Cation exchange and adsorption on clays and clay minerals

Dissertation

Submitted for the degree “Dr. rer. nat.”
of the faculty of mathematics and natural sciences
Christian-Albrechts-Universität
Kiel

Submitted by

Lars Ammann

Kiel 2003

Referent: .....Prof. Dr. Dr. h.c. G. Lagaly

Koreferent: .....Prof. Dr. F. Tuczek

Tag der mündlichen Prüfung: 12.11.2003

Zum Druck genehmigt: Kiel, den .....

.....

Der Dekan

First of all, I would like to thank Prof. Dr. Dr. h. c. G. Lagaly to accept me in his workgroup. Thank you for the interesting topic, the helpful discussions and to let me pursue so many own ideas.

Thank you very much:

- Faiza Bergaya, Amina Aouad and Tushar Mandalia for the great time in Orléans which gave the intention for the chapters four and five.
- Klaus Beneke and Britta Bahn.
- the whole group for the positive and constructive ambience. Special thanks are dedicated to Arno Nennemann, Marián Janek, Sönke Ziesmer, Ingo Berndt, Nils Rickertsen, Heiko Frahm, Matthias Dugaro and Enno Bojemüller.
- Stacy Pyett for checking the language.
- the students Sarah Gebhard, Andreas Beck and Christin.
- the team of Mensa, who always encouraged me to finish as soon as possible.
- my wife Sandra Ammann and Jan & Pierre.

1 Introduction

Clays and clay minerals are two terms which are easily confused, especially by people who do not work in the field of clay science or are newcomers to the field. A natural clay is not composed of one clay mineral only. Impurities such as calcite, quartz, feldspars, iron oxides and humic acids are the most common components in addition to the pure clay mineral. Calcite, iron oxides and humic acids can be removed by chemical treatments. Quartz and feldspars can be removed by sedimentation if the particle size is bigger than that of the clay minerals but traces of quartz are often found in the purified samples. A method for the purification of clay samples is described in Chap. 2.2. In many cases purified samples do not contain one pure clay mineral. Mixtures of clay minerals are very common. Samples with alternating stacking of clay mineral layers of different composition are called mixed-layer clay minerals or interstratified clay minerals. Qualitative and quantitative analyses of mixed-layer clay minerals are usually performed by X-ray diffraction after several chemical pre-treatments.

A number of adsorption experiments with samples containing illite/smectite mixed layer clay minerals were conducted to see if these data can be correlated with the X-ray diffraction data. Another aim was the evaluation and improvement of two experimental techniques which are often carried out by clay scientists. The first is the determination of the cation exchange capacity. A number of methods have been developed, and the determination became comfortable in the last years. Two methods using metal organic complexes have been intensively studied and were compared to the ”standard” ammonium acetate method. Nevertheless the two methods as described in the literature do not give identical results. It seems that the experimental conditions must therefore be evaluated in more detail. The second experimental method investigated is the potentiometric titration of clay dispersions. This experiment is usually carried out to study the surface properties of the samples. Unfortunately, the presentation of the data is often rather poor. An attempt was made to improve the presentation and evaluation of titration data.

2 Material

Several sets of samples were used for this work. They can be divided into five groups:

- Bentonites, on which a lot of research has already been done in our institute, and which can be considered as ”standard samples” of our institute.
- Clays with different contents of smectite, illite, kaolinite and chlorite supplied from other groups. To avoid confusion with the term ”clay”, these samples were called ”common clays”.
- Pillared clays from the group of Dr. F. Bergaya, Orléans.
- A number of samples were employed to evaluate the methods for the determination of the cation exchange capacity. All of them were taken from the sample archive of our group.
- Reduced charge montmorillonites prepared by the Hofmann – Klemen effect (Chap. 2.1).

Most of the work has been done on samples which were purified by the method of Tributh and Lagaly (1986), namely the ”standard samples” of our institute and the common clays. The sample which was chosen to prepare the reduced-charge montmorillonites has also been purified by this method. The procedure of the purification is described in Chap. 2.2.

Bentonites

The so called ”standard samples” of our workgroup are:

- M40a, Na-Bentonite, Volclay, Wyoming
- M47, Ca-Bentonite, Bavaria, Germany
- M48, Ca-Bentonite, Milos, Greece

These samples were received from Süd-Chemie, Germany. The samples were purified by the method of Tributh and Lagaly (1986) (Chap. 2.2). To discriminate purified from raw samples, the purified samples are labelled with the index ”$_{TL}$”, e.g. M47$_{TL}$. The purified samples are assumed to contain only montmorillonite and they are called montmorillonites[1]; the raw samples are called bentonites.

[1] Besides traces of quartz only smectite was detected in the X-ray diffractograms of the purified samples.

Tab. 2.1 : Chemical composition[2] and layer charge ξ of the montmorillonites.

	$M40a_{TL}$	$M47_{TL}$	$M48_{TL}$
SiO_2 [%]	55.06	53.12	55.58
Al_2O_3 [%]	19.39	17.24	17.62
H_2O [%]	16.56	19.47	18.14
Fe_2O_3 [%]	3.41	3.24	1.94
Na_2O [%]	2.68	2.64	2.55
MgO [%]	2.23	3.19	2.94
K_2O [%]	0.181	0.465	0.44
TiO_2 [%]	0.143	0.187	0.209
CaO [%]	0.054	0.084	0.228
MnO [%]	0.007	0.014	0.012
layer charge ξ (alkyl ammonium method)	0.291[3]	0.30[4]	0.33[5]
layer charge ξ (chemical composition)	0.39	0.44	0.43

Common clays[6]

A set of samples with different contents of smectite, illite, kaolinite, chlorite and mixed-layer minerals was chosen for a series of adsorption experiments. The samples Augzin and Friedländer were supplied by Dr. Thorsten Permien, the samples Teistungen, Thierfeld and Plessa by Dr. Jörn Kasbohm, Greifswald University, Germany, and the HS7 sample by Dr. V. Feeser, Kiel University, Germany. All of these samples were purified by the method of Tributh and Lagaly (Chap. 2.2) and labelled with the index ”TL”, e.g. $Augzin_{TL}$. However, experiments were also carried out with the non-purified samples. The raw clays were dispersed in distilled water and passed through a 67 µm sieve, freeze-dried and ground to powder. These samples are labelled with the index ”sieved”, e.g. $Augzin_{sieved}$.

[2] The chemical analyses were performed by K. Emmerich (2002), Braunschweig, personal communication.

[3] Beneke, 1996, personal communication.

[4] Blum, 2001.

[5] Ewald, 1995.

[6] The meaning of ”clay” is ambiguous. The meaning of clay can be the <2µm soil fraction. In this case, the clay minerals are not specified. If the minerals are specified, terms like bentonite (contains mainly smectites) or kaolin (contains mainly kaolinite) are used. In this context the meaning of clay is the very common case of a

Tab. 2.2 : Mineralogical composition of the common clays as received (% w/w).

	smectite	illite	kaolinite	chlorite	mixed layer	quartz	feldspar	hematite	rutile/ anatase
Augzin[7]	34	48	10		8				
Friedländer[2]	48	35	13		4				
HS7[8]	<1	70	27			3			
Plessa[9]			24,4		28,5	40,8	5		
Teistungen[5]			11,2	7,9	25	34,4	19,1	1,8	<1
Thierfeld[5]			19	6,4	28,5	32,6	7,7	4,5	1,5

Pillared clays

A set of pillared clays was chosen for the titration experiments. The samples were prepared by Dr. T. Mandalia, Orléans (Mandalia et al., 1998). A 2% w/w Wyoming montmorillonite dispersion was treated with pillaring solutions containing different ratios of Fe and Al polyhydroxy cations, 10 mmole polyhydroxy cations per gram of clay. The dispersion was aged one day at room temperature, then washed with distilled water until chloride ions were no longer detected. Finally, the samples were calcined at 300°C for 3 hours.

Tab. 2.3 : Composition of the pillared clays.

sample name	composition
PC 100	100% Fe-pillars
PC 50	50% Fe-, 50% Al-pillars
PC 0	100% Al-pillars
Wyoming raw	Na-Wyoming bentonite
Wyoming purified	Na-Wyoming bentonite, < 2µm

Clays from the archive at Kiel

mixture of e.g. smectite, illite, kaolinite and/or mixed-layer minerals. To avoid confusion, this set of samples is called ”common clays”.

[7] Data from Behrens, 1996.

[8] Personal communication, Dr. Feeser.

Tab. 2.4 : Samples from the archive of our group.

Sample	Origin	Supplier
B2	Beidellite from Unterrupsroth, Germany	
Bei 18/4	Beidellite form Unterrupsroth, Germany	
Cameron	Montmorillonite #31, (Bentonite), Cameron, Arizona 48W1310	CMS
Cream	Montmorillonite #22b, (Cream), Amory, Mississippi 48W1221	CMS
de Maio	Bentonita 25 de Maio, Brazil	
H3	Hectorite, California (SHCa-1)	SCMR
KGa-1	Kaolin, well crystallised, Washington County, Georgia, USA	SCMR
Kunipia A	Na-Montmorillonite, Tsukinuno mine, Yamagata, Japan	
M3	Bentonite, Cyprus	
M26	Montmorillonite, Upton, Wyoming	
M34	Bentonite, Camp Berteau	
M39	Bentonite from Niederschönbuch, Germany	
M41	Na-Montmorillonite, Wyoming, (SWy-1)	SCMR
M42	Ca-Montmorillonite, Texas (STx-1)	SCMR
M46	Bentonite from Linden, Germany	
M50	Ca-Bentonite, Ordu, Turkey	Süd-Chemie
Otay	Montmorillonite #24, (Bentonite), Otay, California 48W1240	CMS
Oxidizable blue	Montmorillonite #22a, (oxidizable blue), Amory, Mississippi 48W1221	CMS
Polkville	Montmorillonite #21, (Bentonite), Polkville, Mississippi 45W1210	CMS
Schwaiba	Bentonite from Schwaiba, Germany	
Upton	Montmorillonite #25, Upton, Wyoming 48W1250	CMS

SCMR: Source clay minerals repository, Department of geology, University of Missouri, Columbia, Missouri 65201 U.S.A

CMS: Clay mineral standard, Ward's natural science establishment Inc., P.O. Box 1717 Rochester, New York 14603

2.1 Synthesis of reduced charge montmorillonites

Hofmann and Klemen (1950) reported that the layer charge of Li^+ containing montmorillonite is reduced by heating the samples to 110°C or more. The cation exchange capacity was reduced and the material obtained did not expand upon hydration. Hofmann and Klemen assumed that lithium ions migrate from the interlayer space into the octahedral sheet of the clay mineral to compensate the charge imbalance due to isomorphic substitution. The degree of charge reduction can be controlled by the temperature (Hrobárikova et al, 2001) or by

[9] For these samples only the sum illite + smectite was given. Resultate von Ringanalysen, Ernst-Moritz-Arndt-

mixing different amounts of Na^+ and Li^+ saturated montmorillonite before heating to an appropriate temperature (Brindley and Ertem, 1971, Jaynes and Bigham, 1987). A procedure similar to that of Jaynes and Bigham was applied.

Experimental

M48 bentonite was purified by the method of Tributh and Lagaly (1986) as described in Chap. 2.2. After the sedimentation step the montmorillonite dispersion was coagulated with sodium chloride to reduce the volume. To remove excess salt, the dispersion was centrifuged and dispersed in distilled water[10] several times until the clay mineral did not settle in a centrifugal field of 8000 g. The dispersion was divided into two parts. One was centrifuged and dispersed in ethanol two times, dried at 75°C and ground to powder. This part will be referred to as Na-M48[11]. The other part of the dispersion was dispersed with 1 N LiCl solution and shaken overnight. The sample was centrifuged, the supernatant discarded and the sediment dispersed in 1 molar LiCl solution. This procedure was repeated two times. This part was also washed[12] until the clay did not settle at 8000 g and then washed three times with ethanol. After drying at 75°C the Li^+ saturated montmorillonite could not be ground to powder, the material remained sticky. Therefore, a dispersion of the Li^+ saturated montmorillonite of 2.5% w/w solid content was prepared.

The cec of the purified Na-M48 has been determined in earlier experiments (Ammann, 2000) as 0.97 meq/g. Thus, the equivalent amount of 1g of Na-M48 is 0.9844 g Li-M48, which was calculated by replacing 0.97 mmole of sodium ions by lithium ions. 11 samples with varying molar ratios of Na/Li from 0 to 100% Na were prepared by adding appropriate amounts of dried Na-M48 to the Li-M48 dispersion (Tab. 2.5). The samples are called HK (Hofmann Klemen) followed by the percentage of sodium ions, e.g. HK80 contained 80% sodium and 20% lithium ions (in molar ratios). Water was added to the samples to give app. 2.5% w/w dispersions and the dispersions were shaken for 50 hours, then sonicated for 20 minutes and again shaken over night. The samples were dried at 75°C and filled into a quartz tube (40 mm diameter, 300 mm length). Quartz was chosen to avoid migration of sodium ions from the glass to the sample while heating (Lim and Jackson, 1986, Jaynes and Bigham,

Universtität Greifswald, http://www.uni-greifswald.de/~geo/dttg98/standard/

[10] The distilled water was adjusted to pH 7.

[11] Note that this material has been prepared specially for the reduced charge samples. Though it should have identical properties as the $M48_{TL}$ samples slight differences were observed.

1987). The samples were heated to 260 °C for 24 hours. After heating, the samples were dispersed in 1 molar sodium chloride solution, then centrifuged, washed with distilled water and again centrifuged. This procedure was repeated two times. The dispersions were washed with distilled water until the dispersed particles did not settle completely in a centrifugal field of 8000 g, were dispersed in distilled water and the <2µm-fraction was separated by sedimentation[13]. The supernatant was coagulated by addition of sodium chloride to reduce the volume and then washed with distilled water. Both fractions were dialysed in dialysis bags until salt free. The distilled water was adjusted to pH 7 by addition of a few drops of sodium hydroxide solution. Finally, the dispersion was finally freeze-dried.

Unfortunately a large part of the montmorillonite sintered and could not be used for further experiments.

Tab. 2.5 : Reduced-charge montmorillonites.

	Na-M48 g	Li-M48 g	% Na molar ratio
HK100	66.34	0	100.00%
HK90	45.08	4.96	90.09%
HK80	40.39	10.17	79.88%
HK70	35.22	14.92	70.24%
HK60	30.26	19.75	60.50%
HK50	25.14	24.73	50.41%
HK40	20.26	29.52	40.70%
HK30	15.19	34.53	30.55%
HK20	10.23	39.74	20.47%
HK10	5.2	44.70	10.42%
HK0	0	85.04	0.00%

[12] Being washed means centrifugation and then dispersing in the washing solution.

[13] See Chap. 2.2 for details on the sedimentation and dialysis procedure.

2.2 Purification of clays by the method of Tributh and Lagaly

The purification of clays by the method of Tributh and Lagaly (1986) is designed to remove as many impurities as possible to obtain a somehow ”pure” clay mineral. However, the purified material may still contain impurities like e.g. quartz. The purification procedure contains five steps:

- First the carbonates are removed. Since calcium carbonate is barely soluble it may be a source of Ca^{2+} ions even if the clay was sodium saturated.
- Iron oxides are removed by a combination of reduction to Fe^{2+} and complexation with citrate ions.
- Organic material like humic acids are removed by oxidation with hydrogen peroxide.
- The < 2 µm-fraction is obtained by sedimentation.
- Finally the clay is dialysed until salt-free, freeze-dried and ground to powder.

Removal of carbonates

To dissolve carbonates, 100 g raw bentonite were dispersed in 100 ml 1 N sodium acetate-acetic acid buffer (8.2 g sodium acetate and 6 g pure acetic acid per 100 ml of water, pH = 4.8). The slurry was stirred from time to time and left a few days until no more carbon dioxide bubbles indicated the presence of carbonates. Then the slurry was centrifuged.

Removal of iron oxides

The centrifuged bentonite was dispersed in 270 ml citrate buffer of 115 g (0.37 mole) sodium citrate dihydrate, 8.5 g (0.1 mole) sodium hydrogencarbonate and 70g (1.2 mole) sodium chloride per litre. If needed, buffer was added to adjust pH to 8.3. 20g (0.23 mole) of sodium dithionite were added and the slurry was stirred for 70 hours. Then it was centrifuged and washed[14] four times with a solution of 0.5 mole sodium chloride and 0.025 mole hydrochloric acid per litre. The whole procedure of iron removal was repeated one more time, or, in the case of M47, two more times.

[14] Being washed means centrifugation and then dispersing with the washing solution

Removal of organic matter

0.5 l of 0.1 N sodium acetate solution and 170 ml 30% w/w hydrogen peroxide solution were added. The slurry was stirred for 10 hours at 90°C and then for 20 hours at room temperature. The clay was washed three times with 1 N sodium chloride solution.

Fractionation

The clay was washed with distilled water to remove excess salt until the dispersion did not settle completely in a relative centrifugal field of 8000 g. The dispersion was then diluted with distilled water to about 15 litres and poured into an acrylic glass tube (height 1m, diameter 15 cm). The height of the solution above the outlet was 80 cm. After 60 hours all particles with a Stokes equivalent diameter of >2 µm were below the outlet. However for the first sedimentation step 60 hours were exceeded to be sure that a higher viscosity due to the clay content would not permit particles >2 µm to remain in the supernatant. The sedimentation was repeated once more with the sediment of the first step.

Dialysis

After sedimentation, the dispersion had to be concentrated. Therefore it was flocculated with sodium chloride. The sediment was washed with distilled water and dialysed. For the fractionation, final washing and dialysis, pH of the distilled water was adjusted to 7 by addition of a few drops of sodium hydroxide solution since the pH of the water from the ion exchange resin without exclusion of carbon dioxide is about 5. Dialysis bags were washed before use by boiling several times in distilled water. Finally, the slurry was shock-frozen with liquid nitrogen and freeze dried. The dry clay was then ground to powder.

Samples which have been purified by the method of Tributh and Lagaly are labelled with the index "$_{TL}$", e.g. M47$_{TL}$.

3.1 X-ray diffraction - experimental

Qualitative analysis

X-ray diffraction is the most important tool for qualitative analyses of clay mineral samples. It is easy and fast to carry out and provides a large amount of information. Expanding clay minerals change their (00l) spacing upon ethylene glycol adsorption substantially. Therefore, ethylene glycol solvation was employed to detect smectites. All samples were investigated as air dried powders and ethylene glycol solvated. The procedures for the sample preparation and the identification of the clay minerals were performed as described by Moore and Reynolds (1989). An even more sensitive procedure to detect smectites was published by Weiss et al. (1971) and Lagaly (1981). If the clays are exchanged with alkylammonium ions, even very small amounts ($\leq$ 1%) of smectites can be identified on X-ray diffraction patterns. This procedure was applied to all samples, which did not reveal smectites after EG solvation.

If a clay sample contains chlorite, further work is required to check for kaolinite, because the even order chlorite reflections superimpose with the kaolinite reflections. Kaolinite can be expanded to 11.2 Å by dimethyl sulfoxide (DMSO) intercalation (Calvert, 1984). Therefore, all chlorite containing samples were also investigated after DMSO solvation.

Quantitative analysis

Quantitative analysis of clay minerals is more difficult to carry out than qualitative analysis, and a very good sample preparation is needed. The reflections of mixed-layer minerals are usually found between the those of the pure compounds (Mérings principle, Moore and Reynolds, 1989). The location of the reflections reveal the ratio of the components. For ethylene glycol solvated illite/smectite interstratified minerals, the (001/002) reflection is located between the 10 Å reflection of illite and the ~16 Å reflection of the EG-smectite. The location of the reflection of the mixed layer mineral permits an estimation of the illite/smectite ratio. An even more precise estimation is based on the difference in °2Θ between the (001)/(002) and (002)/(003) reflections, since the difference increases with increasing illite content.

A quantitative estimation of the contained minerals was performed as described by Tributh and Lagaly (1991). For the estimation, the peak size of the first order basal reflections

are determined. The peak area is multiplied with a factor for each clay mineral to give the corrected intensity I. The factors are given in Tab. 3.1. The portion of each mineral is calculated with equation (1) considering illite as example. However, this procedure provides only an estimate.

equation (1) :

$$\text{illite content} = 100\% * \frac{I(illite)}{I(illite) + I(kaolinite) + I(chlorite) + I(montmorillonite) + I(quartz)}$$

Tab. 3.1 : Correction factors for peak intensities

mineral	factor
illite	1
kaolinite	0.24
chlorite	1
montmorillonite	0.22
quartz	2.3

Experimental

The samples were investigated with a Siemens D 5000 diffractometer, (curved germanium 111 monochromator, 1 mm soller slits, a 0.6 mm receiving slit, copper K_α radiation). The samples were applied on a glass sample holder, then passed over several times with a glass slide in an attempt to achieve texture. The dry samples were analysed on a Si (001) sample holder. Since the height adjustment of this sample holder was not perfect, at low values of 2Θ a slight deviation of angle can be noticed between ethylene glycol solvated samples and dry samples. This deviation was not observed when both samples were investigated on the same sample holder. Diffractograms were recorded from $2\Theta = 2°$ to 60° in steps of 0.02° or 0.04° with 15 s counting time for each step.

To obtain ethylene glycol solvation, the samples were put in a desiccator over ethylene glycol at 60° C for eight hours and then stored at room temperature over ethylene glycol until analysis. The samples were moistened with two drops of ethylene glycol before application onto the sample holder.

DMSO solvation of chlorite containing samples was performed as described by Calvert (1984). App. 200 mg of dry clay were ground in an agate mortar with 1 g caesium chloride. 20 ml of 80°C 85% hydrazine monohydrate were added and the mixture was kept at 80°C for five minutes under continuous stirring. The liquid was separated from the sample

with a vacuum filter apparatus and two 20 ml increments of 100° C DMSO were passed through the filter cake. The samples were kept overnight with excess DMSO.

The preparation of the alkylammonium exchanged samples is described in Chap. 6.4.

3.2 X-ray diffraction - results

Augzin$_{TL}$

In the Augzin$_{TL}$ diffractograms (Fig. 3.1) chlorite, illite and quartz can easily be detected. The reflections at 2 Θ = 24.84° and 25.12° (10) could indicate kaolinite in addition to chlorite, but DMSO solvation does not reveal the presence of kaolinite. A reflection at 2 Θ = 5.32° reveals the presence of smectite. The illite reflections (3), (5) and (11) are not affected. The sample does not contain an illite/smectite mixed layer mineral.

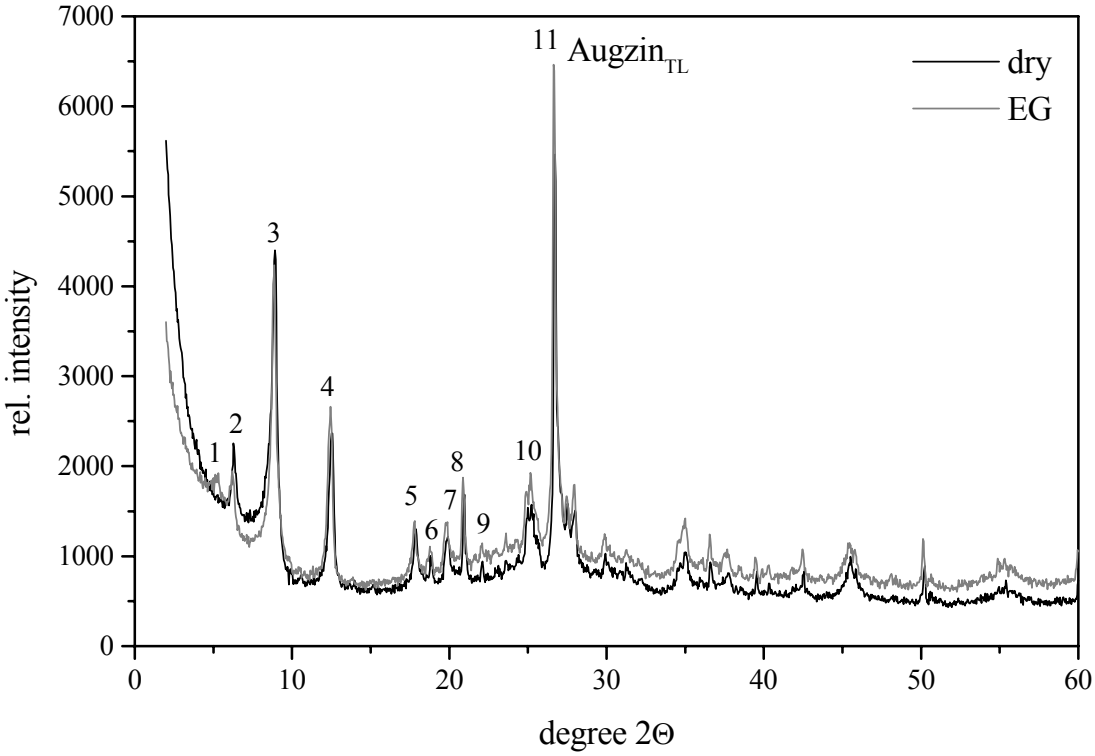

Fig. 3.1 : X-ray diffractogram of Augzin$_{TL}$.

Table 3.2 : Reflections of air dried and EG solvated Augzin$_{TL}$ clay.

	dry		EG		
	deg.2 Θ	d (Å)	deg.2 Θ	d (Å)	
1			5.32	16.61	EG smectite (001)

2	6.28	14.07	6.16	14.35	chlorite (001)
3	8.92	9.91	8.80	10.05	illite (001)
4	12.54	7.06	12.36	7.16	chlorite (002)
5	17.88	4.96	17.68	5.02	illite (002)
6	18.80	4.72	18.68	4.75	chlorite (003)
7	19.92	4.46	19.70	4.51	clay (020)
8	20.96	4.24	20.80	4.27	quartz (100)
9	22.12	4.02	21.96	4.05	cristobalite
10	25.00	3.56	25.12	3.55	chlorite (004)
11	26.72	3.34	26.56	3.36	quartz (101) / illite (003)

Friedländer$_{TL}$

Illite, kaolinite and quartz are detected in the diffractogram of the air dried sample. (Fig. 3.2). Except the EG-smectite (001) reflection, no significant changes are observed after EG solvation, the sample does not seem to be interstratified. Whereas in the Augzin$_{TL}$ and in the Plessa$_{TL}$ sample smectite is difficult to detect, the Friedländer sample contains more smectite.

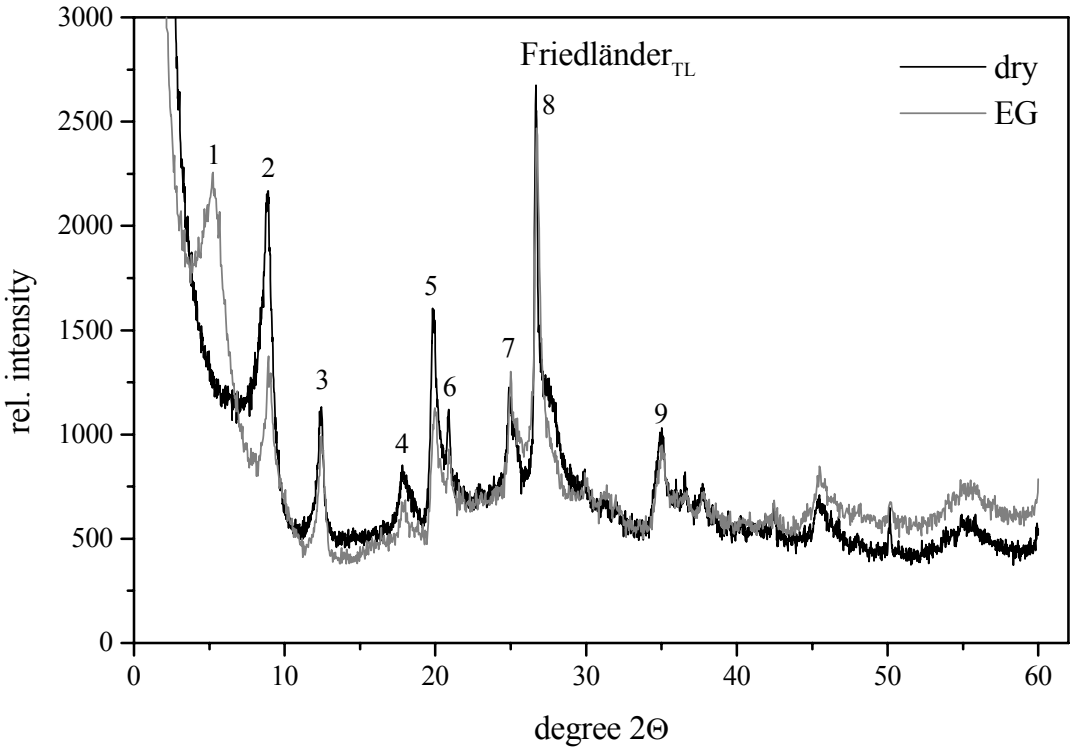

Fig. 3.2 : X-ray diffractogram of Friedländer$_{TL}$.

Tab. 3.3 : Reflections of air dried and EG solvated Friedländer$_{TL}$.

	dry		EG		
	deg.2 Θ	d (Å)	deg.2 Θ	d (Å)	
1			5.24	16.86	EG smectite (001)
2	8.90	9.94	8.92	9.91	illite (001)

3	12.42	7.13	12.44	7.12	kaolinite (001)
4	17.78	4.99	17.76	4.99	illite (002)
5	19.82	4.48	19.96	4.45	clay (020)
6	20.88	4.25	20.88	4.25	quartz (100)
7	24.88	3.58	25.00	3.56	kaolinite (002)
8	26.66	3.34	26.72	3.34	quartz (101) / illite (003)
9	35.02	2.56	35.04	2.56	clay (200)

HS7$_{TL}$

Illite, kaolinite and quartz are the components of HS7$_{TL}$. EG solvation does not affect the diffraction pattern (Fig. 3.3) and smectite cannot be detected. Even the alkylammonium exchanged samples do not reveal any amount of smectites.

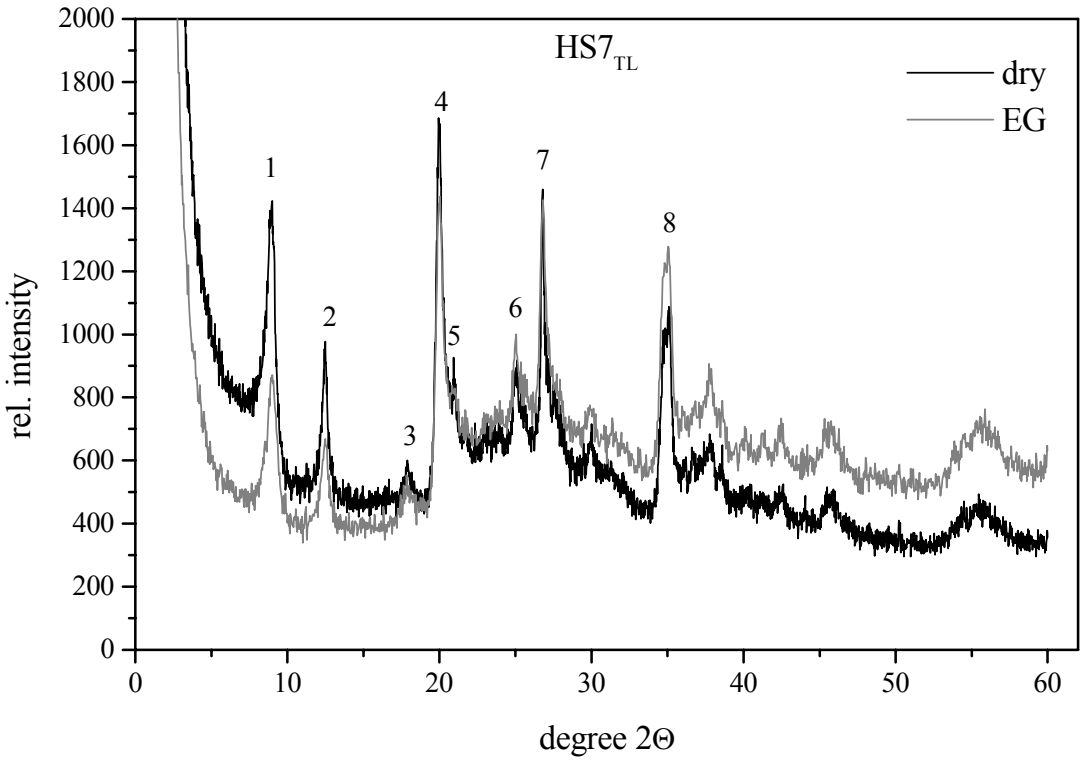

Fig. 3.3 : X-ray diffractogram of HS7$_{TL}$.

Table 3.4 : Reflections of air dried and EG solvated HS7$_{TL}$.

	dry		EG		
	deg.2 Θ	d (Å)	deg.2 Θ	d (Å)	
1	9.00	9.83	9.00	9.83	illite (001)
2	12.48	7.09	12.52	7.07	kaolinite (001)
3	17.88	4.96	18.00	4.93	illite (002)

4	19.94	4.45	20.04	4.43	clay (020)
5	20.94	4.24	20.84	4.26	quartz (100)
6	25.10	3.55	25.04	3.56	kaolinite (002)
7	26.78	3.33	26.80	3.33	quartz (101) / illite (003)
8	35.06	2.56	35.04	2.56	clay (200)

Plessa$_{TL}$

Illite, kaolinite and quartz can be identified in the Plessa$_{TL}$ diffractogram (Fig. 3.4). A broad shoulder at the low angle side of the (001) illite reflection (2) hints to smectite. The EG solvated sample did not clearly reveal whether smectite is present. Another scan of the EG solvated sample was performed from $2\Theta = 2°$ to 20° with a 0.2 mm receiving slit and 30 s counting time (Fig. 3.5). A reflection at $2\Theta = 5.12°$ indicates the presence of a smectite.

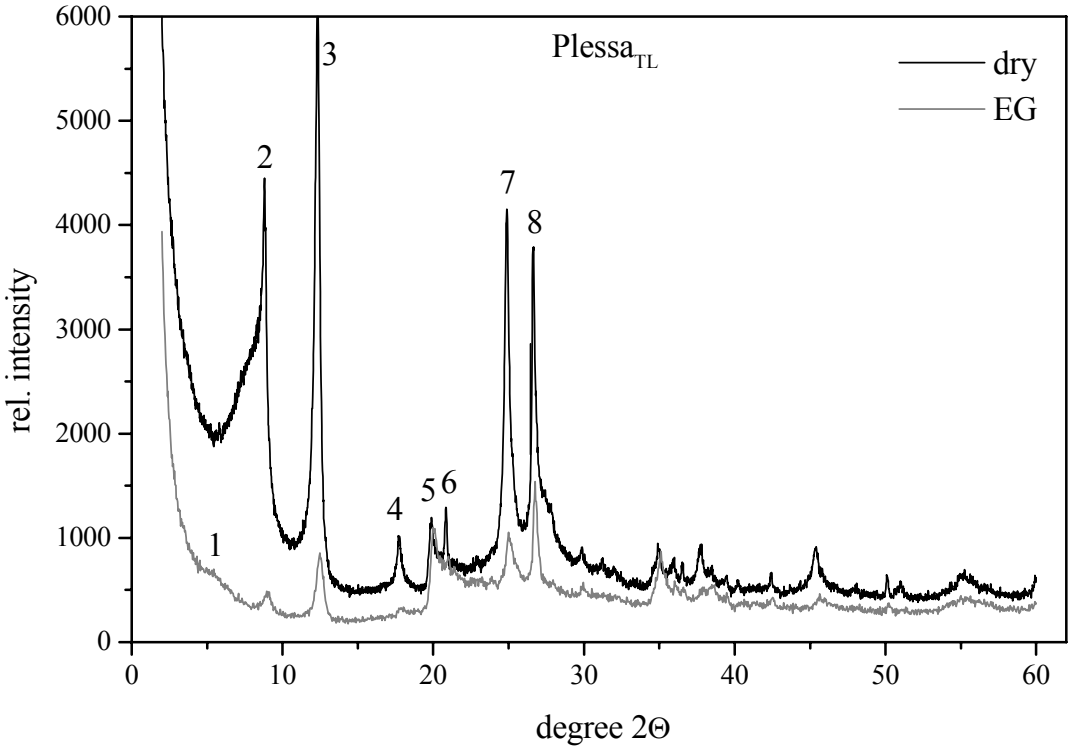

Fig. 3.4 : X-ray diffractogram of Plessa$_{TL}$.

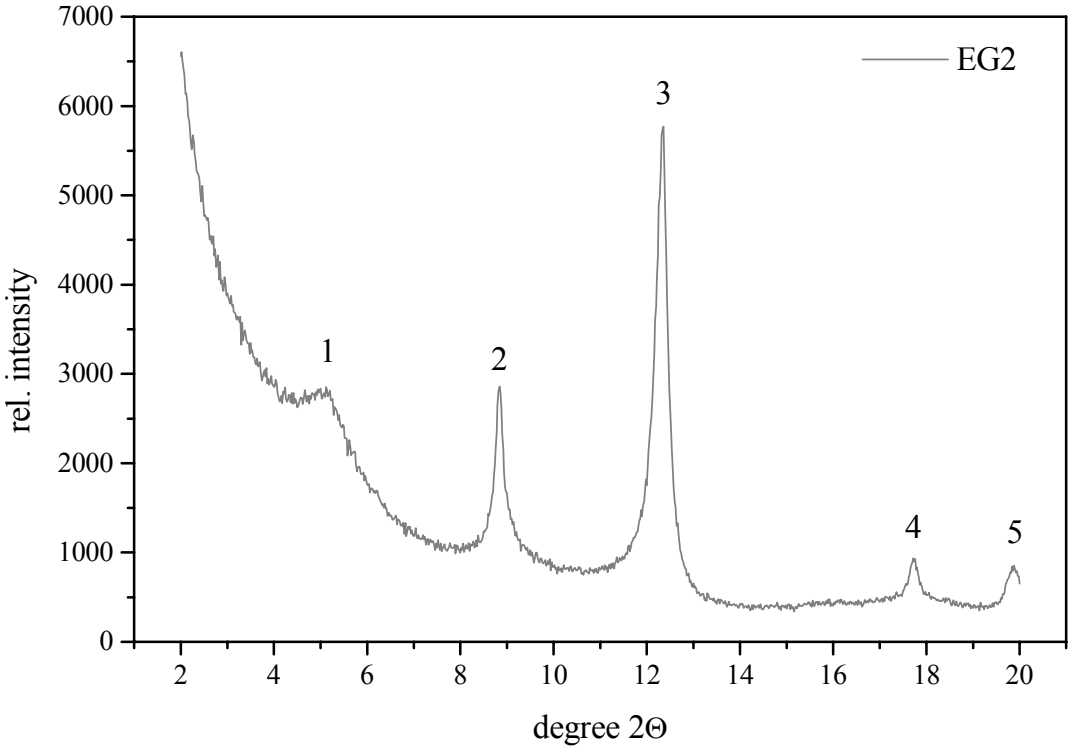

Fig. 3.5 : High resolution diffractogram of EG-solvated $Plessa_{TL}$.

Tab. 3.5 : Reflections of air dried and EG solvated $Plessa_{TL}$.

	dry		EG		
	deg.2Θ	d (Å)	deg.2Θ	d (Å)	
1			5.12	17.26	EG smectite (001)
2	8.78	10.07	8.84	10.00	illite (001)
3	12.30	7.20	12.36	7.16	kaolinite (001)
4	17.76	4.99	17.76	4.99	illite (002)
5	19.86	4.47	19.86	4.47	clay (020)
6	20.80	4.27	21.00	4.23	quartz (100)
7	24.88	3.58	25.00	3.56	kaolinite (002)
8	26.60	3.35	26.76	3.33	quartz (101) / illite (003)

$Teistungen_{TL}$

$Teistungen_{TL}$ consists of chlorite, illite and quartz. EG solvation does not reveal any changes in the diffractogram (Fig. 3.6). Thus, smectites were absent. Two additional reflections (2), (5) of the DMSO solvated sample at °2Θ=7.7 and °2Θ=19.86 reveal the presence of kaolinite. The samples exchanged with decyl-, dodecyl- and tetradecylammonium ions were also analysed by X-ray diffraction. No additional reflections are observed for the decylammonium ion exchanged sample (Fig. 3.7). Two additional peaks are observed for the

tetradecylammonium ion exchanged sample. The dodecylammonium ion exchanged sample reveals a very weak first order reflection at °2 Θ =3.92.

Müller-Vonmoos et al. (1994) reported that long chain alkylammonium ions can enter illite interlayers. The additional reflections likely correspond to expanded illite interlayer spaces, since no reflection is detected for the decylammonium derivative as typical for smectites.

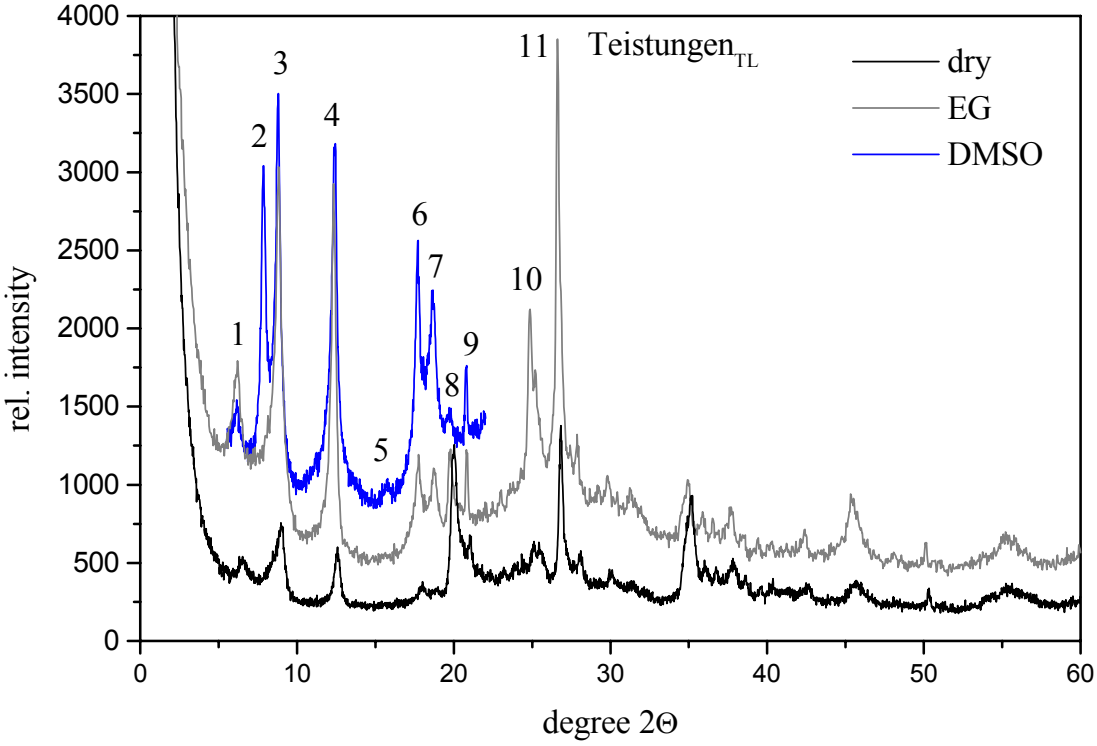

Fig. 3.6 : X-ray diffractogram of Teistungen$_{TL}$.

Tab. 3.6 : Reflections of air dried and EG- and DMSO solvated Teistungen$_{TL}$.

	dry		EG		DMSO		
	deg.2 Θ	d (Å)	deg.2 Θ	d (Å)	deg.2 Θ	d (Å)	
1	6.42	13.77	6.28	14.07	6.16	14.35	chlorite (001)
2					7.86	11.25	DMSO-kaolinite (001)
3	8.98	9.85	8.84	10.00	8.80	10.05	illite (001)
4	12.58	7.04	12.32	7.18	12.44	7.12	chlorite (002)
5					15.78	5.62	DMSO-kaolinite (002)
6	18.02	4.92	17.76	4.99	17.72	5.01	illite (002)
7			18.72	4.74	18.68	4.75	chlorite (003)
8	20.04	4.43	19.80	4.48	19.78	4.49	clay (020)
9	21.02	4.23	20.80	4.27	20.80	4.27	quartz (100)
10			24.88	3.58			chlorite (004)
11	26.84	3.32	26.62	3.35			quartz (101) / illite (003)

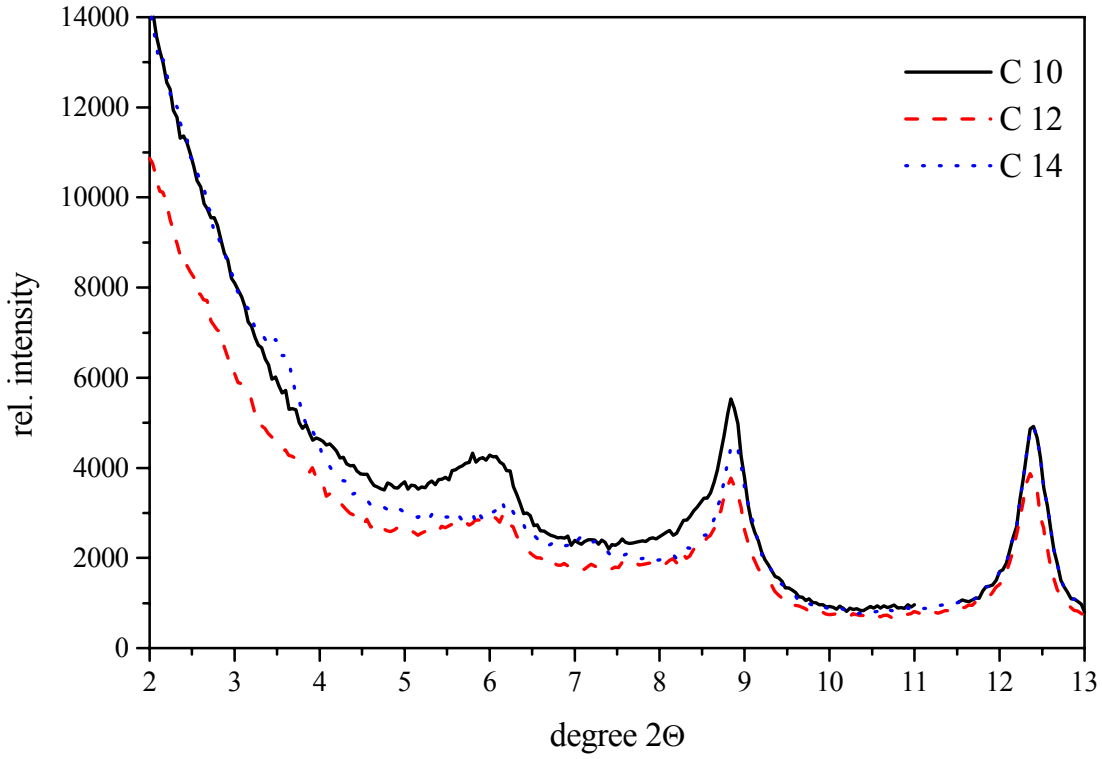

Fig. 3.7 : X-ray diffractogram of alkylammonium exchanged Teistungen$_{TL}$.

Tab. 3.7 : Reflections of alkylammonium exchanged Teistungen$_{TL}$.

	C10		C12		C14		
	deg.2 Θ	d (Å)	deg.2 Θ	d (Å)	deg.2 Θ	d (Å)	
0			3.92	22.54	3.48	25.39	illite (001)
1	6.08	14.54	6.16	14.35	6.16	14.35	chlorite (001)
1b					7.12	12.42	illite (002)
2	8.84	10.00	8.84	10.00	8.88	9.96	illite (001)
3			12.36	7.16	12.40	7.14	chlorite (002) / kaolinite (001)

Thierfeld$_{TL}$

The air dried and EG solvated diffraction patterns of Thierfeld$_{TL}$ (Fig. 3.8) resemble those of the Teistungen sample: Chlorite, illite and quartz are detected and traces of kaolinite are detected in the DMSO solvated sample. Smectite cannot be detected by EG solvation and by exchange with alkyl ammonium ions.

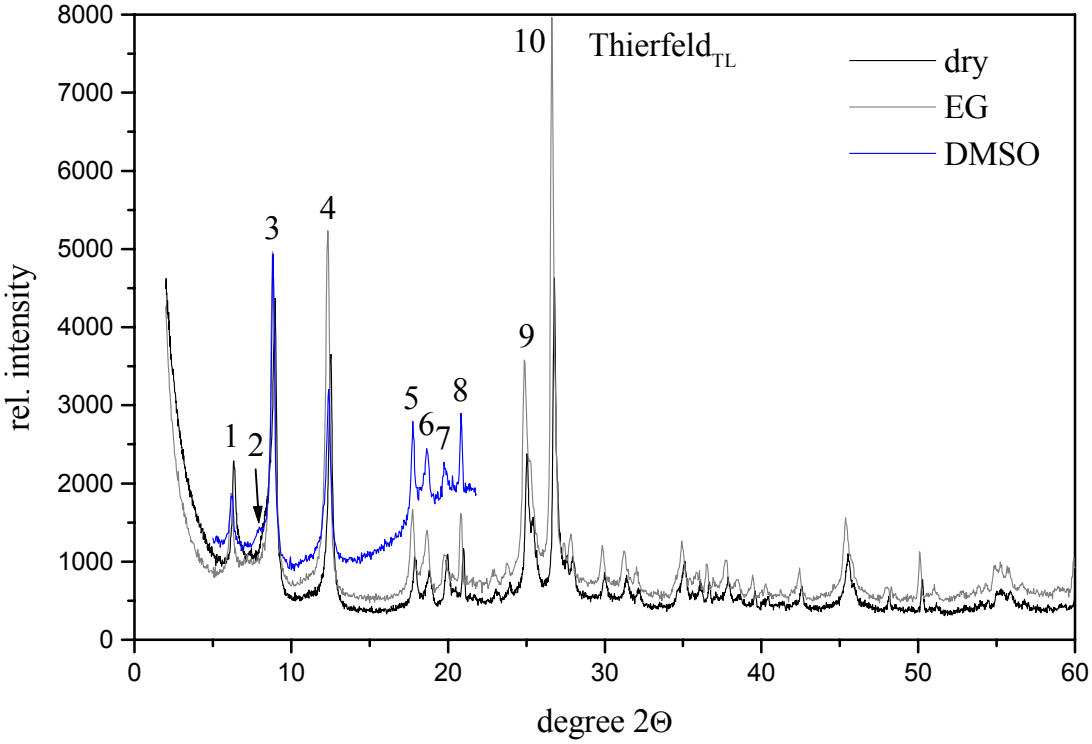

Fig. 3.8 : X-ray diffractogram of Thierfeld$_{TL}$.

Tab. 3.8 : Reflections of air dried and EG- and DMSO solvated Thierfeld$_{TL}$.

	dry		EG		DMSO		
	deg.2 Θ	d (Å)	deg.2 Θ	d (Å)	deg.2 Θ	d (Å)	
1	6.32	13.99	6.16	14.35	6.2	14.26	chlorite (001)
2					7.96	11.11	DMSO kaolinite (001)
3	8.98	9.85	8.80	10.05	8.84	10.00	illite (001)
4	12.54	7.06	12.32	7.18	12.4	7.14	chlorite (002)
5	17.87	4.96	17.76	4.99	17.76	4.99	illite (002)
6	18.80	4.72	18.68	4.75	18.64	4.76	chlorite (003)
7	19.98	4.44	19.88	4.47	19.8	4.48	clay (020)
8	21.00	4.23	20.80	4.27	20.84	4.26	quartz (100)
9	25.04	3.56	24.88	3.58			chlorite (004)
10	26.80	3.33	26.64	3.35			quartz (101) / illite (003)

Conclusions

The results are summarised in Tab. 3.9. All samples contain illite and at least traces of quartz. Chlorite was detected in the Augzin$_{TL}$, Teistungen$_{TL}$ and Thierfeld$_{TL}$ sample. To permit the detection of kaolinite, these samples were also investigated DMSO solvated. Kaolinite in addition to chlorite was detected in the Teistungen$_{TL}$ and Thierfeld$_{TL}$ samples. Kaolinite was also detected in the Friedländer$_{TL}$, HS7$_{TL}$ and the Plessa$_{TL}$ sample. Augzin$_{TL}$, Friedländer$_{TL}$

and $Plessa_{TL}$ contain smectites, but the $Friedländer_{TL}$ sample seems to be the only one with notable amounts of smectite, as seen in the significant changes of the diffraction pattern upon ethylene glycol solvation. All other diffractograms were only slightly affected or not at all by EG-solvation. For this reason the methods to determine the smectite ratio in mixed layer minerals (Srodon, 1980, Moore and Reynolds, 1989) could not be applied. Note that slight differences in the low angle peak positions between dry samples and EG-solvated samples stem from different sample holders. The dry samples were recorded on a Si 001 monocrystal wafer with improper height adjustment.

An estimation of the contained quantities was performed following the procedure proposed by Tributh and Lagaly (1991). Since the third order illite reflections coincide with the (100) quartz reflection, the quartz content could not be determined. For the smectite containing samples the diffractograms of EG solvated samples were used, for the chlorite/kaolinite containing samples the diffractograms of the DMSO solvated samples.

Tab. 3.9 : Estimated content of minerals of the clay samples

	smectite	illite	kaolinite	chlorite	quartz	cristobalite
$Augzin_{TL}$	3%	80%		16%	*	*
$Friedländer_{TL}$	35%	56%	9%		*	
$HS7_{TL}$		91%	9%		*	
$Plessa_{TL}$	9%	52%	39%		*	
$Teistungen_{TL}$		77%	14%	9%	*	
$Thierfeld_{TL}$		80%	3%	17%	*	

4.1 Potentiometric titration: General

Potentiometric titration is applied to study the surface properties of many materials, including clay minerals. Most materials develop charges at the solid/liquid interface due to dissociation or adsorption of ions from the solution. One way to characterise these charges is by potentiometric titration. One may either study the surface charge which is especially important for the colloidal behaviour, or the acid-base behaviour, which is of interest for the catalytic properties. Though the experiment itself seems to be quite simple, two general problems must be considered when performing this kind of experiment: the experimental conditions and the evaluation of the data.

Experimental conditions

The first issue is to find the right experimental conditions. For example, many authors titrate with potassium hydroxide solution and nitric acid because the potassium cation and the nitrate anion have approximately the same size. It is well known that the potassium cation is specifically adsorbed at the hexagonal cavities of the tetrahedral sheet of clay minerals (Lagaly, 1993), which causes some question as to whether titration with potassium hydroxide solution is optimal. On the other hand, the pH-dependent charges are located on the edges of the clay mineral's lamellae so that the specific adsorption of potassium ions may not be important. Rosenqvist et al. (2002) pointed out the influence of the equilibration time when performing titrations on gibbsite particles. As a criterion for the equilibration time they chose a maximum drift of 0.2 mVh^{-1} which was usually reached after 8 to 14 hours. Comparing their results to those from Hiemstra et al. (1999), who used two minutes equilibration time, they found up to five times higher amounts of protons adsorbed by the gibbsite particles. If the titration is performed at high pH, further problems have to be considered – the uptake of carbon dioxide from the atmosphere can lead to erroneous results. Bottles, the burette and the titration vessel made of glass can release impurities due to dissolution of the glass matrix (Lagaly et al., 1997). The reference electrode and the glass electrode must be carefully chosen. Electrodes with diaphragms may be plugged if the clay is flocculated at the diaphragm. Using a Pt-wire diaphragm should avoid this problem but flow out of electrolyte can cause other problems. Kallay et al. (1993) proposed inert gas bubbling at the capillary of

the burette and at the diaphragm of the electrode to avoid flow out of electrolyte. The choice of experimental setup depends on the information which are desired.

Evaluation of data

The second problem concerning potentiometric titrations is the evaluation of the titration data. Titration curves of pH vs. the amount of acid or base added are often characteristic but do not reveal a lot of information. Protonation or deprotonation of surface sites with different acidities can overlap in the curve, or the quantity of a site may be too small to appear as a plateau in the curve. A better evaluation technique is necessary. A simple evaluation of titration data can be based on the determination of inflection points which correspond to sites with a certain acidity. Unfortunately, inflection points often cannot be clearly distinguished on titration curves. More information may be obtained by potentiometric titration if the experiment is repeated at different ionic strengths. The ionic strength of a dispersion has an influence on the shape of the titration curve. By increasing the ionic strength surface charges are shielded because the diffuse double layer is compressed at high ionic strength. More charges can develop on the surface and the proton adsorption increases at low pH whereas at high pH the release of protons increases. Only one point of the titration curve is not affected by the ionic strength, the point of zero salt effect (**pzse**) (Parker et al., 1979, Avena et al, 1990). As the titration curves recorded at different ionic strengths intercept at this point, it is also called the common intersection point (**cip**) (Lagaly et al., 1997, Lyklema, 1995). The point of zero salt effect and the common intersection point are synonyms. Not all ions are indifferent to the materials surface. In some cases specific adsorption, also termed surface complexation, occurs. Chorover and Sposito (1995) point out that the difference between ions bound by surface complexation and those adsorbed in the diffuse double layer is the higher degree of hydration of the latter. Lyklema (1995) assumed that the surface charges of oxidic materials are only generated by adsorption of H^+ and OH^- (or release of H^+) whereas other ions are adsorbed in the Stern layer and do not contribute to the surface charge[1]. If this definition is applied, the point of zero net proton charge (**pznpc**) (Wanner et al., 1994) is identical with the point of zero charge (**pzc**). If specific adsorption of cations (anions) occurs,

[1] Lyklema differentiates between three kind of ions : (i) Indifferent ions with only Coulomb interactions to the surface, (ii) Ions which are bound close to the surface in the Stern layer by specific adsorption, which means that non-electrostatic forces play a more or less important role for the adsorption and (iii) ions which become part of the structure as for example Ag^+ and I^- adsorbed on AgI or protons adsorbed on oxides. Only the latter are called potential determining ions and contribute to, or better, create surface charges.

the cip is located at lower (higher) pH than the pzc. One may interpret this phenomenon as a competition for adsorption sites or exchanger-like behaviour (Wanner et al., 1994). Lagaly et al. (1997) conclude that a higher proton concentration (thus lower pH) is required to achieve the pzc if specific adsorption of cations occurs due to the repulsive potential between cations adsorbed in the Stern layer and protons adsorbed on the surface. If no specific adsorption of the electrolyte occurs, the common intersection point (cip, pzse) and the point of zero charge (pzc, pznpc) are identical. If the definition of Lyklema is applied, we conclude:

$pzse = cip = pznpc = pzc$	if no specific adsorption (surface complexation) occurs
$pzse = cip \neq pznpc = pzc$	if specific adsorption (surface complexation) occurs

Unfortunately, other authors (Roempp, 1995, Helmy et al., 1994) do not differentiate between ions adsorbed on the surface and in the Stern layer, as in Lyklema's model. Following their definition of the pzc means that ions bound by surface complexation also contribute to the surface charge and $pznpc \neq pzc$ in the presence of potential determining ions other than H^+ and OH^-. Roempp (1995) defines the isoelectric point (iep) in the way Lyklema defines the pzc, so that charges are only generated by H^+ and OH^- in absence of any other potential determining ions. Furthermore, Roempp defines the pzc as any point of neutral charge. The pzc coincides with the iep only if H^+ and OH^- are the only potential determining ions. Lagaly et al. (1997) mention that the iep is determined by electrokinetic measurement and is a priori independent of the pzc. They also point out that the definition given by Lyklema has certain advantages, but that including the specifically adsorbed ions in the surface charge is also a reasonable point of view, since many experimental methods do not differentiate between charges located on the surface and those located in the Stern layer. Chorover and Sposito (1995) term the point of zero net charge (pznc) for clay minerals as the pH value where the permanent charge, which is due to isomorphic substitution in the crystal lattice, is compensated by adsorption or release of protons and hydroxyls. The authors point out that from model calculations a common intersection point is found for single oxide dispersions but not for arbitrary oxide mixtures.

Conclusions

- The point of zero salt effect and the common intersection point are synonyms.

- Lyklema postulates that only protons contribute to the surface charge (of oxides), and the point of zero charge and the point of zero net proton charge are identical. Other authors define the pzc as any point of charge neutrality, which means that charge neutrality (pzc) can also be obtained by adding specifically adsorbed ions. Furthermore they refer to the pznpc as the iep.
- The usage of pzc and iep is sometimes confusing, but the terminology of pzse, pznpc is clear.

A common way to present titration data is to calculate a proton adsorption isotherm. The number of protons adsorbed by the sample can be calculated in two ways. The simplest way is to calculate an ”expected” pH by the sample volume and the amount of acid or base added. The difference between calculated pH and measured pH is the amount adsorbed by the sample. The more precise method is to perform a titration experiment on a blank sample under identical conditions (volume, temperature, ionic strength...). Performing the blank titration offers the advantage that some possible sources of errors mentioned above are eliminated automatically if the pHs are measured and not calculated. On the surface of clay minerals silanols and aluminols are present. At least two different acidities characterised by their pK_a should be expected. However different co-ordination of aluminols results in different pK_a (Rosenqvist et al., 2002), and more sites with different acidities can be found. In pillared clays a part of the interlayer cations are replaced by polyhydroxy metal cations. On heating, these polyhydroxy metal cations form oxides fixed to the clay mineral layers. The acidity of a clay can be increased by this process and more acidic sites are created (Bandosz et al., 1994).

4.2 Potentiometric titration: experimental

Single batch titration experiment

The titrations were performed with an automatic titrator (Mettler Toledo DL 25) equipped with a 10ml burette. A glass electrode with Pt-wire diaphragm (especially suitable for dispersions, Schott N 6000 A) was used. Calibration of the electrode was performed prior to each measurement. The titrations were carried out at 25°C in a thermostatic vessel that was

continuously stirred. A slow nitrogen stream was bubbled through the dispersion to prevent uptake of CO_2 from the atmosphere. Titrations were performed from acidic to basic (index: ab) and from basic to acidic (index: ba) using 0.1 N sodium hydroxide solution or hydrochloric acid. A volume of 40 ml dispersion was employed in all titrations. Prior to the titration experiment, the pH of the dispersion was adjusted to 3 for ab titrations and to 10 for ba titrations by fast titration (0.02 ml / 30 s). Distilled water was added to give a total volume of 50 ml. The main experiment was performed by adding 0.01 ml base or acid solution in time intervals of 90 s. Up to 1000 data points (corresponding to 10 ml of acid or base added) were collected for each titration by a computer.

Some problems arose during these experiments:

- The pH-equilibrium of the clay dispersion cannot be achieved at once. When the titration speed was changed, the shape of the titration curve changed to have less pronounced plateaux. Therefore, the slowest possible titration speed (0.01 ml / 90 s) was chosen. However, even at this speed the dispersion will not achieve pH-equilibrium (this may take up to some hours).
- Up to 10 ml of acid or base solution were added which is a significant change in total volume. The use of more concentrated solutions was excluded because it would result in an faster change of pH value.
- Titrations in the ab and ba directions did not yield matching results. Plateaux or shoulders were more or less pronounced and sometimes shifted to different pH values when the direction of the titration was inverted.
- At very high and very low pH the solid phase could dissolve. For this reason, the fast titration prior to the main experiment was stopped at pH 3 or 10. The main titration was stopped at pH $\approx$ 2 or 11.
- The response of the electrode was not stable in all cases. When a calibration was performed before and after the experiment, a drift of the response could be observed. The error due to the drift of the electrode during one titration was within 0.1 pH. A precipitation of flocculated clay at the diaphragm caused by flow-out of electrolyte as reported by Bojemüller (personal communication) was not observed.

Multibatch titration experiments

To avoid the problems mentioned above, another type of titration experiment was designed. The titration was performed as one would make an ordinary adsorption experiment, i.e. as a multibatch experiment. 30 samples of $M40a_{TL}$ and $M48_{TL}$ (100.5 mg ± 0.5 mg) were weighed in 15 ml polystyrene bottles. Distilled water, 0.01 N sodium hydroxide solution and 0.01 N or 0.1 N hydrochloric acid were added to yield 12 ml. The samples were shaken and the pH was read after 2.5 hours and one day for the $M40a_{TL}$ sample and after 2 minutes and one day for the $M48_{TL}$ sample. A blank curve was also recorded. The data were analysed by $\Delta V/\Delta pH$ plots (Chap. 4.3). To plot all samples into one diagram the volumes of acid or base added were taken into account as "0.1 N hydrochloric acid equivalents", e.g. 1 ml 0.01 N sodium hydroxide solution corresponds to –0.1 ml 0.1 N hydrochloric acid. For the single batch titration up to 1000 data points were recorded whereas for the multibatch experiment only 30 points were measured. In this case the polynomial interpolation is needed to calculate the consumption of acid or base to achieve certain pHs. A volume correction as applied to the automatic titrations was not required since all samples were of the same volume (12 ml). No inert gas atmosphere was applied. Since the bottles were almost full the remaining gas volume was relatively small and the effect of carbon dioxide was neglected. There are several advantages of this procedure:

- No sophisticated experimental setup is required.
- The solid content is constant for the whole pH range since the sample is not diluted by adding the acid or base solutions.
- The ionic strength can be kept constant if required.
- The kinetics of the proton adsorption or release can be studied since the pH of each sample can be measured several times.
- The pH can be measured after a sufficiently long equilibration time, e. g. after one day.
- In normal titration experiments one has to choose either dilute solutions for a high resolution or more concentrated solutions for a larger pH range. In the multibatch experiment, solutions with different concentrations can be combined.

Shortcomings of this method are

- The consumption of sample and solutions is higher.
- For non-purified clays 100 mg might be a too small quantity if the clay is very inhomogeneous.

Recommendations

- If a purified clay (<2µm fraction) is going to be analysed, one might consider the use of a dispersion instead of weighing the dry clay. Stirring the bottle with the stock dispersion while taking the subsamples would prevent sedimentation of particles.
- Since pH is a logarithmic quantity, the amount of acid or base between two adjacent samples may be doubled.

4.3 Evaluation of the titration data: $\Delta V / \Delta pH$ plots

To obtain as much information as possible from the titration experiments, an evaluation of the data was performed. The calculations are free of assumptions or models. The three steps of the evaluation are illustrated in a set of graphs (Fig. 4.1 to 4.4). As an example citric acid was analysed to show the capability of the method.

Experimental

0.1927 g (0.917 mmole) of citric acid were dissolved in 50 ml of 0.1 N hydrochloric acid to ensure complete protonation of the acid. The titration was carried out as described in Chap. 4.2 except 1 N sodium hydroxide solution was used and the equilibration time was reduced to 30 s before reading the pH and adding the next increment. As a blank, 50 ml of 0.1 N hydrochloric acid were titrated at the same conditions.

Fig. 4.1 shows the titration curve of the citric acid and the blank solution. Though there is a significant difference between the two curves one can not recognise directly the number of acidic sites involved. Even the hydroxide adsorption isotherm (Fig. 4.3) does not reveal more information.

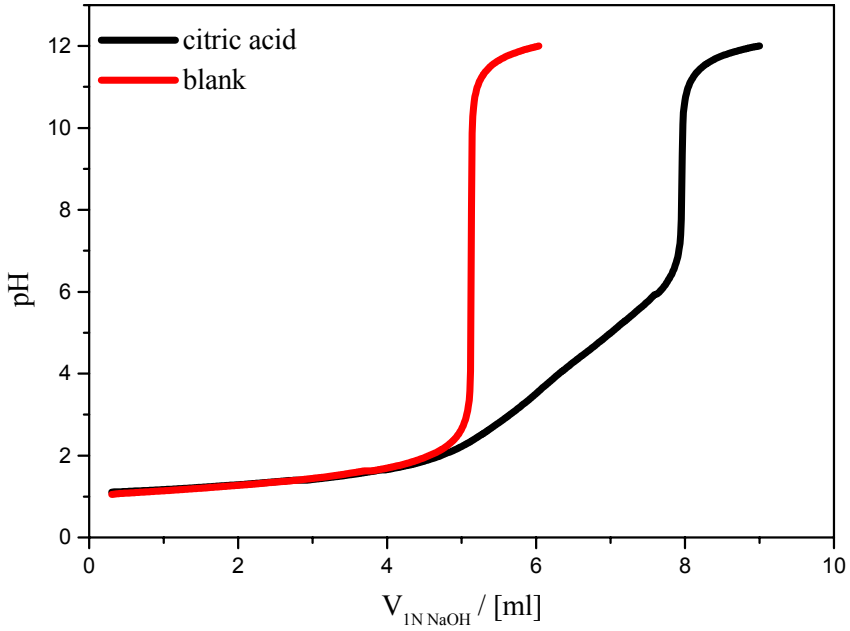

Fig. 4.1 : Titration curve of citric acid and blank solution.

Evaluation

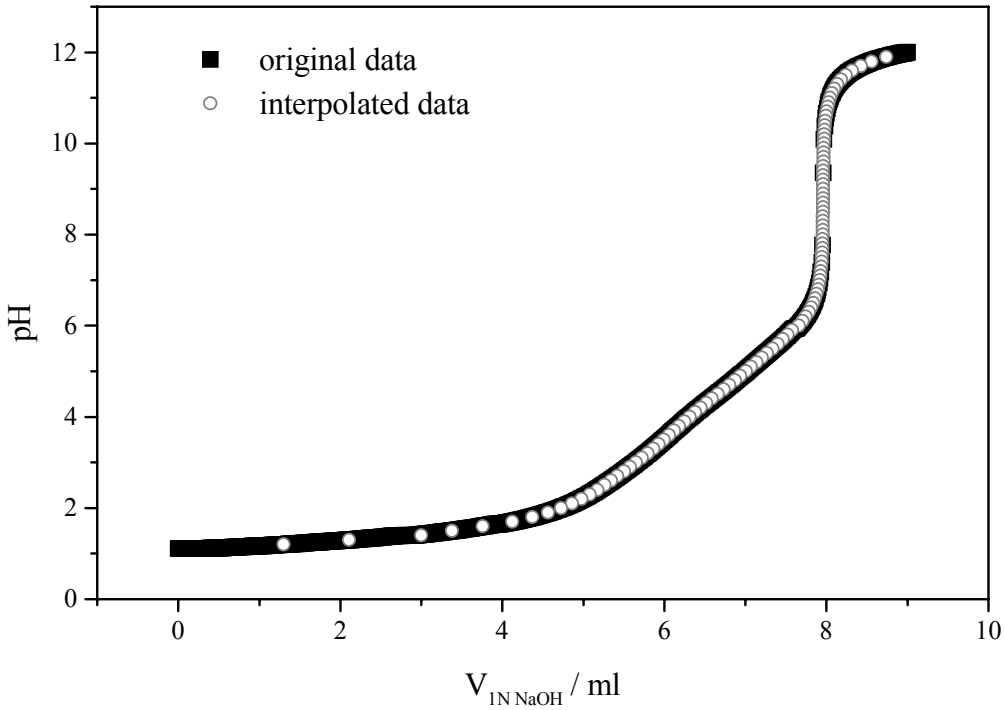

Fig. 4.2 : Original data and interpolated data equidistant in pH.

The evaluation was done in three steps:

- interpolation of the data to calculate the consumption of acid or base to reach a number of given pHs,
- subtracting the consumption for the blank at each pH gives the adsorption isotherm,
- differentiation of these data, smoothing and, finally, plotting $\Delta V / \Delta pH$ vs. pH.

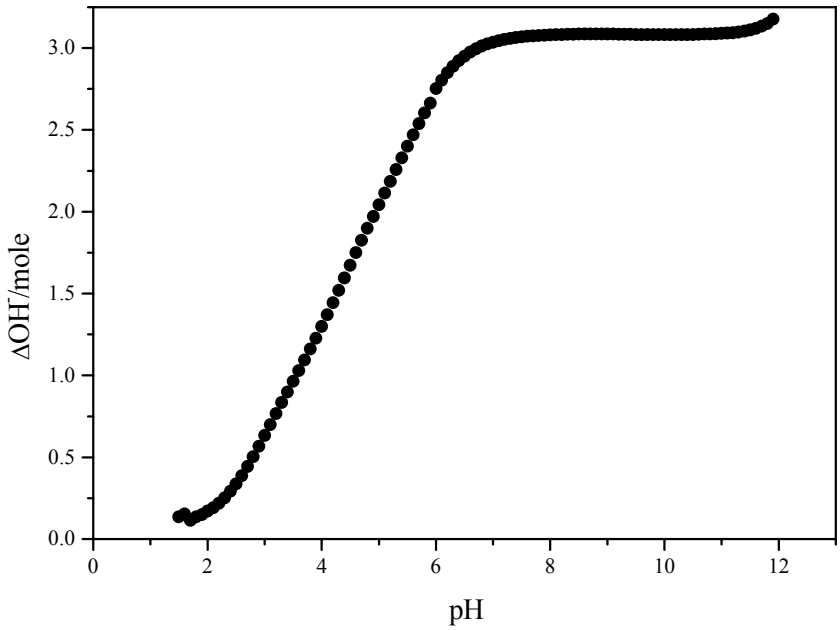

Fig. 4.3 : Hydroxide adsorption isotherm of the citric acid. Note that the axes have been exchanged from the previous figure.

The required volume of acid (or base) to obtain a set of given pHs (e.g. pH 10 to 2.4 in steps $\Delta pH = 0.1$) was calculated by interpolation of the data with a LaGrange polynomial[2] using 4 data points (Fig. 4.2). However, linear interpolation would be sufficient as well since the volume increment is very small (0.01 ml).

The amount of protons (or hydroxide) adsorbed by the sample was calculated by subtracting the acid (or base) consumption of the blank solution from the consumption of the sample for the whole pH-range. Plotting the moles of protons (or hydroxide) adsorbed by the sample vs. pH gives a proton (or hydroxide) adsorption isotherm (Fig. 4.3).

For clay samples the amount of protons (or hydroxide) adsorbed was divided by the initial weight of the clay, for the citric acid it was divided by the number of moles dissolved. To reach a higher accuracy, the consumption of the blank solution was normalised by the

[2] The interpolation was done by an Excel®-macro. The algorithm is given in the appendix.

factor (volume of the dispersion at $pH_i + 2\Delta pH$[3]) / (volume of the blank solution at $pH_i + 2\Delta pH$) to take into account that the volume of acid (or base) added may have changed the dispersion volume in a significant way. (Note that the start volume is 50 ml and up to 10 ml of acid or base were added during the titration !)

The consumption of acid (or base) to decrease (or increase) the pH by $\Delta pH = 0.1$ was calculated, $\Delta V/\Delta pH$. These data were smoothed due to noise at high pH. Smoothing was done by calculating the required volume of acid (or base) to take the dispersion from pH_i to $pH_i + 4\Delta pH$ and dividing it by four. Smoothing was not necessary for the citric acid sample. Plotting $\Delta V/\Delta pH$ vs. pH represents the differentiation of the adsorption isotherm. The graphs obtained by this method resemble spectra where the centre of the peak is the pK_a of the acidic group and the peak area is the amount of protons adsorbed or desorbed by the group. For the citric acid (Fig. 4.4) three acidic sites were found, all about of the same size. The pK_as found are in good agreement with the literature data: $pK_1 = 3.1$ (lit.[4] 3.08), $pK_2 = 4.4$ (lit. 4.74) and $pK_3 = 5.5$ (lit. 5.40).

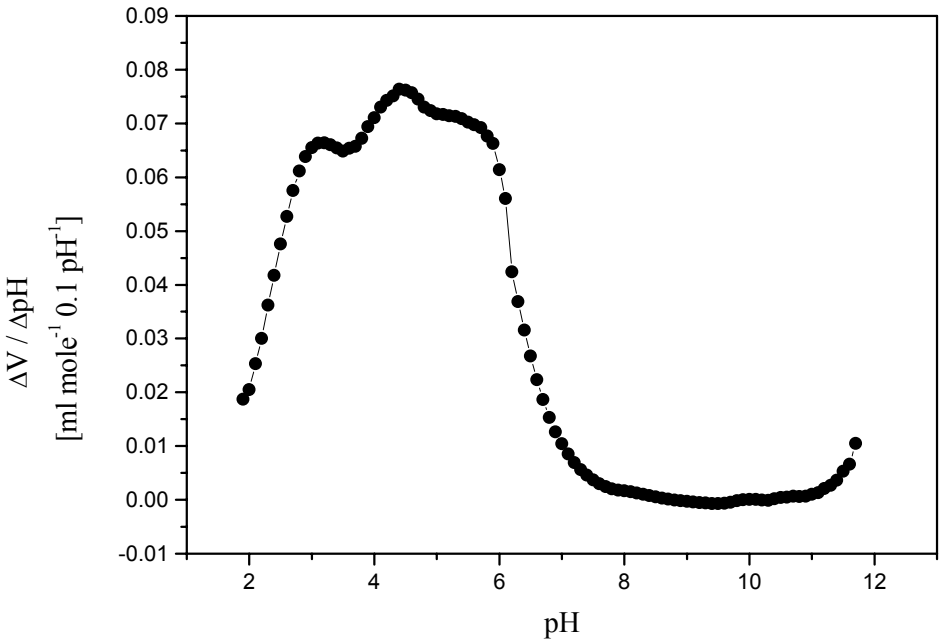

Fig. 4.4 : $\Delta V/\Delta pH$ plot of the citric acid titration.

[3] For titrations of the clay mineral samples, the data were smoothed by averaging four adjacent points, from pH_i to $pH_i + 4\Delta pH$. Therefore, the volume in the centre of the interval, at $pH_i + 2\Delta pH$, was chosen for the correction factor. The data of the citric acid titration were not smoothed, therefore the volume of the citric acid solution and the blank solution at $pH_i + \Delta pH$ was chosen.

[4] Handbook of Chemistry and Physics, 49th edition

4.4 SAIEUS evaluation of titration data

The SAIEUS (solution of adsorption integral equation using splines) software (Contescu et al. 1993, Jagiello, 1994) is designed to take more information from titration data than can be done by simple mathematics (e.g. derivative, subtraction of curves). It permits calculation of the pK_as and the portions of an ensemble of acidic sites with different acidities. The evaluation is done in three steps:

1. First, a proton binding isotherm is calculated by taking the difference of the amount of protons expected (admitting the sample was pure water and accounting for the amount of acid or base added and the salt content) and the amount of protons found (by measuring the pH). This isotherm is considered to be a superposition of a set of Langmuir isotherms.
2. The isotherm is approximated by a least-square fit using a cubic spline function. This function is chosen because it permits calculation of a second derivative in any of its points.
3. Acidic sites are posed where the second derivative of the generated binding isotherm has a minimum. This gives the pK_a of each acidic site, represented as a peak in the final diagram. The area of the peak represents the amount of protons adsorbed or released by each site and is fitted so that the theoretical and the experimental adsorption isotherms match.

4.5 Potentiometric titration of pillared clays

Three samples of different pillared clays were investigated. They are based on Wyoming bentonite which was modified by Dr. T. Mandalia, Orléans (Mandalia et al., 1998). The pillars are 100% Fe_2O_3 (PC 100), 50% Fe_2O_3 and 50% Al_2O_3 (PC 50) and 100% Al_2O_3 (PC 0). The titrations were performed from acidic to basic (ab titration) and from basic to acidic (ba titration). PC 100 ab means titration of the pillared clay with 100% Fe_2O_3 pillars with base.

Ab titration of the pillared clays (Fig. 4.5) reveals significant differences between the samples. With increasing Al-content the samples buffer more base. PC 0 shows a plateau at pH ≈ 4.5 and a shoulder at pH ≈ 6.2. The titration curves of PC 100 and PC 50 are similar. Both curves have inflection points at pH ≈ 5.5 and plateaux at pH 3.5 (PC 50) or pH < 3 (PC

100). Note that the ”natural” pH of the PC 100 dispersion was already below 3 (Tab. 4.2), so it was not necessary to adjust the pH prior to the experiment.

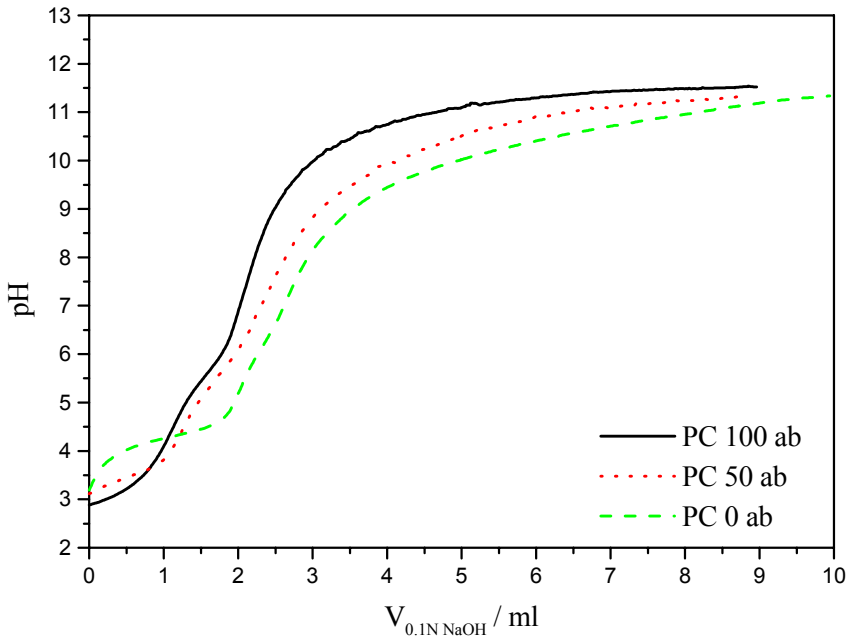

Fig. 4.5 : ab titration of pillared clays.

The ba titration curves of PC 50 and PC 0 were more similar (Fig. 4.6). They buffer more acid and have inflection points at pH 5.5 and 9.5. Again, the PC 50 sample behaved as an intermediate between the two other titration curves. The PC 100 sample did not show any significant characteristics.

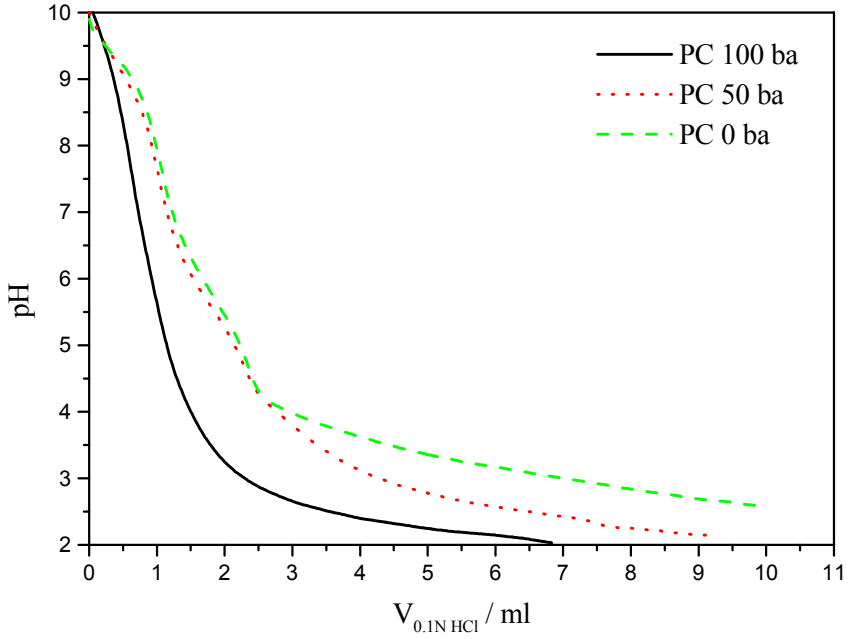

Fig. 4.6 : ba titration of pillared clays.

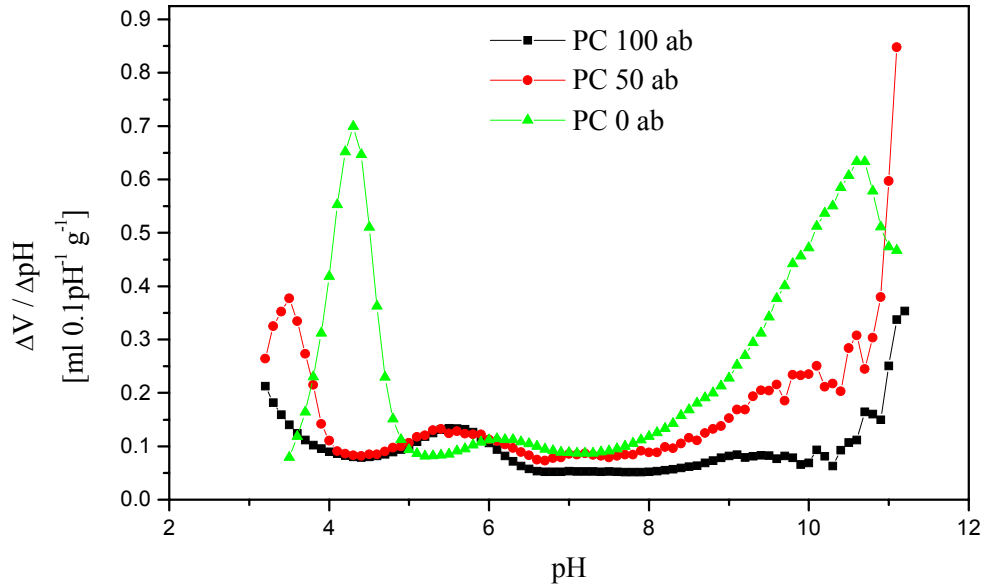

Fig. 4.7 : Δ V/ Δ pH plot of ab titration of pillared clays.

Fig. 4.7 and 4.8 show the evaluated data of the ab and ba titrations of the pillared clays. At pH > 10 the data of PC 100 and PC 50 were scattered despite smoothing. The PC 50 data again lie between the PC 0 and PC 100. An acidic site of approximately the same size between pH 5 and 6 is detected in all experiments except the PC 100 ba titration. Other acidic sites were observed for PC 0 at 4.3 (ab) and 3.9 (ba) and for PC 50 at 3.5 (ab) and 3.9 (ba). A site at pKa < 3 was indicated for PC 100 in the ab experiment but is not seen in the ba experiment. The PC 0 sample has the highest acid and base consumption of all samples. The results are listed in Tab. 4.1.

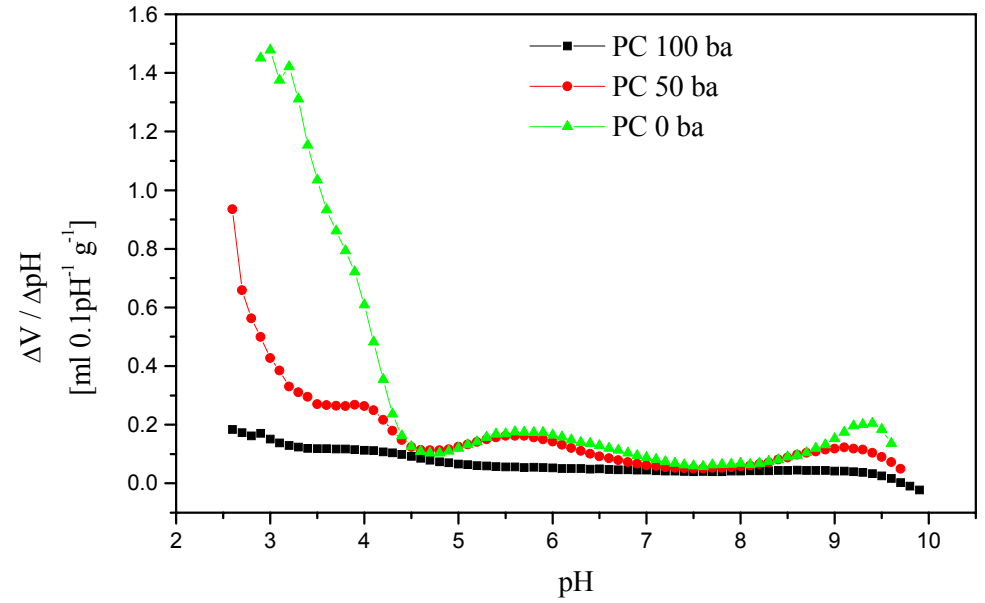

Fig. 4.8 : Δ V/ Δ pH plot of ba titration of pillared clays.

Performing two titrations in opposite direction did not yield matching results. The height and the position of the peaks were quite different. Knowing that pH equilibrium cannot be achieved between addition of two increments, one would expect peaks to occur at higher pH for ab titrations and at lower pH for ba titrations. However, this behaviour was not observed. Peaks at low pH were higher for the ba titrations and peaks at high pH were larger for ab titrations. This could be explained by irreversible reactions of the sample. If irreversible reactions occur at low pH, they would have occurred before the ab titration, because the pH of the dispersion was pH = 3 prior to the experiment. In the ba experiment this leads to a higher consumption of acid at low pH.

Saieus evaluation of the titration data

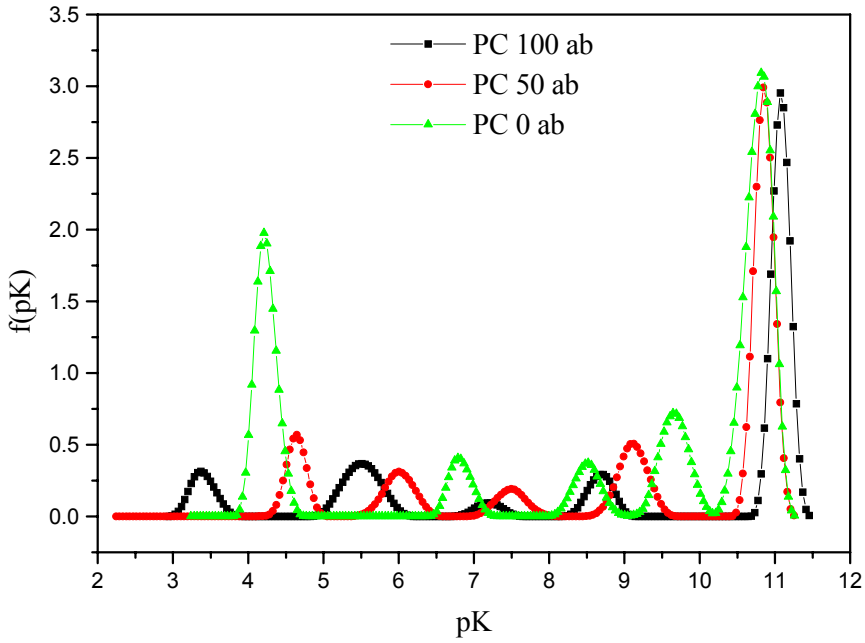

Fig. 4.9 : SAIEUS evaluation of ab titration of pillared clays.

Saieus evaluation was also performed on the titration data of the pillared clay samples. In fact it was the spectra-like appearance of the Saieus results (Fig. 4.9 and 4.10) with a dominant baseline and very sharp peaks led to the development of our evaluation method. Saieus is the more sophisticated method, but more dependent on theory. Saieus evaluation requires the input of fitting parameters which influence the result. Therefore, the results can be ”tuned” in a certain range. Comparing the results obtained by the Saieus software one finds additional peaks which in some cases can be distinguished as shoulders or inflection points in the $\Delta V/\Delta pH$ plot, so that the Saieus plot seems to be the deconvoluted result of the $\Delta V/\Delta pH$

plot. The strongest acidic site of the PC 50 ab experiment is located at an incorrectly high pH when evaluated with the Saieus software.

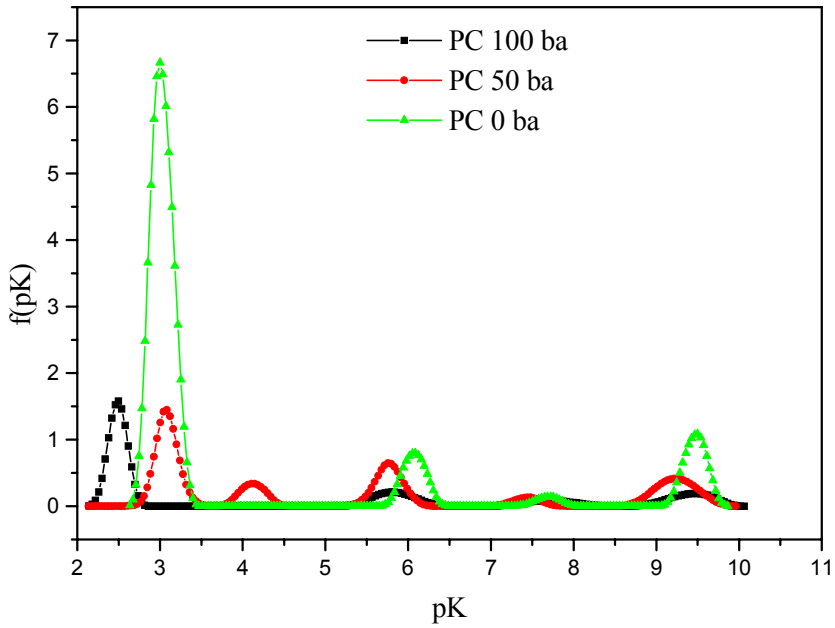

Fig. 4.10 : SAIEUS evaluation of ba titration of pillared clays.

Tab. 4.1 : Results of $\Delta V/\Delta pH$ plot and SAIEUS (in parenthesis) evaluation of PC titration data.

	pKa ab	peak area ml g^{-1}	integration limits	pKa ba	peak area ml g^{-1}	integration limits
PC 100	<3.2 (3.4)	*	*	<2.6 (2.5)	*	*
	5.5 (5.5)	2.31	4.4 / 6.7	3.8 (5.8)	1.83	3.5 / 5.4
	(7.2)			(7.7)		
	9.4 (8.7)	1.47	7.9 / 9.9	(9.5)		
	>11.2 (11.1)	*	*			
PC 50	3.5 (4.6)	2.74	3.2 / 4.4	<2.6 (3.1)	*	*
	5.4 (6)	2.43	4.5 / 6.7	3.9 (4.1)	2.85	3.5 / 4.8
	7.2 (7.5)	6.58	6.8 / 7.5	5.7 (5.8)	2.95	4.9 / 7.5
	10.1 (9.1)	*	*	(7.4)		
	>11.1 (10.8)	*	*	9.1 (9.3)	1.85	7.6 / 9.7
PC 0	4.3 (4.2)	5.50	3.5 / 5.2	3 (3)	14.81	2.9 / 4.8
	6.1 (6.8)	1.94	5.3 / 7.2	5.6 (6.1)	3.48	4.9 / 7.6
	(8.5)			(7.7)		
	(9.6)			9.4 (9.5)	2.33	7.7 / 9.6
	10.7 (10.8)	12.24	7.3 / 11.1			

Tab. 4.2 : Data of the pillared clay dispersions used for potentiometric titration.

	initial pH of the dispersion	solid content of the dispersion (determined at 120°C)
PC 100	2.8	0.0095 g/ml
PC 50	3.9	0.0098 g/ml
PC 0	4.9	0.0086 g/ml

Conclusions

Peaks at high pH are assigned to dissociation of silanols and basic attack of Si-O-Si bonds. The central peaks at pH 5-6 are assigned to dissociation of hydrated aluminium ions at the edges or aluminium ions released from the octahedral layer and/or the Al-pillars. A peak at pH 4.3 in the PC 0 ab experiment and a shoulder at pH ≈ 4 in the corresponding ba experiment are probably due to the Al_{13} polyhydroxy cation. With increasing iron content the strongest acidic site is shifted to lower pH values. At low pH protons are consumed upon exchange of interlayer cations and dissociation of hydrated $[Fe(OH)_6]^{3+}$. A more detailed discussion is given in Chap. 4.6.

4.6 Potentiometric titration of bentonites and illite

A number of experiments was performed to characterise different samples and in order to find the optimum parameters for the experimental study.

Variation of solid content

Different volumes of a stock dispersion of $M48_{TL}$ containing 17.6 g bentonite per litre were used for ab-titrations (Fig. 4.11). Volumes of 10, 20 and 40 ml of this dispersion corresponding to 176, 352 or 704 mg of dry bentonite were diluted to 40 ml with distilled water.

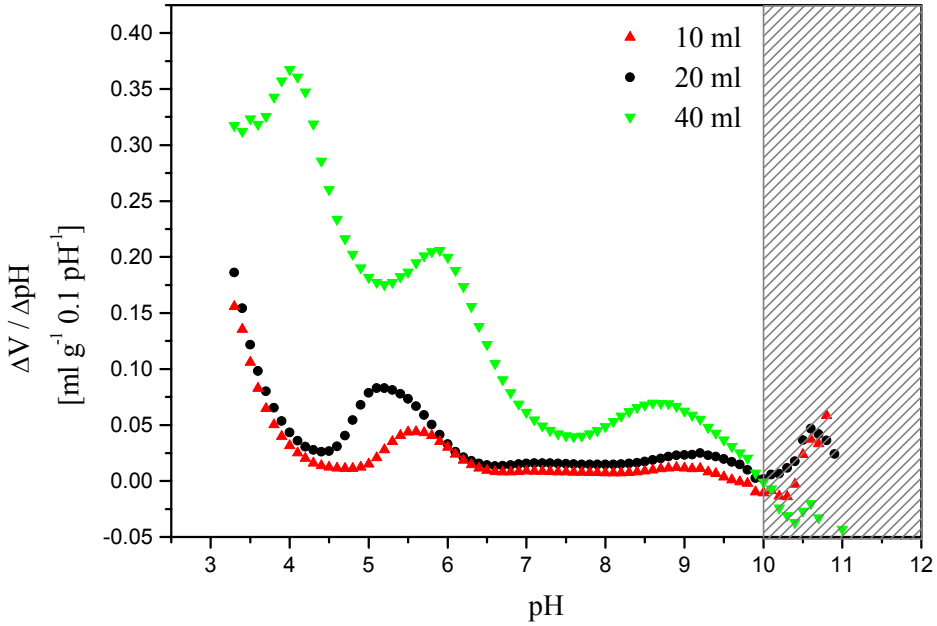

Fig. 4.11 : ab titration of $M48_{TL}$ - variation of solid content.

Though the graphs were normalised on the weight of bentonite, the peak area increased with the solid content of the dispersion. The peaks were more pronounced in the more concentrated sample. The pK_a are <3.3, 5.6 and 8.9 for the 10 ml sample, <3.3, 5.1 and 9.2 for the 20 ml sample and 4, 5.9 and 8.6 for the 40 ml sample. This experiment shows that by increasing the solid content qualitative and quantitative results are changed. However, the error was within $\pm$ 0.4 pH for the pK_a values. The change in position and height of the peaks may be due to the slower relative titration speed. Though the increments are added after the same time, the change in pH is slower since more protons have to be exchanged with increasing solid content.

Purified (< 2 µm) and raw Wyoming bentonite

The peaks for the purified sample were higher than for the raw clay (Fig. 4.12). Ab titration and ba titration of the raw material did not yield identical results but the patterns of the titration curves were similar. The pK_a are < 3.3, 5.2 and > 9.5 for the purified sample (ab), < 3.2, 4.6 and 8.9 for the raw (ab) and 3.6, 6.1 and 9.1 for the raw (ba) bentonite. The area at pH > 9.5 is shadowed since significant scatter occurs. The purification process enriches the montmorillonite content so that a larger amount of protons is adsorbed or desorbed.

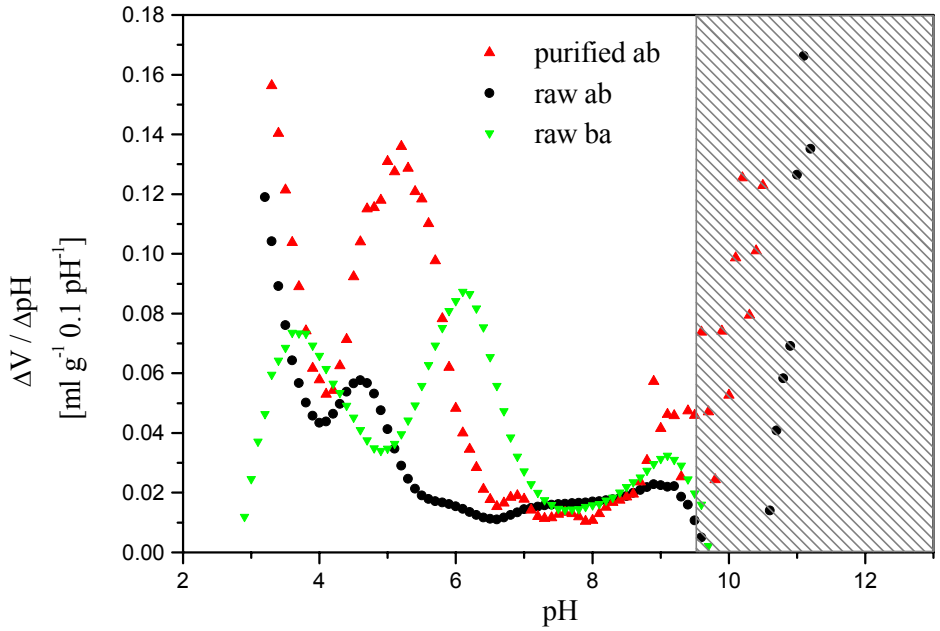

Fig. 4.12 : Titration of purified and raw Wyoming bentonite.

Titration speed and direction

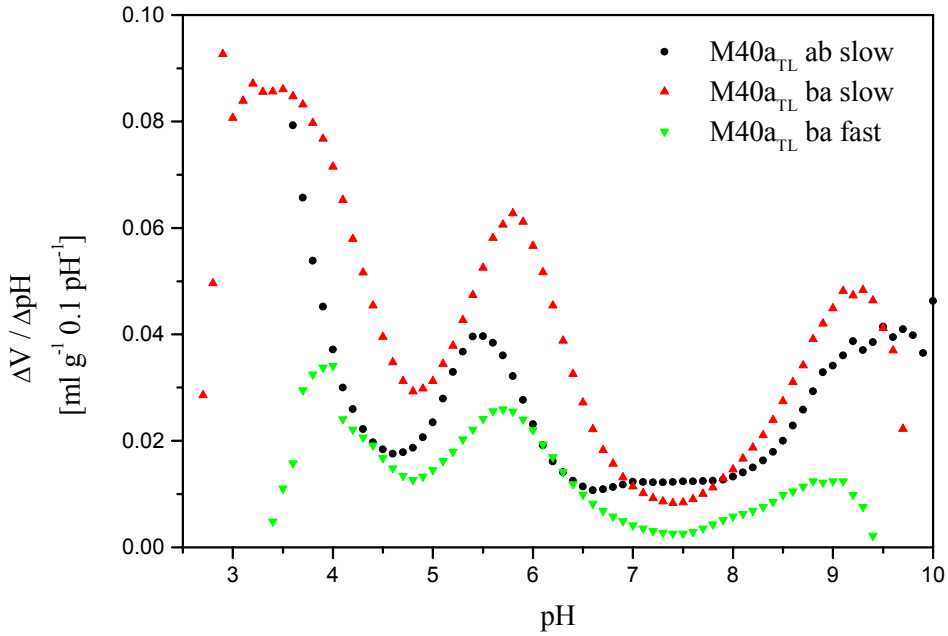

Fig. 4.13 : Titration of M40a$_{TL}$ – variation of titration speed and direction.

A dispersion of purified wyoming montmorillonite M40a$_{TL}$ was titrated in ab direction and in ba direction at 0.01 ml / 90 s and at 002 ml / 90 s. The patterns of the curves (Fig. 4.13) were similar, despite some small differences in peak position. However, the peak areas for the three experiments were quite different. In the slow ba titration experiment the largest amount of

protons was adsorbed. In the fast titration less protons were adsorbed, possibly due to an insufficient equilibrium time.

Titration of illite HS7$_{TL}$

To check the diagnostic value of potentiometric titration, an illite sample was also analysed. Ab and ba titration (Fig. 4.14) are in good agreement concerning the peak's positions but ab titration released much more protons than were adsorbed in ba titration. The pK_a are < 4.3, 6.4 and ≈ 10.1 for ab titration and 3.9, ≈ 5.4 and 9 for ba titration.

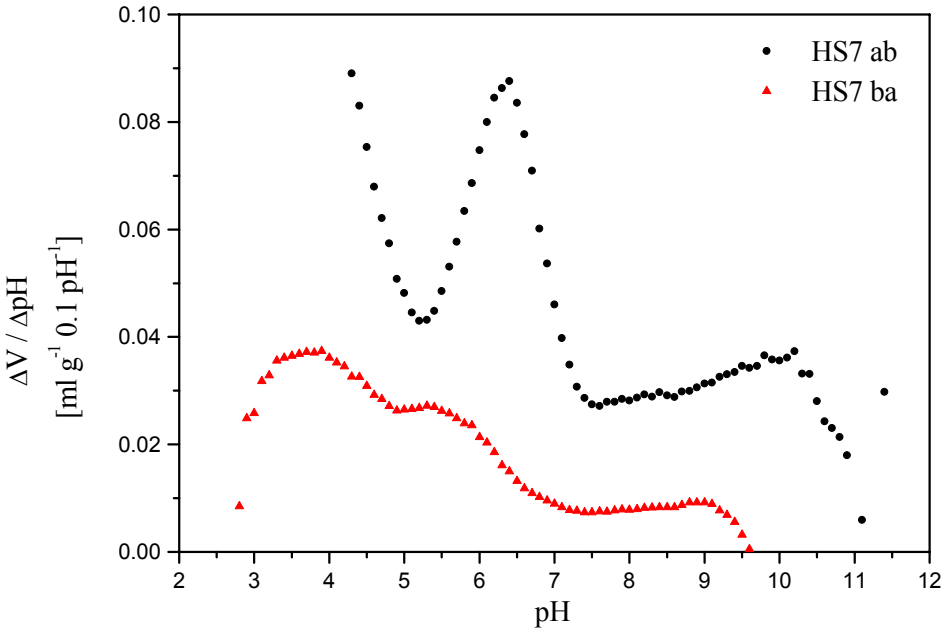

Fig. 4.14 : Titration of illite HS7$_{TL}$.

Reduced charge montmorillonites

Two samples of the reduced charge montmorillonites (Chap. 2.1) were also investigated by titration: a 100% Na-exchanged (HK100) and 100% Li-exchanged (HK0) sample, both calcined at 260°C. Both curves (Fig. 4.15) matched well at pH > 5. Below pH = 5 many more protons were adsorbed by the HK100 sample with the high layer charge. One may conclude that the aluminol groups at the edges of the clay mineral particle are not affected by the charge reduction, so that both samples show the same acidity at $pK_a \geq 5$. Thus, the titration experiment also reveals that the Li^+ cations of the heated montmorillonite are difficult to exchange even by protons.

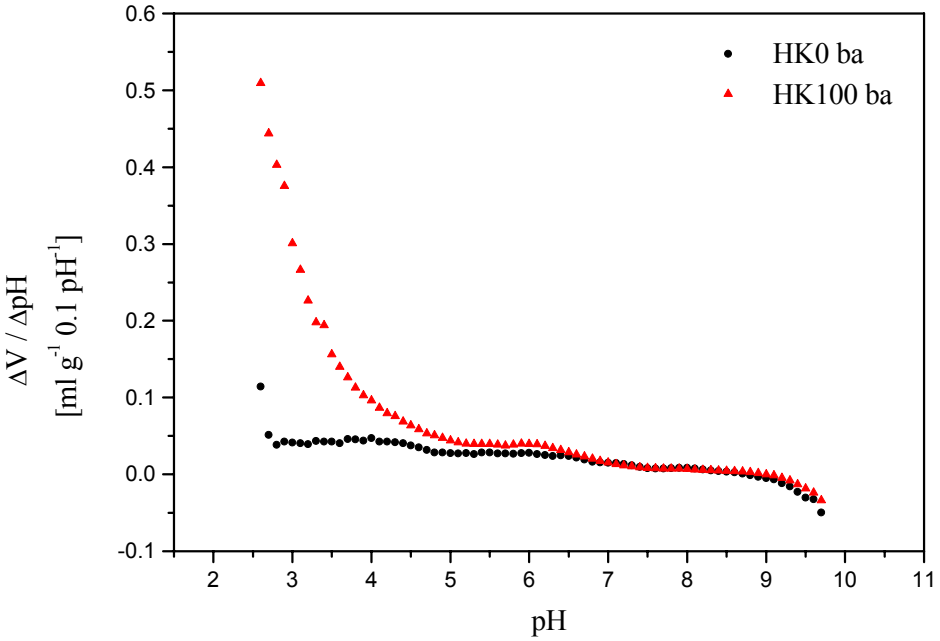

Fig. 4.15 : Titration of reduced charge montmorillonites HK0 and HK100.

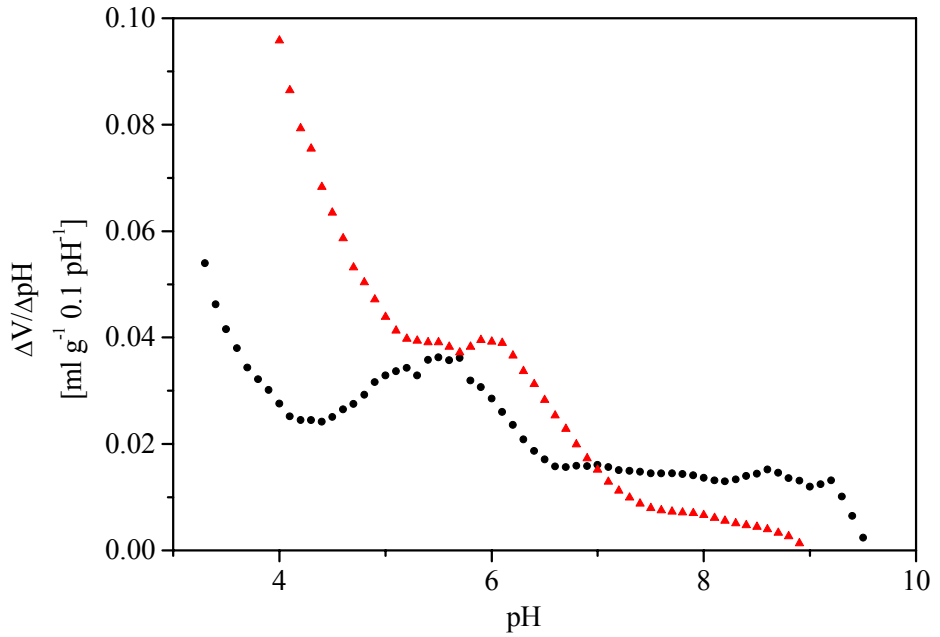

Fig. 4.15b : Enlargement of Fig. 4.15. Titration of reduced charge montmorillonites.

Conclusions

The $\Delta V / \Delta pH$ plots permit qualitative and quantitative evaluation of titration data but application to clay dispersions is risky. The derived pK_a values and amounts of different acidic sites depend on the experimental conditions. Changing the solid content or the titration speed leads to varied results. Performing acidic to basic (ab) and basic to acidic (ba) titration also does not produce identical results. At pH > 10 the data suffer from extended scattering.

In some cases even negative values of $\Delta V / \Delta pH$ are calculated at very high and very low pH indicating that the blank sample adsorbs or releases more protons than the clay sample which has no physical sense. One possible reason for this error is the use of too dilute solutions. Up to 10 ml of the solutions had to be added to 50 ml dispersion to attain pH 2 or 11. If the change in pH is too small compared to the volumes added, the data will be of bad quality. If this is the reason the problem could be solved by using more concentrated solutions. Unfortunately, the titrator Mettler Toledo DL 25 could not perform sufficiently slow titrations. Since the slowest possible titration speed was used, increasing the concentration of the solutions would result in a faster change of pH. However, potentiometric titration of clay minerals requires long time to reach equilibrium, especially at very low and very high pH. The titrations were carried out by adding 0.01 ml increments of acid or base every 90 s.

Even at this titration speed pH equilibrium was not attained before adding the next increment. At low pH metal ions from the octahedral layer are leached by protons, this effect is called autotransformation (Komadel et al., 1997, Janek et al., 1997, Janek and Komadel, 1999, Janek and Lagaly, 2001). As a result, a silica network remains, which is known as bleaching earth. The autotransformation is usually carried out by heating the clay mineral and an appropriate amount of acid to a temperature below 100°C for a few hours (Lagaly, 1993, Srasra et al., 1989). However, this reaction occurs even at room temperature and is likely the reason why equilibrium is attained slowly at low pH. Another reason can be the dissolution of calcite, if it is present in raw clay samples. At high pH a basic attack on Si-O-Si bonds is probably the reason why the equilibrium is attained slowly.

Komadel et al. (1997) and Janek and Lagaly (2001) investigated freshly prepared proton saturated and autotransformed samples by potentiometric titration and evaluation with the Saieus software. The authors assigned peaks at pH 3, 5.5 and 8.3 to $[Fe(H_2O)_6]^{3+}$, $[Al(H_2O)_6]^{3+}$ in solution or attached to clay mineral particles and $[Al(OH)_4]^-$, respectively, assuming that the cations were released from the octahedral layer due to autotransformation. The weakest acidic site at pH 11.3 was assigned to deprotonation of silanols on the edges of the clay mineral lamellae and to basic attack of Si-O-Si bonds. Janek and Lagaly (2001) observed that the strongest acidic site of proton saturated samples at pH 2.8 disappeared after autotransformation. The authors assigned this peak to protons exchanged for the exchangeable interlayer cations. Upon autotransformation these protons migrate into the octahedral layer and replace the structural cations. Therefore, after autotransformation these protons cannot be detected, but the released cations are observed. However, a ferruginous

smectite revealed a peak at pH 2.8 after autotransformation which was assigned to the $[Fe(H_2O)_6]^{3+}$, which are distinctly more acidic than the hydrated aluminium ions. The experiments of Komadel et al. and Janek and Lagaly show that the process of autotransformation is not finished on freshly prepared proton saturated bentonites, thus the octahedral cations can not be completely leached during a titration experiment and the aluminols on the edges should be considered.

Multibatch titration experiments

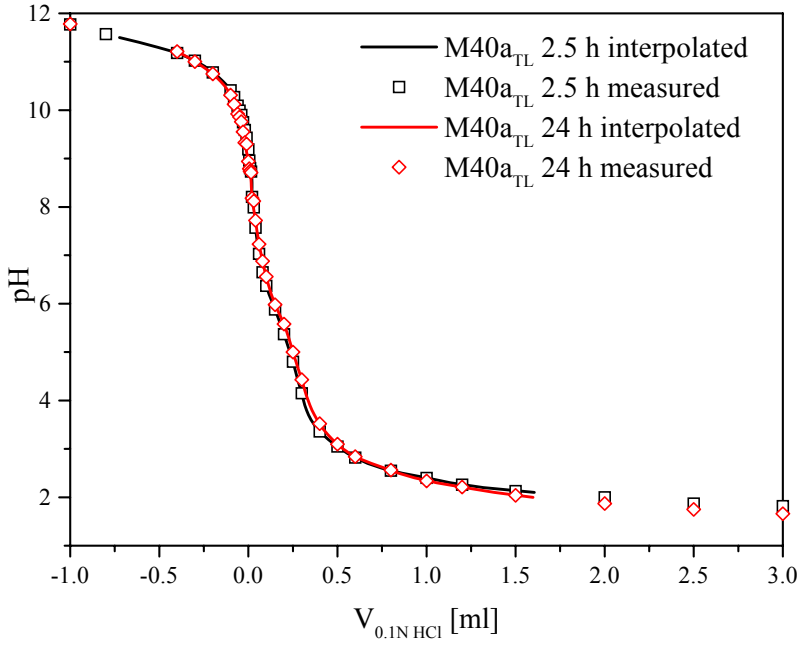

Fig. 4.16 : Multibatch titration experiment: pH of M40a$_{TL}$ dispersion after 2.5 and 24 h.

Two clay samples, M40a$_{TL}$ and M48$_{TL}$ were investigated with the multibatch titration technique. The pH of M40a$_{TL}$ samples was measured after 2.5 and 24 hours (Fig. 4.16). The titration curves are very similar, only slight changes are observed after 24 hours. At pH > 9 the pH decreases after 24 hours, at pH < 7 it increases. At pH 5 – 6 a shoulder indicates adsorption of protons. This shoulder is also found in the $\Delta V / \Delta pH$ plot as a peak (Fig. 4.17).

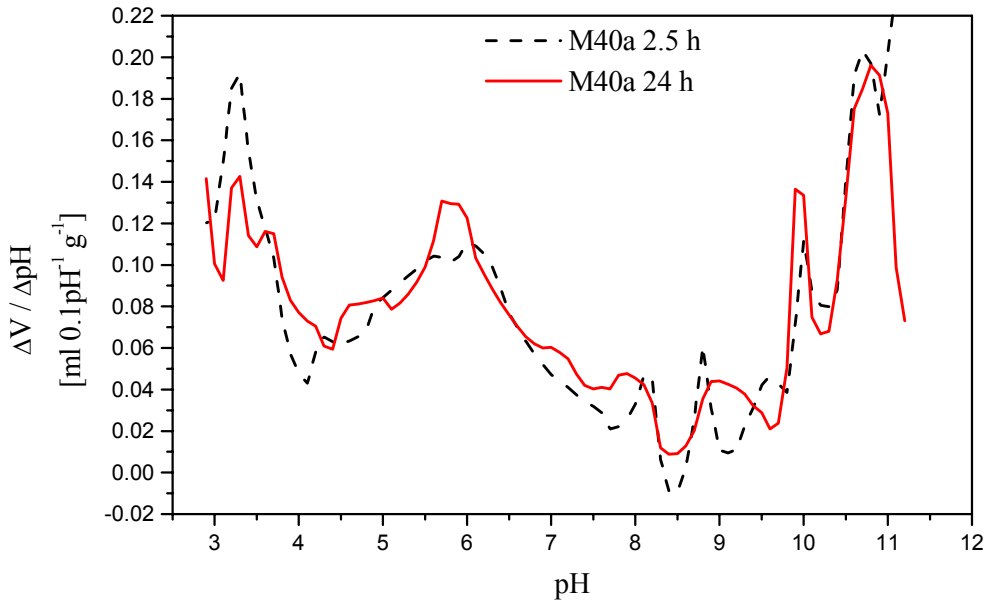

Fig. 4.17 : ΔV / ΔpH plot of the M40a$_{TL}$ multibatch titration experiment. Evaluation 2.5 and 24 hours after addition of acid and base.

The ΔV / ΔpH plots are similar for reaction times of 2.5 and 24 hours, indicating that the dissociation state of the sample does not change between the two measurements. As in the single batch titration experiments, a strong acidic site at pH 3.2 (3.3), a central peak at pH 5.5 – 6 (5.8) and a very weak acidic site at pH 10.7 (10.7) are observed (pH values after 24 hours in parenthesis). It is difficult to determine whether the other smaller peaks refer to acidic sites of the sample or if they are simply experimental errors. Regardless, the experiment reveals that adsorption of protons and hydroxyls does not change between 2.5 and 24 hours.

The M48$_{TL}$ sample was investigated immediately[5] after adding acid or base and after 24 hours (Fig. 4.18). The differences between the two curves are more pronounced. The adsorption of protons does not seem to occur completely within 2 minutes. More information can be taken from the ΔV / ΔpH plot (Fig. 4.19 and 4.19b). The ΔV / ΔpH plots for reaction times of 2 minutes and 24 hours are similar at pH < 4 and pH > 8. A strong acidic site at pH 3.2 (3.2-3.3) with a shoulder at pH 3.7 (3.6) is observed, two weak acidic sites at pH 10.6 (10.6) and pH 11.5 (11.5) (values after 24 hours in parenthesis). The central peak is shifted from pH 5.3 after 2 minutes to a sharper peak at pH 6.5 after 24 h. Comparing the two plots reveals that the protonation/deprotonation reactions at low and high pH occur immediately, but not for the acidic site at pH 5.3 – 6.5. The protonation kinetics of this site

[5] At high pH the electrode required approximately two minutes to obtain a ”stable” pH reading, therefore all data were measured two minutes after the addition of the solutions.

depends on the proton concentration: at pH 6.5 it takes more than a few minutes to adsorb protons.

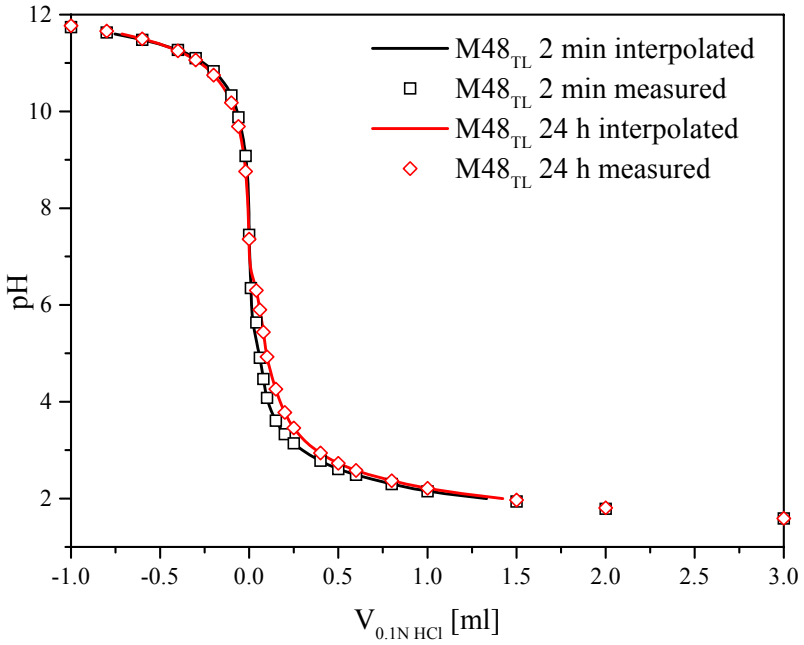

Fig. 4.18 : Multibatch titration experiment: pH of $M48_{TL}$ dispersion after 2 minutes and 24 h.

At a ten times higher proton concentration, protonation occurs immediately. The same effect was observed in the single batch experiment with different amounts of $M48_{TL}$ (Fig. 4.11). At the highest solid content the central peak shifted to a higher pH, probably because the change of pH per time was the smallest.

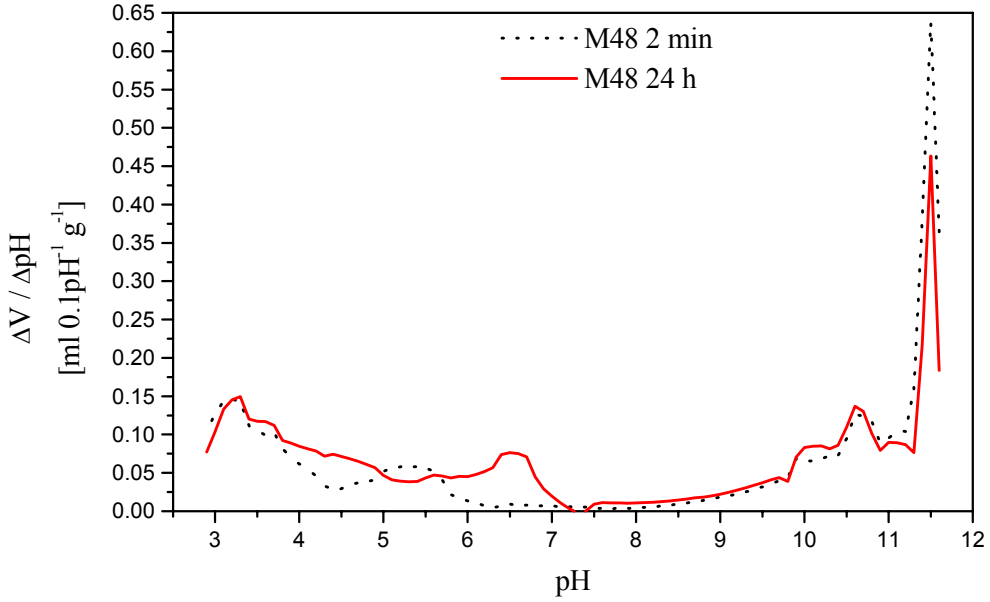

Fig. 4.19 : $\Delta V / \Delta pH$ plot of the $M48_{TL}$ multibatch titration experiment. Evaluation 2.5 minutes and 24 hours after addition of acid and base.

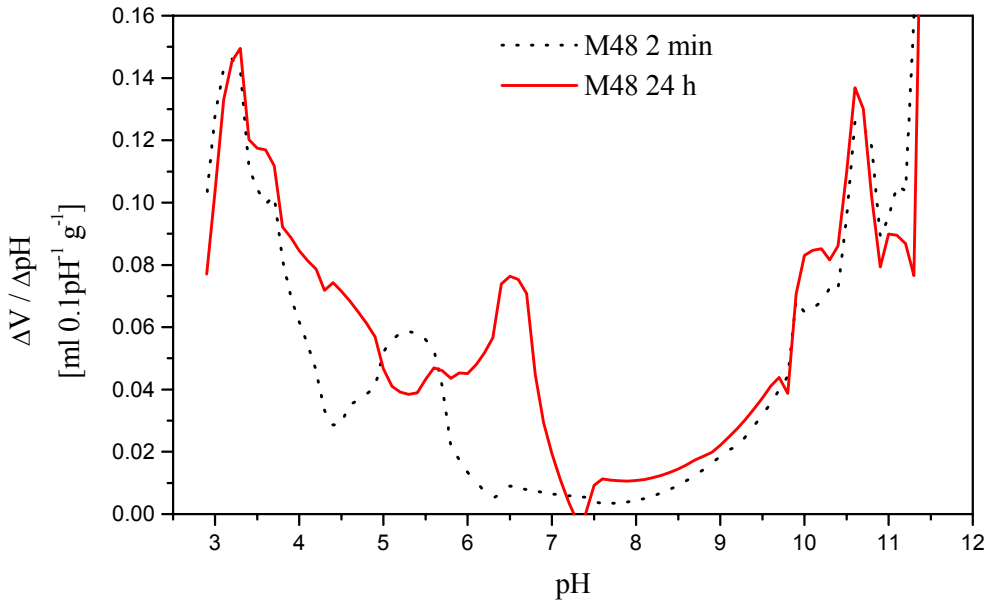

Fig. 4.19b : Enlargement of Fig. 4.19. Δ V / Δ pH plot of the $M48_{TL}$ multibatch titration experiment.

Comparing the results for $M40a_{TL}$ and $M48_{TL}$ (Fig. 4.20) shows very similar acid-base properties for pH < 4 and pH > 10. The central peak which is assigned to dissociation of aluminols is located at pH 5.8 for the $M40a_{TL}$ and pH 6.5 for the $M48_{TL}$ sample.

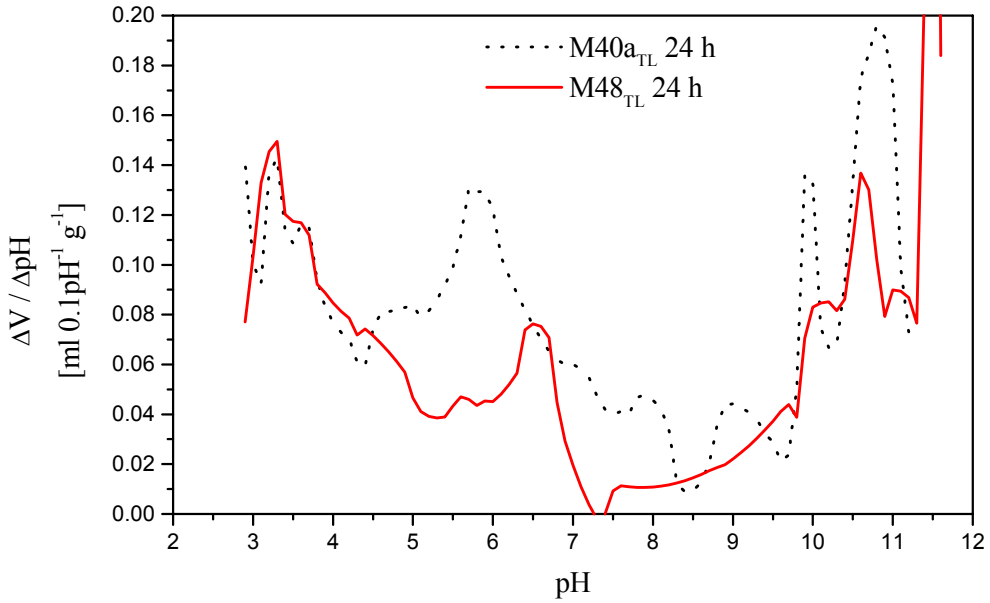

Fig. 4.20 : Δ V / Δ pH plot of $M40a_{TL}$ and $M48_{TL}$ after 24 hours.

Conclusions

The multibatch titration experiments offer several advantages compared to the single batch experiment. Every sample can be measured several times at any time after addition of the solutions. A proton and hydroxide adsorption isotherm can be recorded at a fixed volume combining solutions of different concentrations. The sample volume is not diluted to high volumes to attain very high or low pH values. This increases the accuracy of the experiment, e.g. smoothing was not necessary. On the other hand it is difficult to determine whether the number of smaller peaks is due to a higher resolution or to errors from the restricted number of data points.

For the $M40a_{TL}$ sample pH equilibrium seems to be attained after 2.5 h. Measuring after 24 h did not yield different results. Measuring the $M48_{TL}$ sample after two minutes and after 24 h reveals that only the acidic site 5.3 – 6.5 is not equilibrated after two minutes. Thus, the main source of error in the single batch titration experiment is probably the large amount of acid or base required to attain the extreme pH values and not the equilibration time. Though the equilibration time in the single batch experiment was even less than two minutes, one has to consider that the total amount of acid or base is added in successive steps and not in one time as in the multibatch experiment.

5.1 Cation exchange capacity - general

The cation exchange capacity (cec) is one of the basic properties of clay minerals. It has two origins. One origin is isomorphic substitution in the tetrahedral- and/or octahedral sheet of the clay mineral layer. Substitution of aluminium by magnesium or of silicon by aluminium leads to a negative net charge. This part of the cec is considered to be constant since it is almost not sensitive to the pH of the system. The second origin is dissociation of aluminol groups on the edges. Since the acidity of these groups is weak, the edge charges are pH dependent and the cec depends on the pH. At pH 7 about 20% of the cec of smectites is located at the edges (Lagaly, 1981). Several methods to determine the cec have been developed. In the early days of clay science determination of the cec was performed by saturating the clay with one cation, then washing out excess salt and finally replacing the cation by several exchange/washing cycles with another cation (Mehlich, 1948). The collected solutions were employed for the determination of the amount of the replaced cation. Another method was developed by saturating the clay with NH_4-ions (Hofmann and Giese, 1939). The amount of ammonium ions adsorbed was determined by Kjeldahl distillation (Chap. 5.2). Further methods were proposed by using cationic surfactants (Kloppenburg, 1997, Janek and Lagaly, 2003). The general problem when using surfactants is that an excess will adsorb on the clay, requiring determination of the point when the equivalent amount is adsorbed. One method using cetylpyridinium ions (Kloppenburg, 1997) is discussed in Chap. 5.3. Finally, metal-organic complexes are employed as exchange cations. The affinity of the clay minerals towards this type of cation is high, so that complete exchange can be achieved in one single treatment step (Pleysier and Cremers, 1975). An excess of the complex is added to the clay dispersion and one has only to determine the remaining concentration after the exchange reaction. Cobalthexamine (Morel, 1958, Mantin and Glaeser, 1960, Orsini and Remy, 1976), silver-thiourea (Chhabra et al., 1975, Dohrmann, 1997), copper bisethylenediamine (Bergaya and Vayer, 1997) or copper triethylenetetramine (Meier and Kahr, 1999) can be used for this purpose. The methods using copper complexes are described in Chap. 5.4 and 5.5. Finally, two modified procedures are proposed (Chap. 5.6 and 5.10).

5.2 Determination of the cec with ammonium acetate

Although the determination of the cec with metal-organic complexes is fast and precise, the ammonium acetate method is still important. It is often used to verify other methods, despite being very time-consuming. The samples must be prepared, distilled and finally titrated. Many steps are involved, and errors may easily occur. In this work, the method was carried out as described by Dohrmann (1997). The sample is first ammonium exchanged, then the ammonium ions in the supernatant are deprotonated into ammonia with sodium hydroxide solution and determined by distillation into a known amount of acid and which is back-titrated (Kjeldahl-method).

Ammonium exchange

Tab. 5.1 : Preliminary experiments

Washing	cec meq/g
2x water	1.01
2x water, 1x ethanol	0.94
2x water, 2x ethanol	0.93
2x water, 3x ethanol	0.93
3x ethanol	0.97
4x ethanol	0.96

231 g (3 moles) of ammonium acetate were dissolved in water to give one litre solution. The pH was adjusted to seven if needed. Approximately 0.5 g of clay (1 g if the cec is too low) were weighed in centrifugal tubes and shaken overnight with 50 ml of ammonium acetate solution. The sample was centrifuged, the supernatant discarded.

At this point a modification of the method was inserted. The sample was dispersed in distilled water, shaken over night and centrifuged. This step was included to enable better accessibility of the interlayer surface. Since the ion exchange is carried out at high ionic strength the clay is completely flocculated. By decreasing the ionic strength the dispersion of the clay is improved and the clay particle surfaces are made more easily accessible.

Two more exchange/washing cycles were performed with 40 ml ammonium acetate solution to ensure complete exchange of cations by ammonium ions. The excess of

ammonium ions in the sediment was removed by dispersing the sample in distilled water and shaking it overnight. Again the sample was centrifuged and the supernatant discarded. This step could be repeated only once since at decreasing salt concentration the dispersed particles no longer settled. Preliminary experiments with $M48_{TL}$ (Tab. 5.1) showed that at this point the salt excess was not yet completely removed. So the samples were washed four times in the same manner, substituting ethanol for water. The samples were dried at 65°C to remove any remaining ethanol.

Determination of the ammonium content by Kjeldahl distillation

The sample was dispersed in 25 ml of water and then filled into the bulb of a Kjeldahl-apparatus. The centrifugal tube was rinsed three more times with water to ensure that the sample was completely transferred. 10 ml of 0.1 N HNO_3 were placed in the Erlenmeyer flask, the dispersion was heated and 50 ml of 20% w/w sodium hydroxide solution were added to replace the ammonium. The distillation was run for 20 minutes. Before stopping, the distillate was checked for acidic reaction. The nitric acid was then back-titrated with 0.1 N sodium hydroxide solution with an automatic titrator (Mettler Toledo DL25). The data were collected with a computer. The maximum of the first derivative was employed to determine the endpoint.

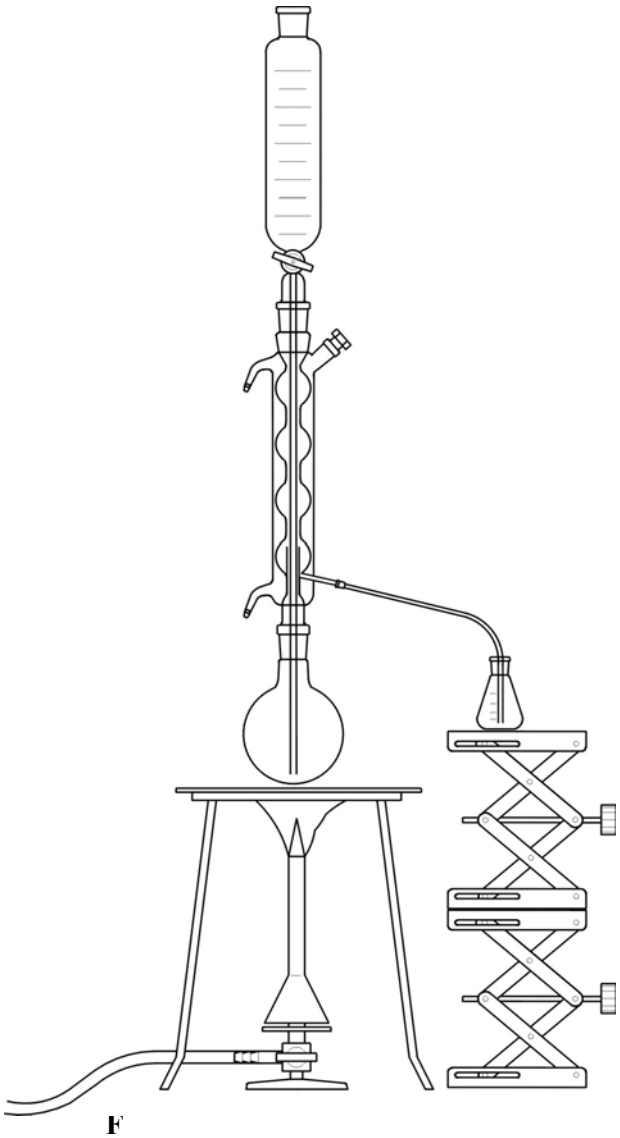

Fig. 5.1 : Kjeldahl distillation.

Determination of ammonium content by CHNS-analysis

A second way to determine the amount of exchanged ammonium ions was tried since the Kjeldahl procedure is very time consuming and errors can be made easily. A set of samples was prepared (ammonium exchanged, excess removed) as described before. The ammonium exchanged samples and the original samples were dried at 120°C, and the nitrogen content was determined in a HEKAtech CHNS Analysator by combustion. Two parallel determinations were performed. The results of the CHNS analyses are given as percent nitrogen. These values refer to the weight of the exchanged clay, while other methods refer to the weight of the clay with its original cations. The cec was calculated as if the clay had been calcium saturated taking into account the nitrogen content of the original clay sample. For interlayer cations other than Ca^{2+} this leads to a small error in the cec. Assuming a cec of 1 meq / g the error for Na^+, NH_4^+, and Mg^{2+} is less than 1%, for K^+ less than 2%. This error can be neglected compared to analytical errors.

Calculation of the cec

ω_N = % w/w nitrogen content of the exchanged sample

$\omega_{N_{blank}}$ = % w/w nitrogen content of the original sample

$\omega_{NH_4^+}$ = % w/w ammonium content of the exchanged sample

cec^* = cation exchange capacity without taking into account the mass of the interlayer cations [meq/g]

$cec_{Ca^{2+}}$ = cation exchange capacity under the assumption that the clay mineral is calcium exchanged [meq/g]

$\omega_{NH_4^+}$ is calculated by subtracting $\omega_{N_{blank}}$ from ω_N , then dividing the result by the molar weight of nitrogen and multiplying with the molar weight of ammonium (eq. 1).

$$\text{eq. 1 :} \qquad \omega_{NH_4^+} = \frac{18}{14} * (\omega_N - \omega_{N_{blank}})$$

The cec^* can be calculated by eq. 2. The factor $\frac{\omega_N - \omega_{N_{blank}}}{14}$ gives the number of charges, the factor $\frac{1}{100 - \omega_{NH_4^+}}$ "eliminates" the weight of the ammonium ions. The factor 10 is required to obtain the dimension of the cec, [meq/g].

$$\text{eq. 2 :} \qquad cec^* = 10 * \frac{\omega_N - \omega_{N_{blank}}}{14} * \frac{1}{100 - \omega_{NH_4^+}}$$

Finally, assuming that the sample is calcium exchanged, the weight of the interlayer cations has to be taken into account (eq. 3). The "additional" weight of the calcium ions is the cec^* multiplied by the equivalent weight of calcium. The equivalent weight of calcium is 0.02 g/meq.

$$\text{eq. 3 :} \qquad cec_{Ca^{2+}} = \frac{cec^*}{1 + cec^* * 0.02 g/meq}$$

The results (Tab. 5.2) of the CHNS analyses were plotted vs. the results obtained with the Kjeldahl method (Fig. 5.2). For the latter the loss on drying at 120°C was taken into account. The two methods are in rather good accordance. However, the cec of the montmorillonites M40a, M47 and M48 (Nr. 1, 2 and 3) were somewhat too low when determined with CHNS analyses. The cec of hectorite H3 (15) was overestimated.

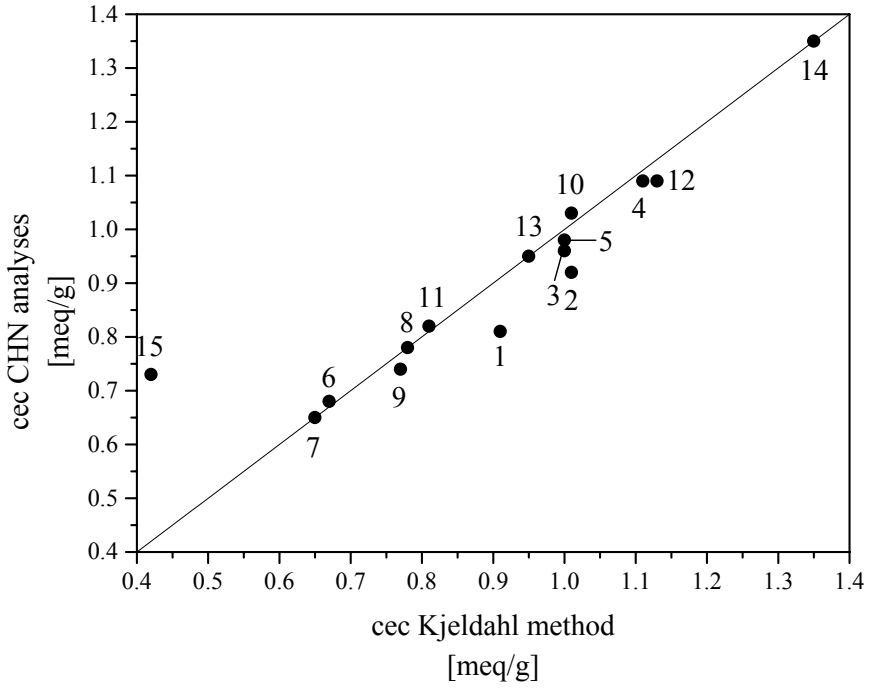

Fig. 5.2 : Ammonium acetate method - comparison of Kjeldahl method and CHNS analyses.

Tab. 5.2 : Ammonium acetate method. Results of the determinations with Kjeldahl method and CHNS analyses.

	sample	Kjeldahl	CHNS
1	M40a	0.91	0.81
2	M47	1.01	0.92
3	M48	1.00	0.96
4	M50	1.11	1.09
5	Polkville	1.00	0.98
6	oxidizable	0.67	0.68
7	Cameron	0.65	0.65
8	Cream	0.78	0.78
9	Upton	0.77	0.74
10	Otay	1.01	1.03
11	M42	0.81	0.82
12	Kunipia	1.13	1.09
13	de Maio	0.95	0.95
14	Bei	1.35	1.35
15	H3	0.42	0.73

5.3 Determination of the cec by adsorption of cetylpyridinium chloride

Clay dispersions can be flocculated with cationic surfactants. The surfactant adsorbs on the clay mineral's surface and neutralises the negative charges, the colloidal stability decreases and the clay mineral coagulates. If the amount of surfactant exceeds the cec, a net positive charge restabilises the clay dispersion. If the amount of surfactant equals the cec, fast flocculation occurs, and a voluminous sediment is created. With increasing concentration of the surfactant, the volume of the sediment increases to give a maximum at the cec (Fig. 5.3). If the cec is exceeded, the volume becomes again more dense. Kloppenburg (1997) used these changes to determine the cec of clays. He proposed two linear fits of the last data before and after the maximum. The point of interception of the extrapolated lines gives an even more precise value of the cec.

The advantage of this method is that it can be carried out with simple materials. The preparation of the samples is easy and fast to carry out.

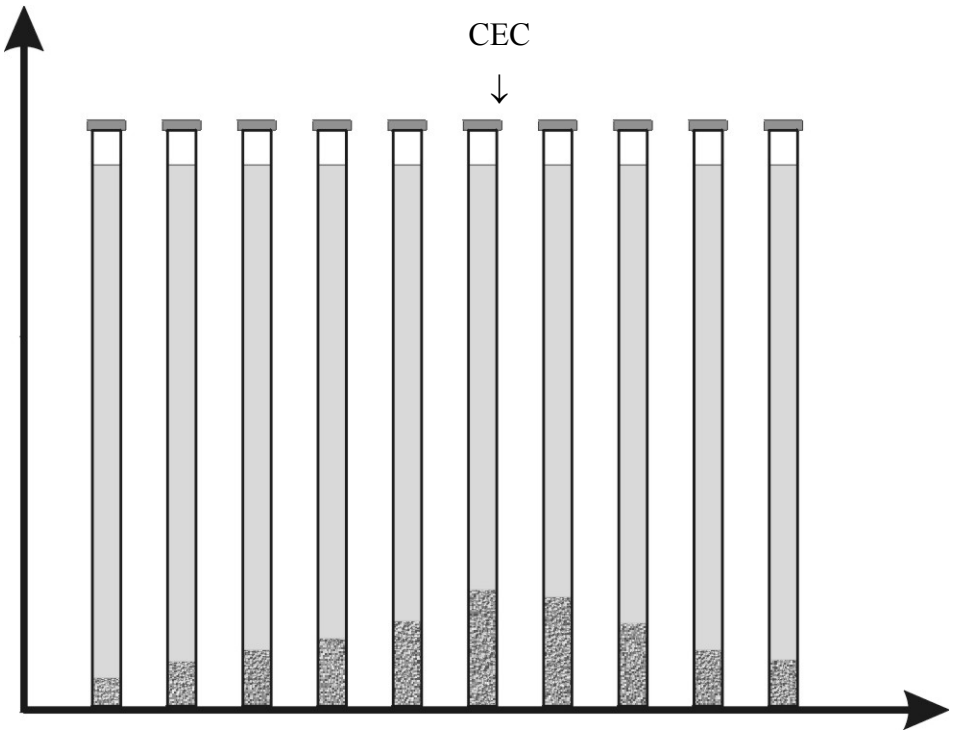

Fig. 5.3 : Determination of cec with cetyl pyridinium chloride. Increasing concentration from left to right.

Experimental

Flat-bottomed glass tubes 190 mm in length and 12 mm in diameter were used. 1 ml clay dispersion containing 0.02 g clay/ml in each glass tube was diluted with water and calculated volumes of 0.01 mole/l cetylpyridinium chloride solution to give 10 ml. For the common samples the range of 0 – 1.1 ml cetylpyridinium chloride solution (corresponding to 0 to 0.55 mmole CPC per gram of clay) was sufficient. The glass tubes were carefully turned three times to mix the components and to avoid formation of bubbles. The glass tubes were left in a vertical position for 24 h before the height of the sediment was determined. Since the filling level of the tubes varied somewhat, the height of the sediment was divided by the height of the total dispersion. The relative height was plotted vs. the amount of CPC per gram of clay (Fig. 5.4). The maximum indicates the cec.

The CPC method was applied only to the common clays.

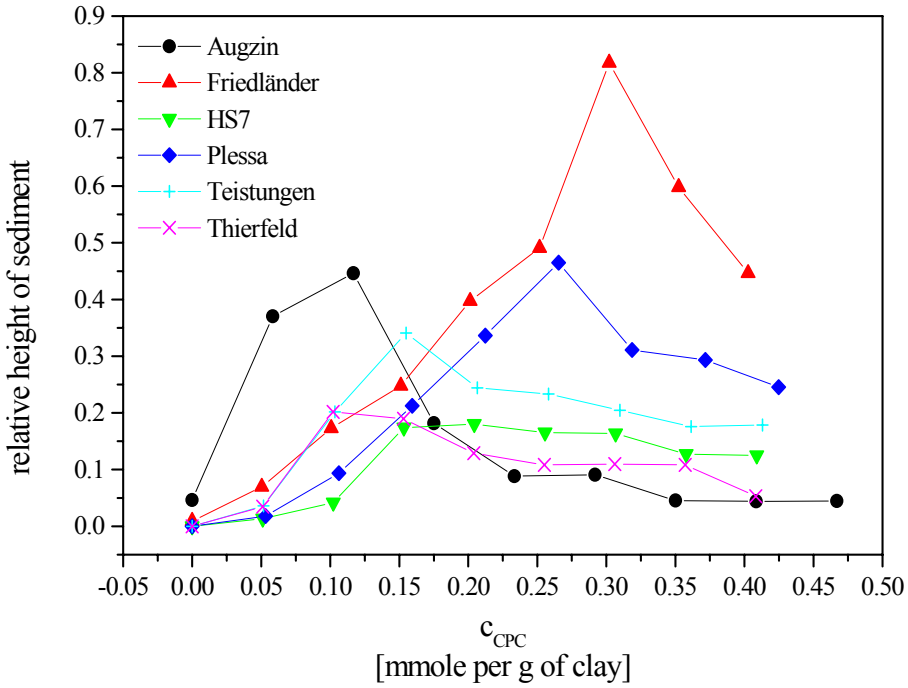

Fig. 5.4 : Relative height of the sediment at different CPC concentrations.

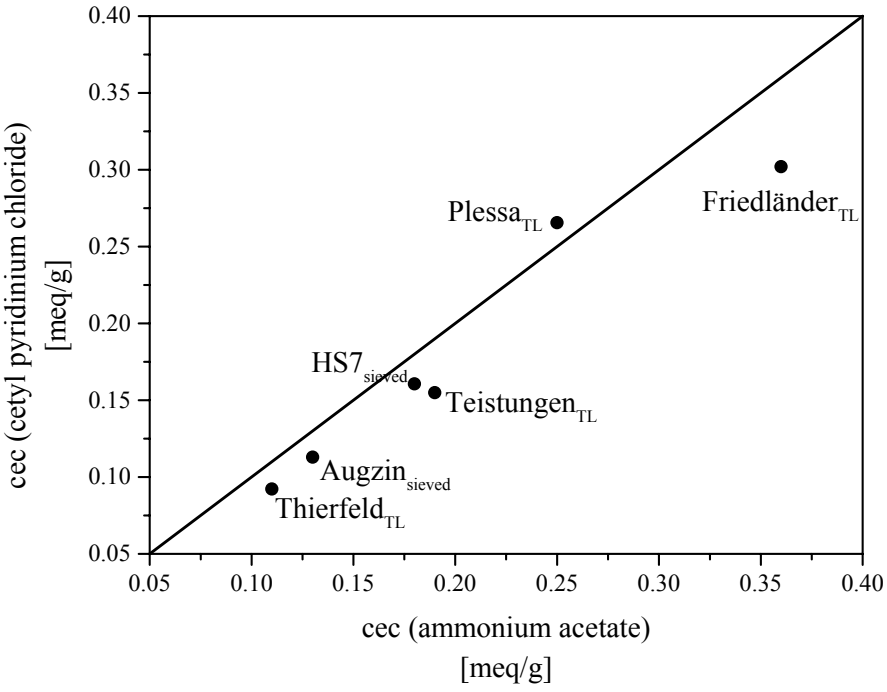

Fig. 5.5 : cec determined with CPC and with ammonium acetate (Kjeldahl method).

The maxima of the relative height of the sediments were in the range of 0.1 to 0.3 mmole/g clay. The Friedländer$_{TL:}$ sample adsorbed the largest amount of CPC and had the highest sediment. The correlation between the results obtained with the ammonium acetate (Kjeldahl)

method and the CPC method (Fig. 5.5) is rather good but the CPC values are too low. However, the CPC method permits a good estimation of the cec.

5.4 Determination of the cec with copper bisethylenediamine

Bergaya and Vayer (1997) proposed the use of copper bisethylenediamine cations to determine the cec. The procedure is described briefly.

$[Cu(EDA)_2]^{2+}$ solution

A 1 molar solution of $CuCl_2$ is prepared by dissolving 26.89 g $CuCl_2$ (0.2 mole) in distilled water to give 0.2 l. If the ethylenediamine requires purification, sodium hydroxide is added to adsorb traces of water. The amine is then distilled. A 1 molar solution of ethylenediamine is prepared by dissolving 30.05 g (33.39 ml, 0.5 mole) ethylenediamine in distilled water to yield 0.5 l. The complex is formed by adding 50 ml of the $CuCl_2$ solution to 102 ml of the ethylenediamine solution. The slight excess of the amine ensures complete formation of the complex. The solution is diluted with water to one litre to give a 0.05 molar $[Cu(en)_2]^{2+}$ solution.

Cation exchange

0.3 to 0.5 g of dry clay are weighed in a centrifugal tube. 2 to 5 ml of the complex solution are diluted with distilled water to 25 ml and added to the clay. The samples were shaken for 30 min and then centrifuged. The concentration of the complex remaining in the supernatant is determined by photometry, atomic absorption spectroscopy or by iodometry.

Comments

- One may doubt whether the sample will disperse well when the complex is added to the dry clay, since the cationic complex flocculates the clay dispersion. Therefore, the experiment was repeated by adding the complex solution to a dispersion which has been shaken overnight. No change in the cec was observed.

- $CuSO_4$ can be substituted for $CuCl_2$ because it can easily be dried at 260°C. The choice of the counter anion does not seem to affect the amount of complex adsorbed.
- Bergaya and Vayer (1997) used atomic absorption spectroscopy and iodometric titration to determine the concentration of the complex remaining in the supernatant. Unfortunately, no details are given how to carry out the titration or a photometric determination. The technique is described in the following paragraphs.

Photometric determination of the complex concentration

Though photometry may be a convenient technique because it is precise and fast to carry out, one has to be aware that mistakes may arise during measurement. Since the extinction coefficient changes at extremely high or low pH the copper bisethylenediamine complex can not be used at all pH values (Chap. 5.6). If the pH remained in the range of pH 7 to 12, the molar extinction coefficient was determined to be 63.7 $mole^{-1}$ cm^{-1} at 548 nm.

Determination of the complex concentration by iodometry

If the concentration of the complex is determined by iodometry, the pH range is only limited by the destruction of the complex at pH $\leq$ 4. Furthermore, in addition to a centrifuge only a burette is required. To determine the remaining complex concentration after centrifugation 15 ml of the supernatant were mixed with 15 ml of 0.1 N HCl to destroy the $[Cu(EDA)_2]^{2+}$ complex. 2 ml of 0.5 g/ml KI solution were added, and the sample was titrated with 0.02 m NaS_2O_3 solution with starch as indicator.

Note: Unlike in simple iodometric titrations, sufficient I^- is required from the beginning since I^- generated during titration is precipitated by Cu^+ !

1) $$2\ Cu^{2+} + 4\ I^- \rightarrow 2\ CuI \downarrow + I_2$$

2) $$I_2 + 2\ S_2O_3^{2-} \rightarrow 2I^- + S_4O_6^{2-}$$

$$2\ Cu^{2+} + 2\ I^- + 2\ S_2O_3^{2-} \rightarrow S_4O_6^{2-} + 2\ CuI \downarrow$$

Calculating the cec

The cec is calculated as two times the amount of complex adsorbed per gram of dry clay. Most authors refer to drying the clay at 105 °C or 120 °C. Bergaya and Vayer recommend,

however, on drying at 1000 °C. The difference between these two temperatures is about 4% for a purified montmorillonite. The result is usually given as milliequivalents per gram of dry clay.

5.5 Determination of the cec with copper triethylenetetramine

Meier and Kahr (1999) introduced the copper triethylenetetramine $[Cu(trien)]^{2+}$ complex to determine the cec. The procedure will be described before discussing some possible modifications.

A 0.01 molar solution of the complex was prepared by dissolving 1.463 g (0.01 mole) triethylenetetramine and 1.596 g (0.01 mole) copper sulphate in distilled water and filling to 1 l. 200 mg of clay were dispersed in 35 ml of distilled water by means of ultrasonication. The sample was filled to 50 ml in a volumetric flask and completely transferred into a beaker. 10 ml of the complex solution were added while the dispersion was stirred. The sample was centrifuged and the concentration of the remaining complex in the supernatant was determined by measuring the extinction at 620 nm.

Comments on the method

- The method as described in the original publication requires many steps. The procedure can be simplified without any loss of precision. A simplified method and an improved method are given in Chap. 5.6.
- The purity of the triethylenetetramine sample as received was ≥97%. Therefore, 1.508 g of the triethylenetetramine were used to obtain a 0.01 molar solution.
- Since the adsorption maximum of the copper triethylenetetramine complex lies at 577 nm the extinction should be determined at this wavelength to reach maximum accuracy. It is probable that Meier and Kahr confused the adsorption maximum of $[Cu(trien)]^{2+}$ with methylene blue at 620 nm.
- The molar extinction coefficient at 577 nm was determined to be 152.1 mol^{-1} cm^{-1}.
- If the pH of the samples is very low, the determination of the remaining concentration by photometry yields wrong results since the extinction coefficient is affected by the pH. For more details see Chap. 5.6.

5.6 Comparison and evaluation of the copper complex methods

The methods of Meier and Kahr (1999) and Bergaya and Vayer (1997) were modified by adjusting the pH of the supernatant solution after centrifugation to increase the precision. An attempt was made to adjust the pH during the cation exchange. Finally, the results were compared to the values obtained by the ammonium acetate method.

Simple methods

To compare the methods of Meier and Kahr (1999) and Bergaya and Vayer (1997), the procedures were slightly simplified without loss of precision:

100 mg ± 25 mg of dry clay were weighed in 25 ml centrifugal tubes. 8 ml of 0.01 molar complex solution were added. The samples were shaken for at least 30 minutes and then centrifuged at a relative centrifugal field of 3000 g for 10 minutes. 3 ml of the supernatant were filled into cuvettes and the adsorption was measured at 577 nm for the copper triethylenetetramine complex and at 548 nm for the copper bisethylenediamine complex. Every determination was carried out with three parallel samples.

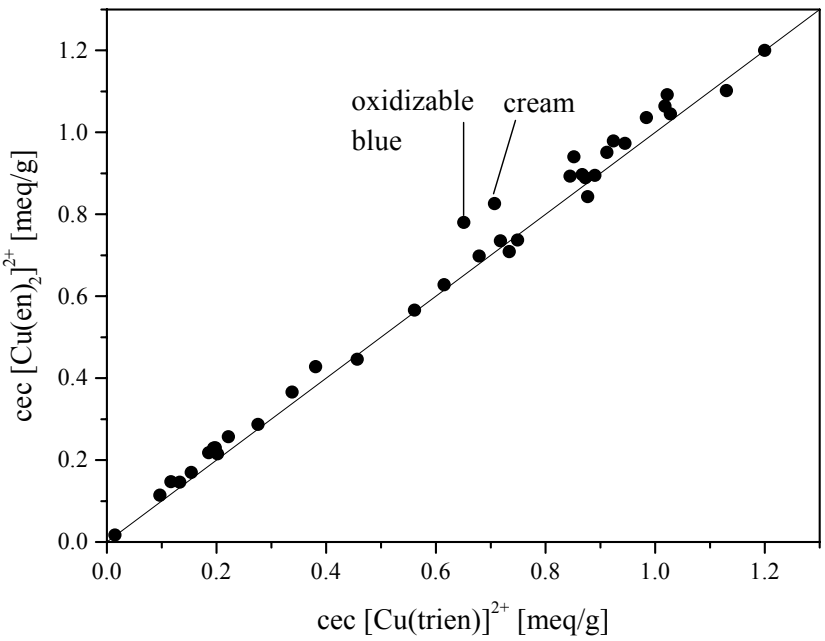

Fig. 5.6 : Plot of cec's determined with the two copper complex methods.

The results measured with that the $[Cu(en)2]^{2+}$ complex were plotted vs. data obtained with the $[Cu(trien)]^{2+}$ complex (Fig. 5.6). The results obtained by both methods are generally in

good agreement. However, the $[Cu(en)_2]^{2+}$ complex gives somewhat higher cec's for some samples. The largest difference of about 20% was found for the "oxidizable blue" clay.

This result induced further experiments. A method was developed to measure competitive adsorption (Chap. 5.7) but a preference for the $[Cu(en)_2]^{2+}$ or the $[Cu(trien)]^{2+}$ complex was not observed. Other experiments revealed that the adsorption coefficient of the two complexes are pH dependent (Fig. 5.7). If the pH of the clay dispersion is too low, the complex is protonated and the absorption coefficient decreases. This pretends the equilibrium concentration to be too small, thus the calculated cec is too high.

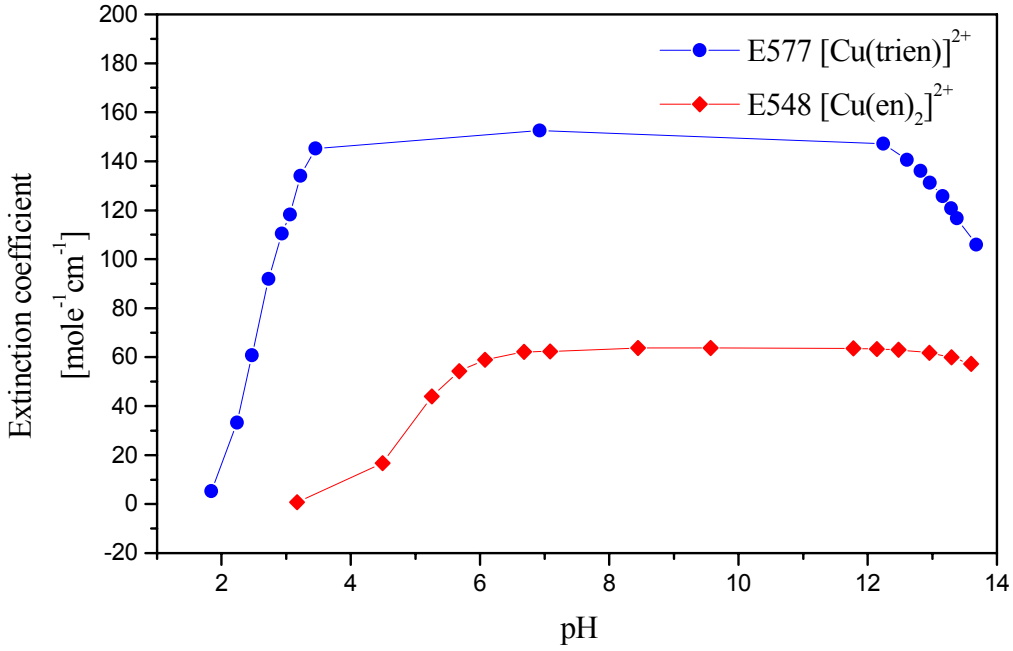

Fig. 5.7 : Extinction coefficients of the two copper complexes at λ_{max} as a function of the pH.

Modified methods

The methods were modified by using a buffer to adjust the pH of the solution. The first idea was to use phosphate buffer. Knowing that phosphate adsorbs on the clay mineral edges, phosphate was not added to the clay dispersion but to the separated supernatant after centrifugation. Phosphate slightly interacts with the complexes by shifting the adsorption maximum to longer wavelengths and decreasing the absorption coefficient. However, the use of phosphate is not recommended since many clays contain calcium as interlayer cation which is displaced by the copper complex and precipitates as $Ca_3(PO_4)_2$[1] in the cuvette.

[1] The use of EDTA to remove Ca^{2+} is not recommended at all because it also forms a (non-coloured) complex with the copper ions which is even more stable than the $[Cu(en)_2]^{2+}$ and the $[Cu(trien)]^{2+}$ complex.

Another buffer investigated was tris(hydroxymethyl)aminomethane (tris). To obtain optimum buffer capacity a 1 molar solution of tris was adjusted to pH = 8 ($\approx pK_a$) by addition of hydrochloric acid[2]. One ml of the solution was added to 3 ml of the supernatant. A calibration curve for both complexes was recorded at the same buffer concentration and indicated that the extinction coefficient was only slightly increased by the buffer. When the buffer was used for the $[Cu(en)_2]^{2+}$ determination, the results were in good agreement with data obtained with the $[Cu(trien)]^{2+}$ complex. Results obtained with this complex were almost not affected by the addition of the buffer. Within 37 samples investigated (Fig. 5.8) only the oxidizable blue and the cream clay showed a notable deviation between determination with and without addition of tris to the $[Cu(trien)]^{2+}$ complex. In both cases this was due to the very low pH of the samples.

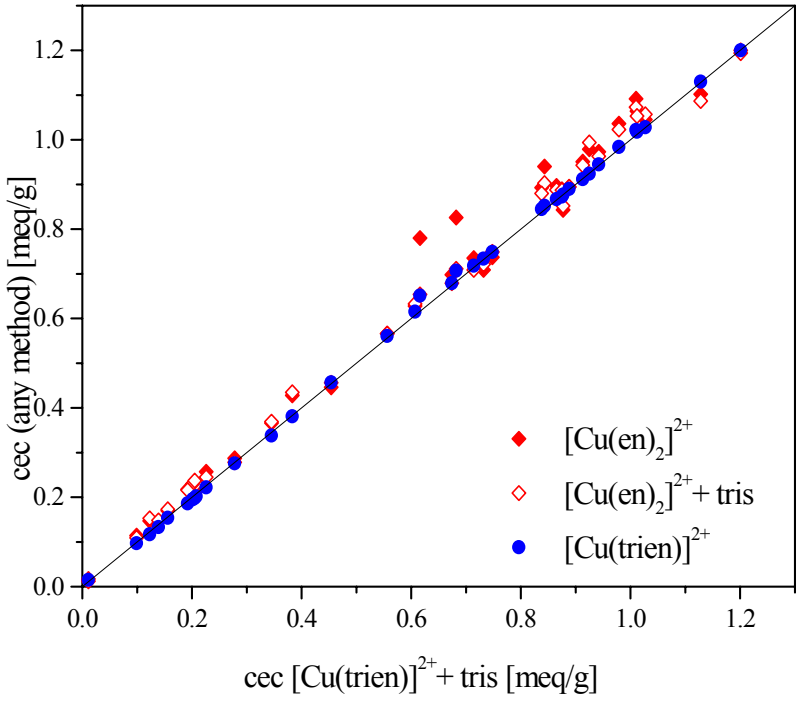

Fig. 5.8 : Comparison of the cec's determined with both copper complexes, Cu-trien^{2+}+ tris -method was chosen as reference. Hollow symbols refer to samples with addition of buffer to the supernatant.

If the $[Cu(en)2]^{2+}$ complex is used, addition of tris buffer is recommended to increase the precision, especially at low pH. All data are reported in Tab. 5.3. When calculating the cec most authors refer to the weight of the clay dried at 105 or 120°C, Bergaya and Vayer (1997) recommend on drying at 1000°C. In Tab. 5.3 the cec's are given for the clays as they were used and the loss on drying is reported in a separate column.

[2] 0.1 mole (12.114 g) tris and 55.8 ml 1 N hydrochloric acid were filled up to 100 ml to obtain a 1 molar pH=8

Some samples adsorbed up to 7 percent more $[Cu(en)2]^{2+}$ than $[Cu(trien)]^{2+}$ even if the tris buffer was applied. The geometry of the complexes was calculated (Chap. 5.9). The cross sectional area of the $[Cu(trien)]^{2+}$ complex (83 $Å^2$) is larger than that of the $[Cu(en)_2]^{2+}$ complex (71 $Å^2$). Typical equivalent areas of montmorillonites are $\approx$75 $Å^2$/charge (Lagaly, 1994). Since this value lies between the values of the copper complexes, it was supposed that a steric hindrance may be the reason for the differences in the cec. For this reason, the cec was determined with both complexes (+ tris) for 18 samples of known layer charge (determined with the alkyl ammonium method, Lagaly, 1994). The ratio of the cec's was plotted vs. the layer charge (Fig. 5.9). No correlation was found indicating that the charge density can not be the reason for the differences between the two methods. The copper complex exchanged samples were washed with distilled water and dried at 65°C in an evacuated chamber. X-ray diffraction of the samples revealed that the d(001) spacing does not depend on the layer charge. The d(001) spacing of the $[Cu(trien)]^{2+}$ exchanged clay was 12.9 Å in dry state and 15.7 Å if swollen in water and 13.1 Å for the wet $[Cu(en)_2]^{2+}$ exchanged samples.

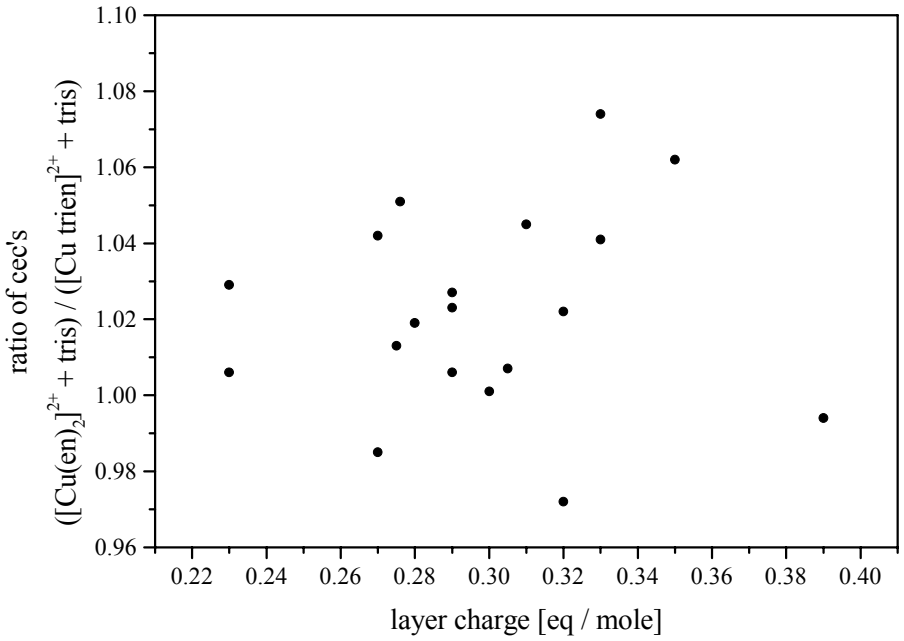

Fig. 5.9 : Ratio of exchange capacities determined with the modified methods vs. layer charge

buffer solution.

pH influence

The ammonium acetate method is automatically carried out at pH 7 because a large excess of ammonium acetate is employed. If silver thiourea is used, pH is adjusted by an excess of ammonium acetate (molar ratio ammonium acetate/silver thiourea = 10). Using the copper complexes, pH is not adjusted. The pH of the exchange experiment is determined by the sample, the amount and the pH of the complex solutions. It was observed that in general, pH during the cation exchange experiment was slightly higher in the presence of the $[Cu(trien)]^{2+}$ complex compared to the $[Cu(en)_2]^{2+}$ complex, except for the samples which yielded a very low pH. This can be explained by the higher pH (8.4) of the $[Cu(trien)]^{2+}$ complex solution and the fact that the $[Cu(en)_2]^{2+}$ complex (pH 8.1) buffers more protons.

It was assumed that different pHs of the exchange experiments could be the reason for the different cec's. Therefore, an attempt was made to adjust the pH already during the adsorption experiment[3]. A series of experiments was carried out to find a way to adjust the pH. Every experiment was performed with both copper complexes as triple measurements.

- The cec experiment was carried out by adding 8 ml of 0.01 molar complex solution and 1 ml of 3 molar ammonium acetate solution to 100 mg of dry clay. A calibration curve for both complexes at the same ammonium acetate concentration was recorded. The pH could be adjusted to 7 but the cec's measured by this method were significantly too low. May be the very big excess of ammonium ions compared to the amount of complex added led to adsorption of NH_4^+ instead of complex cations.
- To adjust pH, the samples were shaken overnight with 15 ml of 3 molar ammonium acetate solution. The samples were centrifuged, the supernatants discarded and the sediments dried at 60°C. Than 8 ml of the complex solution were added. This procedure also yielded too small cec values. The pH was increased but remained below 6. (Only the most acidic samples were investigated in this experiment.)
- As proposed by Chhabra et al. (1975) for the silver thiourea exchange, the samples were buffered with ammonium acetate solution but a much smaller amount than in the previous experiments was added. Chhabra et al. added a tenthfold excess of ammonium acetate compared to the complex. However, the buffer was not capable to adjust the pH to seven and the cec's measured were too low.

[3] Note that in the modified method tris buffer was added to the separated supernatant.

- Adding 1 ml of 1 molar tris buffer adjusted to pH 7 did not improve the results very much, the cec's measured by this method were too low. May be the buffer was adsorbed by the clay mineral because adjusting pH to 7 transformed tris into a cationic species.
- A 1 molar glycine solution at pH 7 was also applied. The advantage of glycine is that its iep is 5.97, so base has to be added to adjust the pH to seven. An anionic molecule is obtained which should not be adsorbed by the clay mineral. However, the cec values were also too low.

A number of buffers was investigated to adjust the pH of the cation exchange experiment but the cec's measured with addition of buffer were lower than those obtained with the ammonium acetate method. The error was almost neglectable for the purified samples but considerable for the raw clays.

Evaluation: Comparison of both the methods

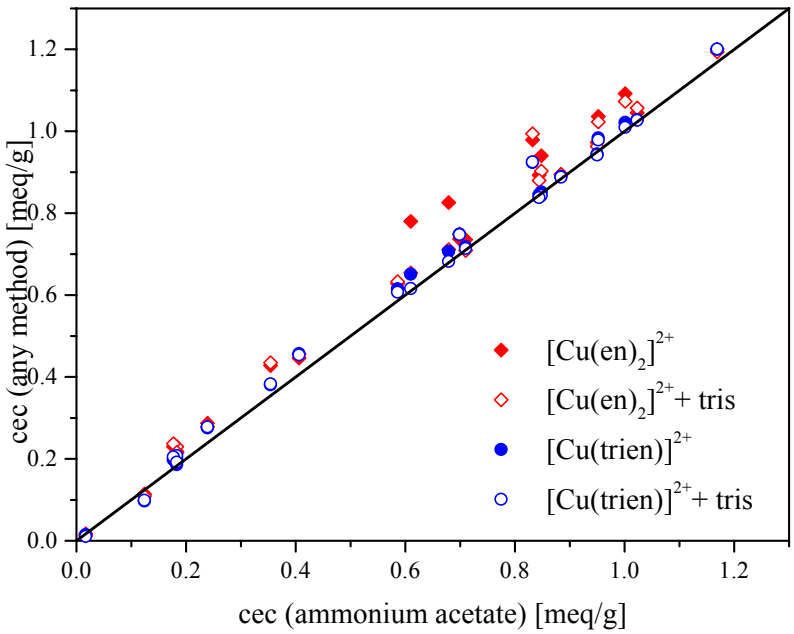

Fig. 5.10 : Comparison of sec's determined with $[Cu(en)_2]^{2+}$ + tris buffer, $[Cu(trien)]^{2+}$ + tris buffer and ammonium acetate.

Results obtained with the $[Cu(trien)]^{2+}$ complex and the buffered $[Cu(en)_2]^{2+}$ complex are in good agreement with the ammonium acetate method (Fig. 5.10). The $[Cu(en)_2]^{2+}$ complex slightly seems to overestimate the cec. For some samples the agreement between the two methods using copper complexes is better than to the ammonium acetate method. Though the

ammonium acetate measurements were carried out as triples, some errors are more likely to occur than for the copper complex determinations.

Results

Sec's measured with both copper complexes are generally in rather good agreement. Compared to the data obtained with the ammonium acetate method the $[Cu(en)_2]^{2+}$ complex tends to overestimate the cec but the accuracy of the method can be increased by adding tris buffer to the separated supernatant.

Addition of tris buffer was not found to be necessary for the $[Cu(trien)]^{2+}$ complex method except for two samples of very low pH.

No way was found to ensure that the cation exchange experiment with the copper complexes is carried out at neutral pH.

Both copper complexes permit a fast and precise determination of the cec. Though the extinction coefficient of the $[Cu(en)_2]^{2+}$ complex is less than half of that of the $[Cu(trien)]^{2+}$ complex, photometric determination is recommended.

Tab. 5.3 : cation exchange capacities[4], layer charge, weight loss on drying[5] and pH[6].

	layer charge eq/mole	ammonium acetate[7] meq/g	$[Cu(en)_2]^{2+}$ meq/g	$[Cu(en)_2]^{2+}$ + tris meq/g	pH	$[Cu(trien)]^{2+}$ meq/g	$[Cu(trien)]^{2+}$ + tris meq/g	pH	loss on drying 120°C	loss on drying 1000°C
					montmorillonites					
$M40a_{TL}$	0.29	0.884	0.895	0.894	6.8	0.890	0.888	7.6	4.9%	8.7%
$M47_{TL}$	0.31	0.952	1.036	1.023	6.6	0.984	0.979	7.3	6.2%	9.9%
$M48_{TL}$	0.32	0.950	0.973	0.963	6.8	0.945	0.942	7.1	6.9%	11.6%
$M50_{TL}$	0.35	1.001	1.092	1.073	6.6	1.022	1.010	7.0	10.9%	15.5%
					bentonites					
Cameron		0.586	0.628	0.633	7.8	0.615	0.607	8.2	7.7%	12.8%
Cream	0.27	0.679	0.826	0.711	6.0	0.707	0.682	4.7	13.2%	17.0%
de Maio	0.28	0.844	0.893	0.880	6.6	0.845	0.838	7.0	12.9%	17.5%
Kunipia A	0.23	1.023	1.045	1.057	8.3	1.028	1.027	8.9	10.4%	14.4%
M3	0.33		1.064	1.053	7.1	1.018	1.012	7.6	10.1%	
M26	0.31		0.698	0.679	6.6	0.679	0.674	6.4		
M34	0.32		0.843	0.852	8.1	0.877	0.877	8.3		
M39	0.29		0.897	0.888	6.8	0.867	0.865	7.4	15.5%	
	layer	ammonium	$[Cu(en)_2]^{2+}$	$[Cu(en)_2]^{2}$	pH	$[Cu(trien)]^{2+}$	$[Cu(trien)]^{2+}$	pH	loss on	loss on

[4] All cec data refer to the undried clay. Loss on drying was determined at 120°C and 1000°C.

[5] The weight loss on drying was determined as (loss on drying)/(dry weight). Therefore, to obtain the cec corresponding to a clay dried at 120°C the value of the undried clay has to be multiplied with the factor 100/(100-%weight loss).

[6] pH refers to the dispersions which have been shaken overnight after addition of the complex solution.

[7] The cec data of the ammonium acetate method reported in Tab. 5.3 were determined with the Kjeldahl method.

	charge eq/mole	acetate[8] meq/g		$^{+}$ + tris meq/g			+ tris meq/g		drying 120°C	drying 1000°C
M41	0.27		0.709	0.721	8.1	0.734	0.732	8.3		
M42		0.710	0.735	0.709	6.8	0.718	0.714	7.0	13.9%	17.7%
M46	0.29		0.951	0.943	7.0	0.912	0.913	7.7		
Otay	0.33	0.832	0.979	0.994	8.0	0.924	0.925	8.4	13.0%	22.1%
oxidizable blue		0.610	0.780	0.654	6.0	0.651	0.616	4.8	11.0%	16.4%
Polkville		0.848	0.940	0.903	6.5	0.852	0.843	6.6	16.4%	21.8%
Schwaiba	0.28		0.889	0.887	7.3	0.873	0.875	8.0	15.5%	
Upton	0.30	0.699	0.737	0.749	7.6	0.749	0.748	8.3	6.4%	12.2%
				beidellites						
B2			1.102	1.087	7.1	1.130	1.128	7.2	0.3%	
Bei 18/4	0.39	1.169	1.200	1.194	7.1	1.200	1.201	7.2	15.8%	23.5%
				kaolin						
KGa-1[9]		0.017	0.017	0.012		0.015	0.011		13.7%	
				hectorite						
H3	0.23	0.406	0.446	0.456	8.5	0.457	0.454	8.5	4.2%	24.1%
				common clays						
$Augzin_{sieved}$			0.147	0.153		0.117	0.123		3.2%	
$Augzin_{TL}$		0.183	0.215	0.230		0.202	0.208		1.7%	
$Friedländer_{sieved}$			0.366	0.369		0.338	0.345		2.1%	
$Friedländer_{TL}$		0.354	0.428	0.435		0.381	0.383		1.7%	
$HS7_{sieved}$			0.229	0.230		0.195	0.201		3.6%	
$HS7_{TL}$		0.177	0.230	0.237		0.198	0.205		2.3%	
$Plessa_{sieved}$			0.257	0.245		0.222	0.226		4.0%	
$Plessa_{TL}$		0.239	0.287	0.278		0.276	0.278		1.6%	
$Teistungen_{sieved}$			0.170	0.173		0.154	0.156		2.8%	
$Teistungen_{TL}$		0.183	0.218	0.216		0.186	0.192		1.1%	
$Thierfeld_{sieved}$			0.146	0.148		0.133	0.139		1.5%	
$Thierfeld_{TL}$		0.124	0.114	0.109		0.097	0.099		1.5%	

5.7 Competitive adsorption

The goal of this investigation was to find out if there is any preference in adsorption when both complexes are present in the solution. The absorption spectra of the two copper complexes differ in a significant way but, unfortunately, the absorption curve of $[Cu(en)_2]^{2+}$ lies below the curve of $[Cu(trien)]^{2+}$ (Fig. 5.11). There is consequently no isosbestic point or a wavelength to discriminate between the complexes.

[8] The cec data of the ammonium acetate method reported in Tab. 5.3 were determined with the Kjeldahl method.

[9] 0.5 g KGa-1 kaolin were weighed for the cec experiments

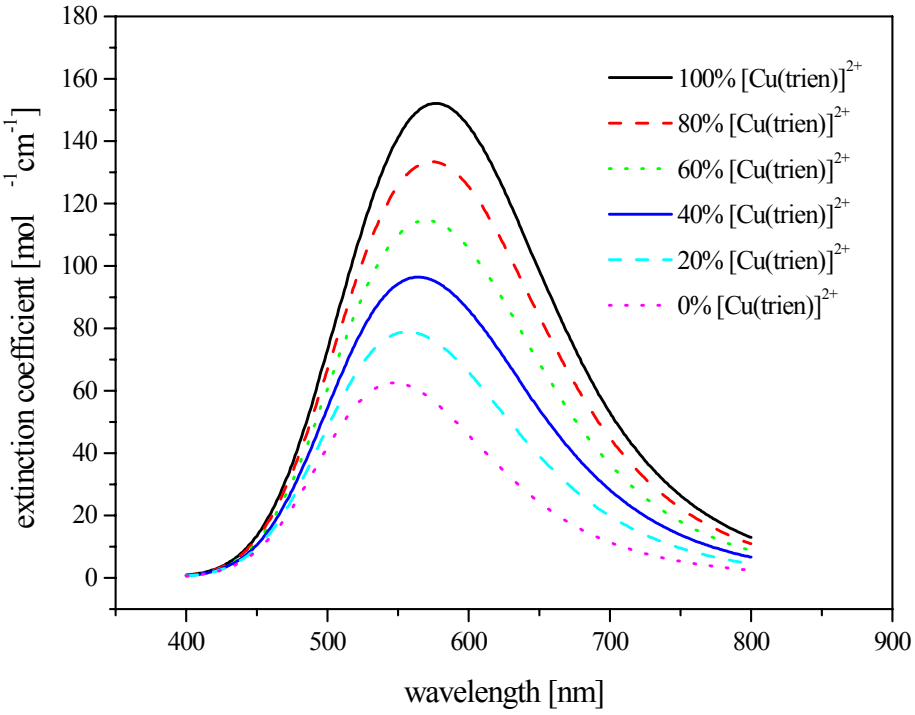

Fig. 5.11 : Spectra of different mixtures of $[Cu(trien)]^{2+}$ and $[Cu(en)_2]^{2+}$ complex.

A method was developed to calculate the concentrations of both complexes from the spectra. The ratio of adsorption coefficients was plotted vs. the wavelength. Two wavelengths with sufficiently high adsorption and a large difference in the ratio $\varepsilon_{[Cu(trien)]^{2+}} / \varepsilon_{[Cu(en)_2]^{2+}}$ (Fig. 5.12) were chosen (Tab. 5.4).

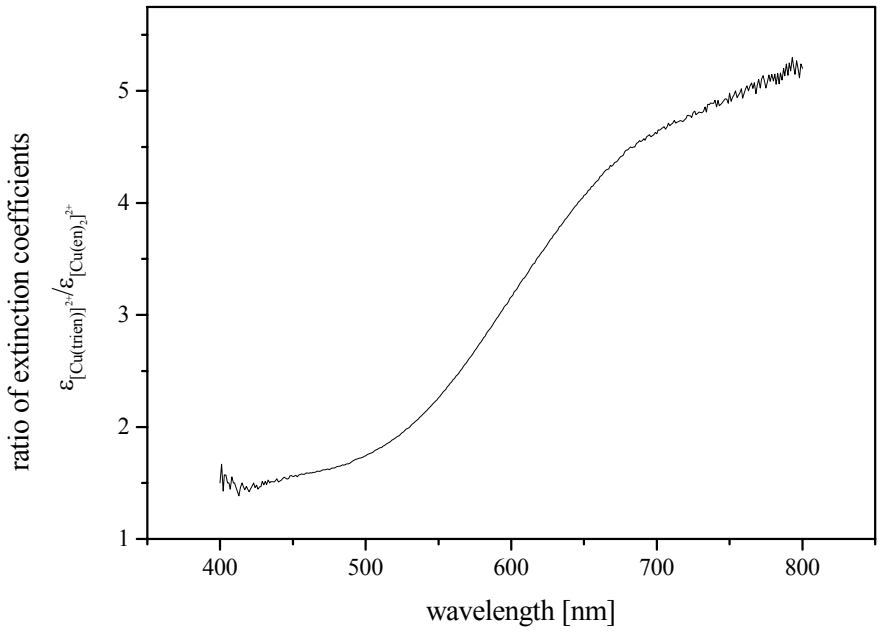

Fig. 5.12 : Ratio of extinction coefficients as a function of the wavelength.

Tab. 5.4 : Molar extinction coefficients

	500 nm	650 nm
$[Cu(en)_2]^{2+}$	41.9	24.2
$[Cu(trien)]^{2+}$	73	98.4
ratio $\varepsilon_{[Cu(trien)]^{2+}} / \varepsilon_{[Cu(en)_2]^{2+}}$	1.74	4.07

A formula was derived to calculate the total concentration and the molar fractions of the complexes by measuring the extinction at these two wavelengths:

(1) $$E_{500nm} = c_{EDA}\varepsilon_{EDA500} + c_{trien}\varepsilon_{trien500}$$

(2) $$c_{EDA} = c_{total}(1 - X_{trien})$$

(3) $$c_{trien} = c_{total}X_{trien}$$

(1b) $$E_{500nm} = c_{total}(1 - X_{trien})\varepsilon_{EDA500} + c_{total}X_{trien}\varepsilon_{trien500}$$

(1c) $$E_{500nm} = c_{total}\left[(1 - X_{trien})\varepsilon_{EDA500} + X_{trien}\varepsilon_{trien500}\right]$$

(1d) $$E_{500nm} = c_{total}\left[\varepsilon_{EDA500} - X_{trien}\varepsilon_{EDA500} + X_{trien}\varepsilon_{trien500}\right]$$

(1e) $$E_{500nm} = c_{total}\left[\varepsilon_{EDA500} + X_{trien}(\varepsilon_{trien500} - \varepsilon_{EDA500})\right]$$

(1f) $$\frac{E_{500nm}}{(\varepsilon_{trien500} - \varepsilon_{EDA500})} = c_{total}\left[\frac{\varepsilon_{EDA500}}{\varepsilon_{trien500} - \varepsilon_{EDA500}} + X_{trien}\right]$$

(1g) $$\frac{E_{500nm}}{(\varepsilon_{trien500} - \varepsilon_{EDA500})} = c_{total}\frac{\varepsilon_{EDA500}}{\varepsilon_{trien500} - \varepsilon_{EDA500}} + c_{total}X_{trien}$$

respectively for E_{650nm}:

(4) $$\frac{E_{650nm}}{(\varepsilon_{trien650} - \varepsilon_{EDA650})} = c_{total}\frac{\varepsilon_{EDA650}}{\varepsilon_{trien650} - \varepsilon_{EDA650}} + c_{total}X_{trien}$$

(1h) $$\frac{E_{500nm}}{(\varepsilon_{trien500} - \varepsilon_{EDA500})} - \frac{E_{650nm}}{(\varepsilon_{trien650} - \varepsilon_{EDA650})} = c_{total}\left[\frac{\varepsilon_{EDA500}}{\varepsilon_{trien500} - \varepsilon_{EDA500}} - \frac{\varepsilon_{EDA650}}{\varepsilon_{trien650} - \varepsilon_{EDA650}}\right]$$

(1i) $$c_{total} = \frac{E_{500nm} - E_{650nm}(\varepsilon_{EDA500} - \varepsilon_{trien500})/(\varepsilon_{EDA650} - \varepsilon_{trien650})}{\varepsilon_{trien500} - \varepsilon_{trien650}(\varepsilon_{EDA500} - \varepsilon_{trien500})/(\varepsilon_{EDA650} - \varepsilon_{trien650})}$$

(1e) $$E_{500nm} = c_{total}\left[\varepsilon_{EDA500} + X_{trien}(\varepsilon_{trien500} - \varepsilon_{EDA500})\right]$$

(1j) $$X_{trien} = \frac{E_{500nm} - c_{total}\varepsilon_{EDA500}}{(\varepsilon_{trien500} - \varepsilon_{EDA500})c_{total}}$$

E_{500nm} = extinction measured at 500 nm

c_{EDA} = concentration of the copper bisethylenediamine (EDA) complex

ε_{EDA500} = extinction coefficient of the copper bisethylenediamine (EDA) complex at 500 nm

c_{total} = sum of the concentrations of both copper complexes

X_{trien} = molar fraction of the copper triethylenetetramine (trien) complex

The accuracy of the method was checked on 6 solutions, all 0.01 molar, with different molar fractions of the copper complexes. The calculated values of c_{total} and X_{trien} are reported in Tab. 5.5. The errors between theoretical and calculated values are in the range of 0.2% for c_{total} and 1% for X_{trien}. These errors are due to erroneous data of the spectra.

Tab. 5.5 : Extinctions at 500 nm and 650 nm and calculated values of c_{total} and X_{trien}.

X_{trien} given	E_{500nm}	E_{650nm}	c_{total} calculated 10^{-2} mole/l	X_{trien} calculated
1	0.73	0.984	1.000	1
0.8	0.669	0.838	1.001	0.803
0.6	0.606	0.689	0.999	0.603
0.4	0.544	0.539	1.002	0.399
0.2	0.481	0.391	0.999	0.202
0	0.419	0.242	1.000	0.000

No significant preference between the two complexes could be observed by this experiment. The molar fractions of the two complexes showed no change for all the samples investigated. There was no preference for either of the copper complexes.

5.8 CEC with copper complexes – particle charge detector

The particle charge detector (PCD) is designed to study the change of some type of streaming potential (which is close to the zeta potential but not identical) during a titration. Clay minerals have a negative surface potential and show in water a negative potential. Any substance that adsorbs on the clay will influence the potential. The aim of this experiment was to see whether any information can be taken from a titration of clays with both copper complexes.

Description of the PCD

The titration vessel and the piston are made of PTFE. The piston moves vertically at a speed of 4 s^{-1}. The dispersion is accelerated and sheared in the gap between the piston and the vessel. A potential can be measured between the two electrodes.

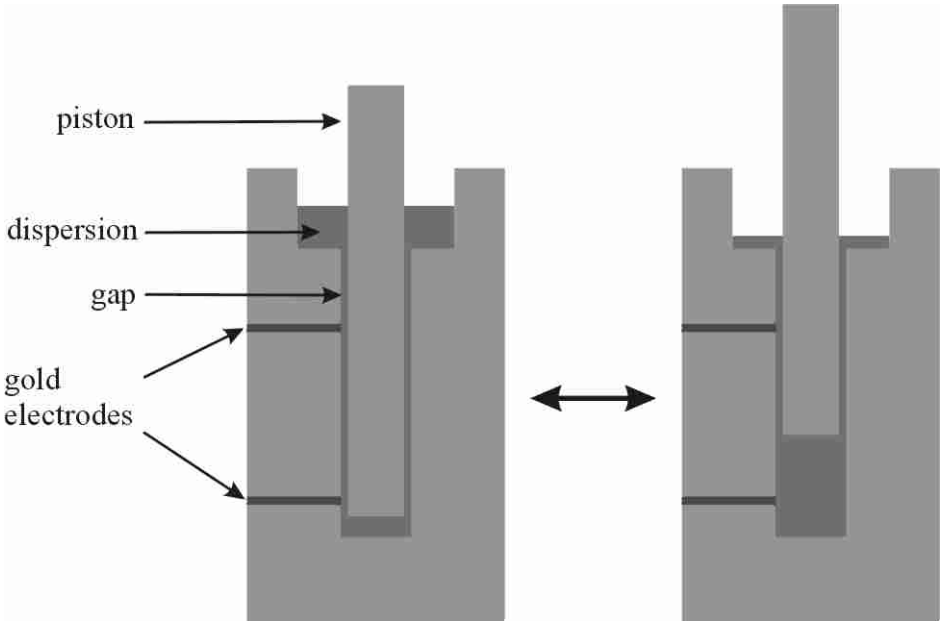

Fig. 5.13 : Schematic assembly of the PCD apparatus.

Experimental and results

0.5 ml to 2 ml of a dispersion (0.02 g/ml) of $M48_{TL}$ was diluted with distilled water to provide 10 ml and filled into the titration vessel. 0.01 molar solutions of the copper complexes were added in 0.05 ml increments every 10 seconds.

The curves (potential vs. added amount of the copper complex) were not optimal. The potential measured at the beginning of the titrations varied in a wide range and the beginning of the curves was not reproducible. Best results were obtained with 0.5 ml of the dispersion. In the beginning the potential decreased slowly, after addition of app. 0.3 ml solution it rapidly dropped and, finally decreased again slowly. At the end of the rapid decrease the amount of the complex added corresponded to the cec. However, it is noteworthy that the potential remained negative even when the amount of added complex corresponded to four times the cec. One may conclude that a part of the complex adsorbed can be desorbed by shearing the dispersion. It may also indicate that no excess of the complexes is adsorbed on the clay. No significant differences between the two complexes were observed.

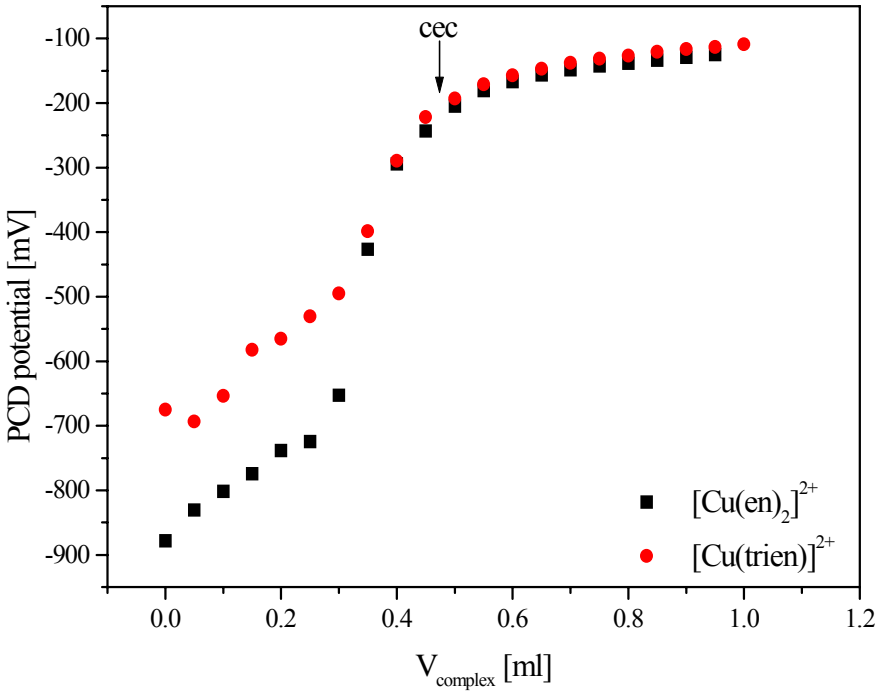

Fig. 5.14 : PCD potential vs. amount of complex added for 0.5 ml of 2%w/w $M48_{TL}$ dispersion.

5.9 Geometry of the complexes

To determine the size of the complexes, the compositions were calculated by quantum mechanics (Gaussian 98 Software[10]). The copper ion was placed in the origin of the axes and

[10] Thanks to Dr. Nicolai Lehnert (Institute of Inorganic Chemistry, Chrisitan-Albrechts University in Kiel, Germany) for performing the calculations.

the data[11] were transformed to fit the plane of the four nitrogen atoms parallel to the xz-plane. According to Burba and McAtee (1977) the orientation of the plane of the four nitrogen atoms is parallel to the clay mineral's surface. Thus, the area of the complex was calculated in the xz-plane. The specific surface area of each complex was calculated by taking into account a Van der Waals radius of 1.32 Å for the hydrogen atoms of the molecule.

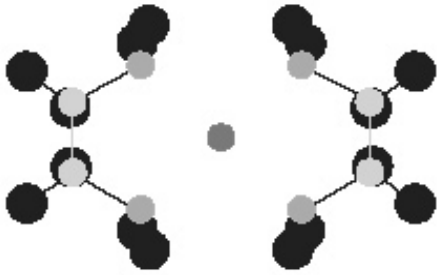

Fig. 5.15 : xz-plot of the $[Cu(en)_2]^{2+}$ complex.

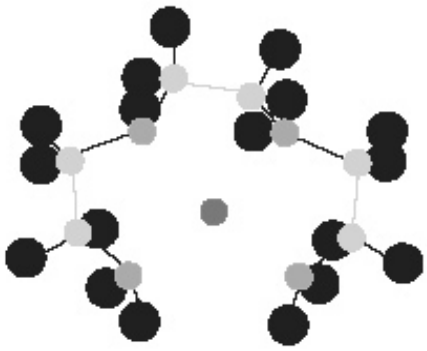

Fig. 5.16 : xz-plot of the $[Cu(trien)]^{2+}$ complex.

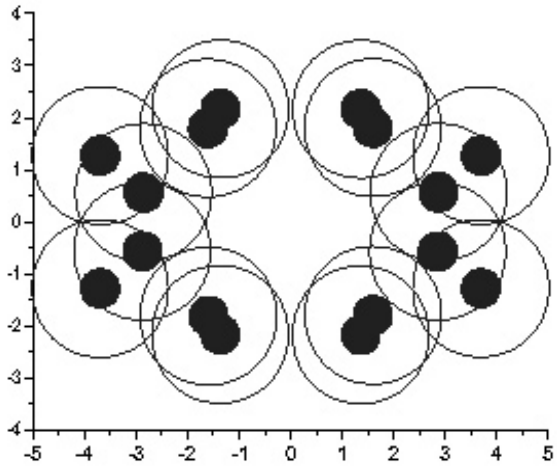

Fig. 5.17 : xz-plot of the $[Cu(en)_2]^{2+}$ complex. Only hydrogen atoms displayed with covalent and Van der Waals radii.

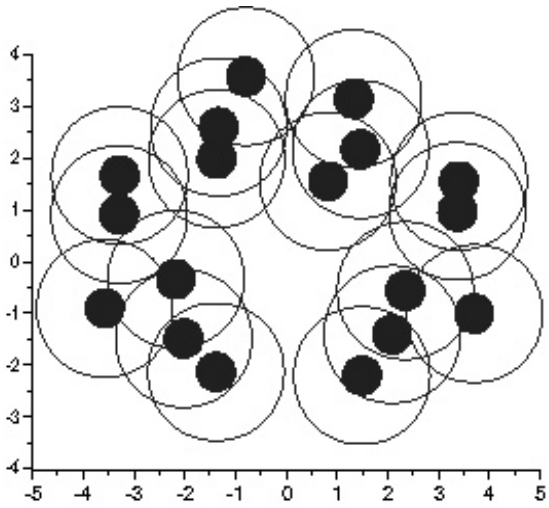

Fig. 5.18 : xz-plot of the $[Cu(trien)]^{2+}$ complex. Only hydrogen atoms displayed with covalent and Van der Waals radii.

[11] Data are reported in the appendix-

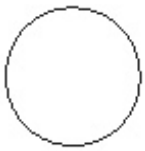

Van der Waals radius of hydrogen

covalent radius of hydrogen

covalent radius of carbon

covalent radius of nitrogen

As can be seen from the co-ordinates and the plots the copper triethylenetetramine complex covers a larger surface area. The calculated surface areas of the xz-planes are 71 $Å^2$ for the $[Cu(en)_2]^{2+}$ complex and 83 $Å^2$ for the $[Cu(trien)]^{2+}$ complex.

5.10 Recommended procedure for the cec determination

The best accordance with the ammonium acetate method was measured with the copper triethylenetetramine $[Cu(trien)]^{2+}$ complex. It depends on the sample whether a buffer is required. Very acidic samples require a buffer. To avoid errors, we recommend addition of buffer as a standard procedure. Note that calibration curves with and without buffer match almost but not completely !

The determination with the copper bisethylenediamine $[Cu(en)_2]^{2+}$ complex is almost as good as with the $[Cu(trien)]^{2+}$ complex. If this complex is chosen and the determination is carried out by photometry, buffer should always be added.

App. 200 mg of dry clay are weighed in 20 ml centrifugal tubes. If the sample has a very low cec, as for example kaolin, the amount should be increased. 8 ml 0.01 molar complex solution are added and the sample is shaken for 30 minutes. Note that though the exchange usually occurs very fast, some calcium-exchanged samples require this equilibration time. The samples are centrifuged and 3 ml of the supernatant are filled into cuvettes. 1 ml 1 molar tris buffer are mixed with the supernatant. The extinction is read at 577 nm for the $[Cu(trien)]^{2+}$ complex or at 548 nm for the $[Cu(en)_2]^{2+}$ complex.

Preparation of the complex solution

100 ml 0.1 molar $CuSO_4$ solution (Merck) and 1.508 g (0.01 mole) triethylenetetramine ≥97% (Fluka) are dissolved in distilled water to give one litre 0.01 molar solution. A slight excess of triethylenetetramine can be employed to ensure complete formation of the complex.

If the $[Cu(en)_2]^{2+}$ complex is chosen, 1.202 g (0.02 mole) ethylenediamine are required. Bergaya and Vayer (1997) proposed addition of a 2% excess of ethylenediamine.

Preparation of the buffer

0.1 mole (12.114 g) trishydroxymethyl aminomethane and 55.8 ml 1 N hydrochloric acid were filled to 100 ml to obtain a 1 molar pH 8 buffer solution.

6.1 Adsorption on clays

Clay minerals have very good sorption properties for a number of substances. There are at least three factors which control the sorption capacity of clays:

- the total number of charges on the clay mineral surface and the charge density,
- the acidity and the number of hydroxyl groups and oxygen atoms on the clay mineral surface, and
- the specific surface area of the clay mineral.

In some cases not only one factor plays a role for every substance to be adsorbed. Kahr and Madsen (1995) proposed determination of the specific surface area *and* the cation exchange capacity of clays by adsorption of methylene blue (MB). Depending on the experimental conditions the charges of the clay mineral or the surface area of the clay mineral control the adsorption rate. At low MB concentration the cec can be determined, while with increasing concentration of methylene blue the adsorption rate is controlled by the surface area of the clay. In this work experiments were also carried out with cetyl pyridinium chloride and alkyl ammonium ions. These molecules are cationic surfactants, therefore, the adsorption rate could be controlled by the number of charges (Kloppenburg, 1997) or the specific surface area (Greenland and Quirk, 1964). The aim was to determine, whether the amount adsorbed can be correlated with the cec or the specific surface area.

The number of anionic charges is called the cation exchange capacity and is discussed in Chap. 5. Lagaly (Lagaly, 1993) pointed out that the cation exchange of di- and tri-valent cations can take place to equivalent or, at low charge density, equimolar capacities. For this reason, the charge density may play a role. The acidic properties of clays were investigated by potentiometric titration (Chap. 4). The following section deals with the specific surface area of clays.

Specific surface area

A comprehensive discussion of the specific surface area of clays requires recognition that there are different ”specific surface areas” for one clay sample. Different methods yield different results. Before discussing the methods, one must carefully consider the meaning of ”surface area”.

The maximum specific surface area can be calculated from crystallographic data. The basal plane surface of montmorillonite covers a specific surface area of 760 m^2/g. Depending on the particle size the edges contribute 40 – 50 m^2/g, thus the total surface area is about 800 – 810 m^2/g. However, this value is valid only for a pure clay mineral whereas natural samples always contain impurities.

In the dry state, clay minerals consist of stacks of silicate layers in face to face orientation. One can distinguish between the external, internal and total surface area. If the adsorbate cannot enter the interlayer space, the amount adsorbed corresponds to the external surface area. However, the usefulness of the external surface is restricted, because pores and holes can also contribute to this value (as for example in gas adsorption measurements). In same cases the layers are collapsed in the centre whereas close to the edges the layers are partly expanded. All of these factors complicate the definition of the external surface area.

Some polar molecules may enter the interlayer space and expand it. To determine the specific surface area it is important to know whether a monolayer (II a) or a bilayer (II b, Fig. 6.1) is present in the interlayer space. If the interlayer is expanded by a bilayer of the adsorbate, the total surface area can be determined.

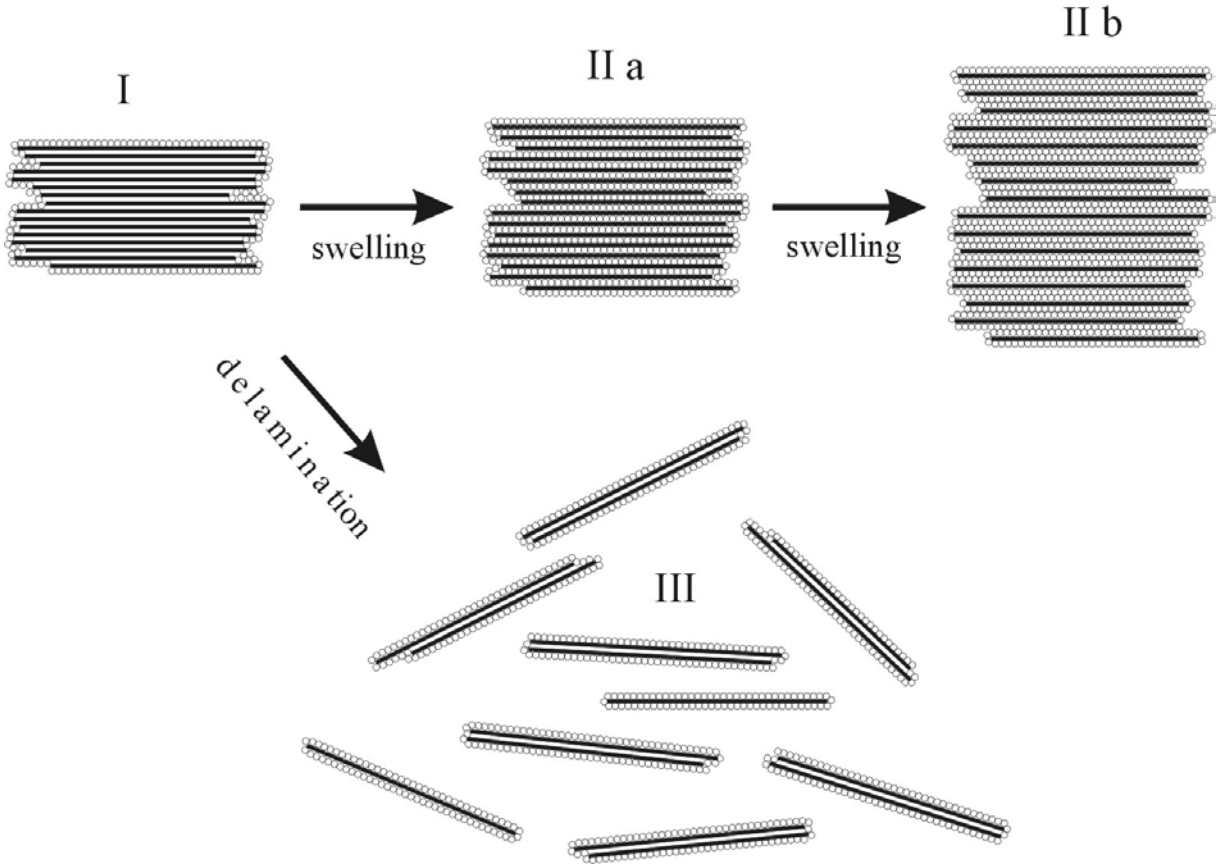

Fig. 6.1 : Swelling and delamination of montmorillonite.

Determination of surface area is even more complicated with smectites. When dispersed in water, the individual particles of montmorillonite delaminate. The degree of delamination depends on the interlayer cation, the ionic strength of the dispersion and the nature of the clay mineral. Schramm and Kwak (1982) found that the average number of attached clay crystallites is 1.7 for a sodium saturated montmorillonite and 6 for a calcium saturated montmorillonite (III, Fig. 6.1). The effect of different degrees of delamination in solution permits a third way to define the specific surface area, the surface which is exposed to the solution. If complete delamination occurs, this value equals the total surface area (IIb, Fig. 6.1). A method which could be employed to measure this surface area is negative adsorption. A number of experiments were carried out to measure negative adsorption (Schofield, 1947 and 1949, Bolt and Warkentin, 1958, Van den Hul and Lyklema, 1967, Polubesova et al., 1989) with the common clays but all experiments failed. Nennemann (1997) and Nennemann et al. (2000) determined specific surface areas of montmorillonites by negative adsorption. However, this method could not be adapted to the common clays, probably because the surface area was too small.

A point to consider is the size of the adsorbate: with decreasing size of the adsorbate the ”specific surface” area increases (Helmy et al. 1998), due to the increased number of accessible sites like holes or pores. This problem leads to the definition of the fractal dimension. An even surface exposes the same area to small and great molecules. A surface with pores, edges, holes and angles exposes a greater area to smaller molecules. If the logarithm of the specific surface area is plotted vs. the logarithm of the size of the adsorbate, usually a straight line is obtained. The slope is referred to as the fractal dimension, which describes the roughness of a surface.

Methods to determine the specific surface area are usually based on the adsorption of polar liquids like water (Newman, 1983, Kraehenbuehl et al. 1987, Kahr, 1991), ethylenglycol (Chap. 6.5) or ethylene glycol monoethylether (Chap. 6.6). Dyes are also employed for surface determinations, e.g. methylene blue (Chap. 6.2) or p-nitrophenol (Ristori et al., 1989). Helmy et al. (1998) compared adsorption of phenanthroline, bipyridine, quinoline, oxine, methylene blue, glycerol, ethylene glycol and ethylene glycol monoethyl ether to determine surface areas of kaolin, α-Fe_2O_3 and hydroxy-Al montmorillonite.

6.2 Adsorption of methylene blue

Adsorption of methylene blue (MB) is a common method to estimate the specific surface area of kaolin and the smectite content of bentonites, especially in the foundry industry. A vast number of publications refer to the application of this method (Hang and Brindley, 1970, Lagaly, 1981, Cenens and Schoonheydt, 1988, Schoonheydt and Heughebaert, 1992, Kahr and Madsen, 1995, Bujdák and Komadel, 1997; 1998, Avena et al., 2001). Correlations between the amount adsorbed and the specific surface area and the cation exchange capacity were discussed by Kahr and Madsen (1995). The arrangement of methylene blue cations on the surface and the area covered by each molecule depend on the layer charge of smectites (Bujdák et al, 1998).

Performing a titration of a clay dispersed in water, Hang and Brindley assumed that monomolecular coverage of the surface is attained at the specific point when traces of free methylene blue are detected in the solution. They refer to this point as the ”optimum flocculation” point, determined by staining the dispersion on filter paper. At low MB loading, all the dye is adsorbed by the clay and only water will flow from the droplet. If the ”optimum flocculation point” is exceeded, free methylene blue can be determined as a halo around the flocculated clay. Kahr and Madsen (1995) proposed to determine this point by photometry. Plotting the amount of MB adsorbed by the clay vs. the amount added, they found a straight for small loadings. They considered the ”optimum flocculation point” to be the point at which the curve deviates from linearity. If non-flocculated clay particles are present in the dispersion, determination of this point becomes difficult. Note that at very low MB concentrations a halo also appears, indicating that a minimum MB concentration is required before adsorption takes place. However, the name ”optimum flocculation point” is confusing, because not the flocculation is investigated but the adsorption. Therefore, this point will be referred to as ”halo point”.

Experimental

20 ml PE bottles with 0.5 ml of a 2% w/w clay dispersion were used. Water and varied amounts of 0.01 mole/l methylene blue solution were added to give 20 ml. Each isotherm consisted of 11 initial concentrations in the range from 0 to 1 mmole/l. Adsorption was carried out overnight in an end-over-end shaker. The samples were centrifuged at a relative centrifugal field of 10000 g for 10 minutes. The extinction of 1 ml supernatant in 1 ml

cuvettes was determined at 663 nm. The halo point was determined as the minimum concentration where free MB was observed. The maximum adsorbed amount (saturation adsorption) was taken as the plateau values of the adsorption isotherms.

6.3 Adsorption of polyvinylpyrrolidone

Since polyvinylpyrrolidone (PVP) easily intercalates smectitic interlayers (Eberl et al., 1998, Sequaris et al., 2001), the amount of PVP adsorbed should correlate with the content of expandable layers. A method was developed to measure the amount of PVP adsorbed by clays.

Preliminary experiments

Preliminary experiments were carried out to find the optimal conditions for the adsorption experiment. Polyvinylpyrrolidones of different chain lengths were tested (PVP K15, M_r ~ 10000, Fluka, pract., PVP K25, M_r ~ 24000 Fluka, purum and PVP, M_r ~ 25000-30000, Merck), the adsorption time was varied, and clay suspensions of different solid contents were tried.

Experimental

A stock solution with a mass concentration of 20 g/l was prepared. From this solution a set of solutions with the concentrations 15, 12, 10, 7.5, 5 and 2 g/l were prepared. 1 ml clay suspension (solid content 0.02 g clay / ml) and 1 ml PVP-solution were filled into 2 ml centrifugal caps. The samples were shaken overnight and centrifuged at a relative centrifugal field of 20000 g. 1 ml of the supernatant was filled into 1 ml shell vials for HPLC analyses. The concentration of the polymer was determined with HPLC without column (!), equipped with a refractive index detector (waters 410). 1.5 µl of sample were injected and the flow rate was 1ml/min distilled water. Each sample was measured three times.

6.4 Adsorption of alkylammonium ions

Alkylammonium ions intercalate in the interlayer space of smectitic minerals. The aim of this investigation was to determine whether the smectite content is correlated with the amount of alkylammonium ions adsorbed on the clay.

Preparation of the solutions

0.01 mole n-alkylamine (chain length C10, C12 and C14) were weighed out and dissolved in 50% v/v ethanol. The pH was adjusted with 2 N hydrochloric acid to 7. The solution of decylamonium ions was diluted to 100 ml with a resulting 0.01 molar concentration. Since the other amonium ions are less soluble they required dilution to 250 ml, yielding 0.04 molar solutions. However the solutions remained opaque, indicating that the amines were not completely dissolved.

Adsorption experiment

5 ml clay suspension (solid content 0.02 g/ml) were filled into 20 ml centrifugal tubes. 0.2 mmole alkylammonium ions (corresponding to at least two times the cec of a montmorillonite) were added and the samples were shaken overnight. The samples were centrifuged, the supernatant discarded and again 0.02 mmole alkylammonium ions added. The sediment was stirred with a spatula and the samples again shaken overnight. This procedure was repeated three times so that the samples were four times exchanged. One exchange was performed in a temperature-controlled shaker at 65°C. The samples were then washed and centrifuged five times with ethanol to remove excess alkylammonium ions. The supernatant of each cycle was analysed with HPLC to determine the required number of washing cycles. The samples were dried overnight at 65°C and ground to powder. They were subsequently dried another night at 65°C in an evacuated chamber. All samples were analysed in a CHN-Rapid Analysator (Haraeus company) for the content of carbon, hydrogen and nitrogen. The nitrogen content was used to calculate the amount of alkylammonium ions adsorbed.

6.5 Adsorption of ethylene glycol

General

The use of ethylene glycol (EG) plays an important role in the identification of clay minerals. Adsorption of EG changes the interlayer spacing of expandable clay minerals, namely smectites, and permits their identification by X-ray diffraction. In illite/smectite, kaolinite/smectite and chlorite/smectite interstratified clay minerals it even permits the determination of the smectite ratio (Moore and Reynolds, 1989). Adsorption of EG can also be carried out to determine the specific surface area of clays. There are two general ways to perform this experiment: adsorption of EG on the dry clay via the gas phase (Eltantawy and Arnold, 1974), or desorption of an excess amount of EG previously added to the clay (Dyal and Hendricks, 1950) (EG retention).

The desorption method is carried out by adding 3 ml of EG to 1 g of the dry clay and placing the sample in a desiccator over anhydrous $CaCl_2$. The weight is measured periodically. After a high loss rate the evaporation of EG slows down indicating that monolayer coverage is obtained. 0.25 g EG were retained per gram of the < 2µm fraction of a Wyoming montmorillonite. Assuming a total surface area of 810 m^2/g (derived from crystallographic data) Dyal and Hendricks calculated a specific adsorption of 0.31 mg EG per m^2. McNeal (1964) found that the amount of EG retained by the clay mineral depends on the interlayer cation. Several modifications were proposed (Bower and Gschwend, 1952, Martin, 1955, Bower and Goertzen, 1959, Sor and Kemper, 1959, Brindley, 1965).

The adsorption method (Eltantawy and Arnold, 1974) is carried out by placing the dry clay and anhydrous $CaCl_2$ or mixtures of $CaCl_2$ and EG, so called ”solvates”, in a desiccator over liquid EG. $CaCl_2$ or the solvates are employed to reduce the vapour pressure of EG. Compared to the desorption technique, Eltantawy and Arnold found a higher amount of EG adsorbed but no dependence on the interlayer cation. They concluded that without liquid EG as a separate phase the vapour pressure of EG is so low that less than the amount corresponding to monolayer coverage is adsorbed or retained. Eltantawy and Arnold found a specific adsorption of 0.45 mg/m^2.

Experimental

The experiment was carried out following the procedure of Eltantawy and Arnold (1974). Ethylene glycol was dried over sodium sulphate and distilled prior to use. Approximately 100 mg of clay were weighed into glass vessels and placed in a desiccator over P_4O_{10} for three days. The samples were weighed again and the P_4O_{10} was removed. An evaporating dish (Ø 80 mm) with fresh ethylene glycol was placed in the desiccator below the samples. About 10 g of $CaCl_2$ which had been dried at 200°C was placed in the dessicator to reduce the vapour pressure of the EG. The desiccator was evacuated and the samples were weighed daily. The experiment was carried out at room temperature. All experiments were carried out in duplicate.

6.6 Adsorption of ethylene glycol mono- and diethyl ether

General

The specific surface area of clay minerals can be determined by retention of ethylene glycol monoethyl ether (EGME) (Heilman et al. 1965, Eltantawy and Arnold, 1973, Carter et al. 1986). Carter et al. and Heilman et al. used identical procedures. The Ca^{2+} exchanged clay mineral is dried over P_4O_{10} until reaching constant weight. 1 g samples of the clay are wetted with 3 ml EGME and placed in a desiccator with dry $CaCl_2$ or $CaCl_2$-EGME mixtures. Heilman et al. found that the choice of $CaCl_2$ or $CaCl_2$-EGME mixtures did not affect the results. Carter et al. measured 23.17 mg EGME retained per gram of a montmorillonite. Division by the max. specific surface area of 810 m^2/g gives 0.286 mg/m^2. The authors found good agreement between their data and those obtained with EG retention (Carter et al., 1965, Heilman et al., 1965) by the method of Dyal and Hendricks (1950). Eltantawy and Arnold (1973) used dry $CaCl_2$ and liquid EGME as separate phases in the desiccator. The amount of EGME retained was up to 50% higher. Though this amount was significantly higher than by the other two methods ($CaCl_2$ or $CaCl_2$-EGME), the d(00l)-spacing of 17.07 Å was not affected. The authors assumed that at low EGME vapour pressure EGME solvates the calcium ions leaving empty space between these complexes. This space can be filled to obtain complete unimolecular coverage by increasing the vapour pressure of the EGME. The authors confirmed their assumption by DTA curves. The amount of 0.302 g EGME retained per gram of montmorillonite was in agreement with the theoretical value of 0.297 g/g calculated from

the liquid density of EGME and assuming a specific surface area of 800 m^2/g. Carter et al. (1986), however, claimed that the measured values of Eltantawy and Arnold were too high. The EGME vapour pressure in the experiments of Carter et al. and Heilman et al. is probably very low, depending on the amount of EGME desorbed and the amount of $CaCl_2$ placed in the desiccator. In the experiment of Eltantawy and Arnold the EGME vapour pressure is distinctly higher. It is probably close to $p/p_0 = 1$, thus almost equal to the equilibrium vapour pressure of liquid EGME. In the following sections the method of Carter et al. and Heilman et al. will be called retention at ”lower vapour pressure” (lvp), the method of Eltantawy and Arnold retention at ”higher vapour pressure” (hvp).

Carter et. al. (1986) used 0.286 mg/m^2 as conversion factor, Eltantawy and Arnold (1973) 0.367 mg/m^2.

Experimental

The EGME retention experiment was performed by two different methods, first at higher EGME vapour pressure (hvp) by the method of Eltantawy and Arnold (1973) and then at lower EGME vapour pressure (lvp) as described by Carter et al. (1986) and Heilman et al. (1965). The same samples were used for both experiments.

2 g of clay were weighed into glasses[1] (20 mm diameter) and dried over P_4O_{10}. Up to 3 ml liquid EGME ($\geq$ 99%, Fluka) were added to each sample. The samples were left for one hour in an evacuated dessicator to adsorb the liquid. Next, approx. 10 g of $CaCl_2$, dried at 200°C, and an evaporating dish with EGME were also placed in the dessicator. The dessicator was continuously evacuated for one hour and the samples were weighed. This procedure was repeated twice per day until the weight remained constant. Then the liquid EGME was removed and the retention was determined at lower EGME vapour pressure.

The experiments were also inadvertently carried out with ethylene glycol diethyl ether (EGDE).

[1] The glasses were engraved with a diamond marker, because at the higher vapour pressure any ink label was unrecognisable and paper labels also adsorbed EGME.

6.7 Adsorption of ethylene glycol, ethylenglycol mono- and diethyl ether

Adsorption of EG, EGME and EGDE was measured on the common clays, the purified bentonites M40a$_{TL}$, M47$_{TL}$ and M48$_{TL}$ and the reduced charge samples.

Ethylene glycol

During the first days of the experiment a fast adsorption was observed for all samples. This phase lasted, depending on the sample, between one and nine days. After this phase, the adsorption rate decreased but continued almost constantly for a period of 60 days. Data were evaluated by two linear regression lines for the fast and slow adsorption phase. The point of intersection was intended to represent the monomolecular coverage. There is, however, some arbitrariness in defining the fast adsorption phase, since its duration depends on the sample and on the amount exposed; there is no sharp transition. Nevertheless the duplicates were in good accordance, the error was within 5%. The adsorption rate also depended on the environmental conditions. For example, 35 days after the start of the experiment in a very warm period, all samples adsorbed more EG than on other days. The time-dependent adsorption is shown in the App. 9.3, the results are summarised in Tab. 6.1.

The samples adsorbed from 0.01 to 0.31 g ethylene glycol per gram of dried clay. The lowest values were observed for the KGa-1 kaolin, the highest for the reduced charge montmorillonite HK90. Taking into account the conversion factor of 0.45 mg/m^2, HK90 has a specific surface area of 688 m^2. The purified montmorillonites M40a$_{TL}$, M47$_{TL}$ and M48$_{TL}$ have specific surface areas between 611 and 644 m^2/g. The common clays adsorbed 0.03 to 0.16 g/g corresponding to 67 to 356 m^2/g. The lithium exchanged Li-M48 sample adsorbed about 0.9 g EG/g of montmorillonite. This would correspond to 2000 m^2/g, which is 2.5 times the maximum specific surface area of a montmorillonite!

Ethylene glycol monoethylether (EGME)

At higher vapour pressure (lvp) the samples attained a constant weight after one week. On the eleventh day of the experiment the evaporating dish with liquid EGME was removed to reduce the vapour pressure. The samples took three days to attain a constant weight at lower vapour pressure (lvp).

0.19 to 0.31 g EGME/g were adsorbed at higher vapour pressure. With the conversion factor of 0.367 mg/m^2 M47$_{TL}$ (0.289 g/g) has a specific surface are of 787 m^2/g. The Li-M48 sample retained as much as 2.8 g EGME/g, corresponding to 7529 m^2/g, which is almost ten times more than the maximum specific surface area of a montmorillonite.

0.06 to 0.19 g EGME/g were retained at lower vapour pressure. M40a$_{TL}$ adsorbed the largest amount which corresponds to 657 m^2/g if the conversion factor of 0.286 mg/m^2 is applied.

Ethylene glycol diethylether (EGDE)

The evaporation rate of EGDE is much lower than of EGME. For this reason the samples took about five weeks to attain a constant weight at high vapour pressure. Amounts of 0.03 to 0.61 g EGDE/g were retained.

When the evaporating dish with liquid EGDE was removed, the samples took one more week to equilibrate and retained 0.01 to 0.21 g EGDE/g at lower vapour pressure. Again, the Li-M48 sample retained much more EGDE than all other samples, especially at high vapour pressure.

Tab. 6.1 : Adsorption of ethylene glycol (EG) and retention of ethylene glycol monoethylether (EGME) and ethylene glycol diethylether (EGDE) at lower vapour pressure (lvp) and at higher vapour pressure (hvp).

	EG g/g	EGME (lvp) g/g	EGME (hvp) g/g	EGDE (lvp) g/g	EGDE (hvp) g/g
			common clays		
Augzin$_{TL}$	0.078	0.032	0.080	0.065	0.179
Friedländer$_{TL}$	0.163	0.069	0.167	0.144	0.244
HS7$_{TL}$	0.090	0.042	0.109	0.077	0.275
Plessa$_{TL}$	0.098	0.044	0.100	0.076	0.175
Teistungen$_{TL}$	0.069	0.034	0.079	0.055	0.144
Thierfeld$_{TL}$	0.036	0.017	0.093	0.029	0.080
Augzin$_{sieved}$	0.031	0.019	0.036	0.018	0.059
HS7$_{sieved}$	0.070	0.036	0.093	0.040	0.238
			kaolin		
KGa-1	0.010	0.006	0.019	0.010	0.029
			montmorillonites		
M40a$_{TL}$	0.290	0.188	0.266	0.141	0.328
M47$_{TL}$	0.286	0.181	0.289	0.161	0.339
	EG g/g	EGME (lvp) g/g	EGME (hvp) g/g	EGDE (lvp) g/g	EGDE (hvp) g/g

$M48_{TL}$[2]	0.275	0.169	0.260	0.142	0.303
Na-M48	0.286	0.163	0.309	0.160	0.352
Li-M48	0.871	0.176	2.763	0.240	2.741
			reduced charge samples		
HK0	0.105	0.053	0.184	0.081	0.393
HK10	0.121	0.057	0.199	0.091	0.427
HK20	0.121	0.057	0.205	0.087	0.424
HK30	0.135	0.068	0.223	0.135	0.510
HK40	0.139	0.068	0.236	0.097	0.492
HK50	0.147	0.065	0.228	0.099	0.332
HK60	0.155	0.068	0.239	0.123	0.354
HK70	0.158	0.071	0.247	0.103	0.335
HK80	0.261	0.130	0.322	0.164	0.599
HK90	0.310	0.176	0.312	0.199	0.610
HK100	0.308	0.178	0.310	0.214	0.433

Comparison of the methods

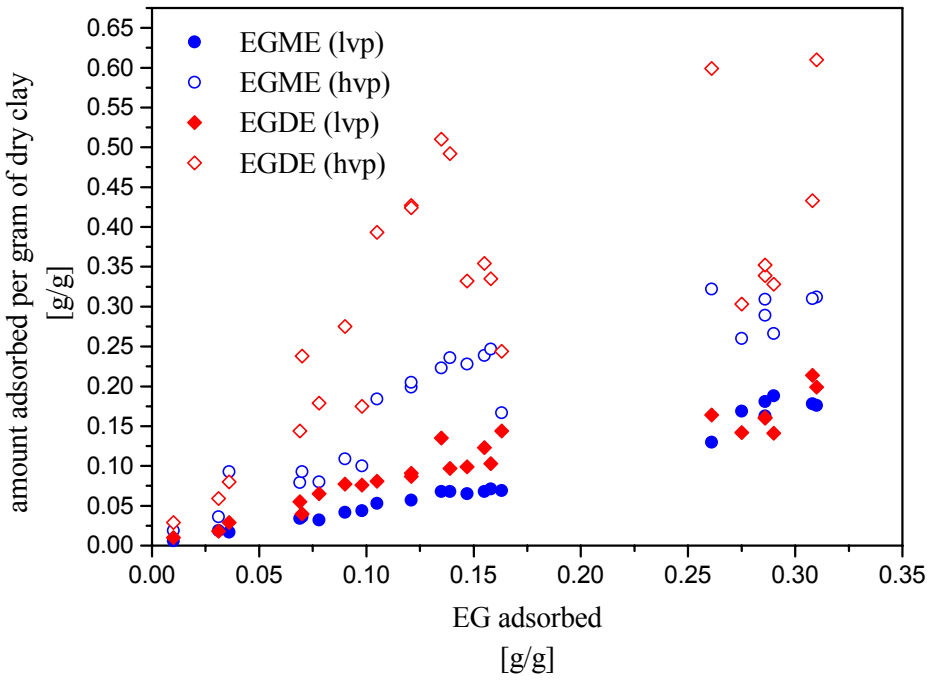

Fig. 6.2 : Adsorption of ethylene glycol (EG), ethylene glycol mono- (EGME) and diethylether (EGDE) at lower vapour pressure (lvp) and higher vapour pressure (hvp).

Eltantawy and Arnold (1974) stated that EG adsorption was in good agreement with EGME retention at higher vapour pressure. In our experiments the correlation was better if EGME

[2] The samples $M48_{TL}$ and Na-M48 were purified by the same procedure but in two runs by different persons.

was retained at lower vapour pressure EGME (lvp). Note that all samples were sodium exchanged, except KGa-1, $Augzin_{sieved}$ and $HS7_{sieved}$. The Li-M48 sample is not displayed.

A rather good correlation is found between EG adsorption and EGME and EGDE retention at lower vapour pressure but not for the adsorption at higher vapour pressure (Fig. 6.2). A good correlation is also found between the amount of EGME retained at lower and higher vapour pressure (Fig. 6.3). Two regions can be distinguished: one region with an almost linear correlation between the two quantities and a second region at higher EGME loading with a smaller (hvp)/(lvp) ratio. Region I contains all mixed layer samples and the samples HK0 to HK70. Region II contains all montmorillonites and HK80 to HK100. Samples of region II are more easily expandable and EGME can enter the interlayer space at lower vapour pressure.

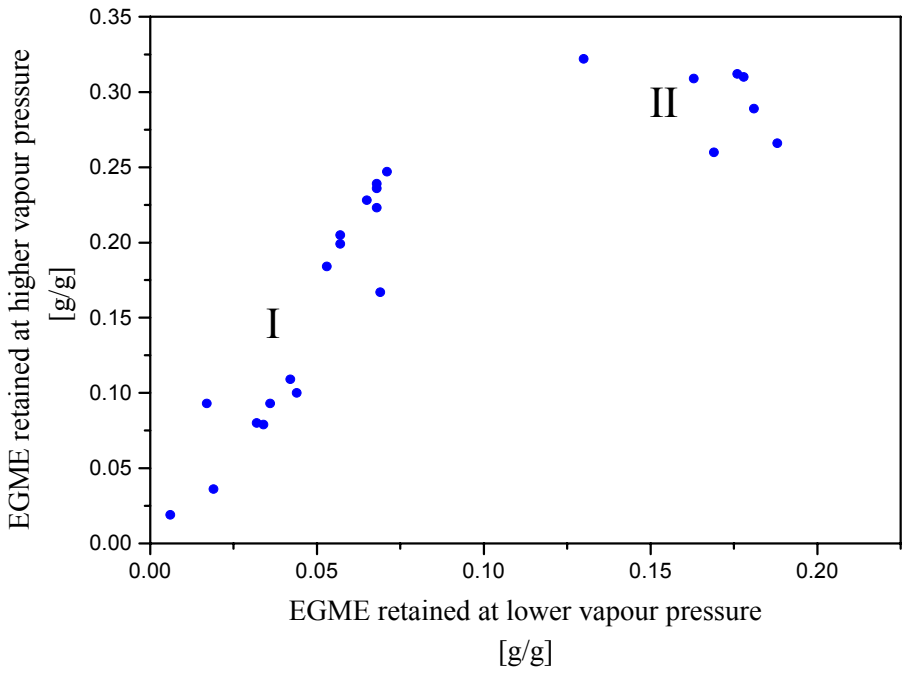

Fig. 6.3 : EGME retention at higher and at lower vapour pressure.

Reduced charge samples

For a better understanding of the adsorption techniques, the reduced charge samples were investigated with the EG, the EGME and the EGDE methods. The cation exchange capacity was determined and the X-ray diffractograms of the EG-solvated samples were recorded. For experimental details of the X-ray diffraction see Chap. 3.1. The ratio of the expanded layers was estimated by dividing the peak area of the expanded layers' reflection at $°2\Theta = 5.2$ by the sum of the peak areas of expanded and collapsed layers at $°2\Theta = 10.0$.

To permit a common plot of all data, the data of each sample were normalised by the values of the HK100 sample. Note that HK100 was 100% sodium exchanged, therefore, no charge reduction was expected for this sample. The data were plotted vs. the sodium content of the HK samples before heating (Fig. 6.4).

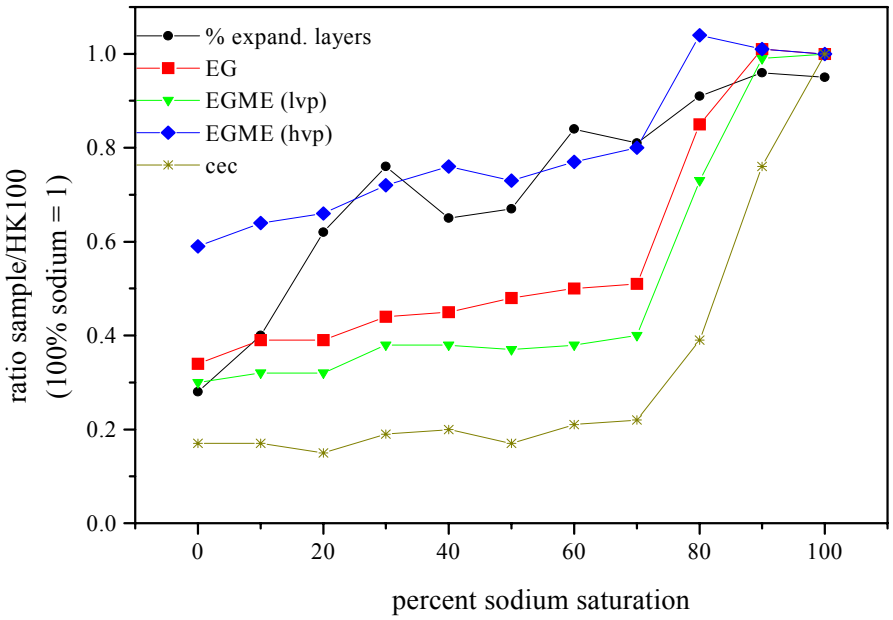

Fig. 6.4 : Influence of charge reduction on the expandability, adsorption of EG, EGME (lvp) and (hvp) and on the cec.

A sharp step between HK0 to HK70 and HK80 to HK100 is observed for the cation exchange capacity, the EG adsorption and the EGME retention at lower vapour pressure. The cec of HK70 is about 20% of the original value, though only 30% of the exchangeable cations were lithium ions. The EGME retention at lower vapour pressure exhibits a similar tendency: with increasing lithium content a strong decrease of the adsorbed amount is observed which remains almost constant from HK70 to HK0. The variation of the EG adsorption is similar but a slight decrease in the amount adsorbed is maintained with increasing lithium content.

EGME adsorption at higher vapour pressure shows a different behaviour. HK0 adsorbed 60% of the amount of HK100. The amount of EGME adsorbed decreases with increasing lithium content. The portion of expandable layers estimated from X-ray diffraction varies nearly in the same way. One should keep in mind that for the X-ray analyses the samples were wetted with excess ethylene glycol, so that these samples correspond to EG adsorption at higher vapour pressure.

Specific surface areas

Specific surface areas were calculated from the EG adsorption and EGME lvp and hvp retention experiments using the conversion factors reported by Eltantawy and Arnold, (1973 and 1974) and Carter et al. (1986). All data are reported in Tab. 6.3. For comparison, specific surface areas were also estimated from cec data. Lagaly (1994) found equivalent areas of ≈ 75Å/charge for montmorillonites. If the cec is known, the basal plane area can be estimated by eq. 1[3] :

$$\text{eq. 1}: \quad S = 2 \cdot 6.02 \cdot 75 \cdot f \cdot cec \qquad [m^2/g]$$

The factor f is applied, because only ≈80% of the charges are located on the basal surfaces, thus f is ≈0.8. The surface areas of the various methods were plotted vs. surface area determined with EG adsorption (6.5).

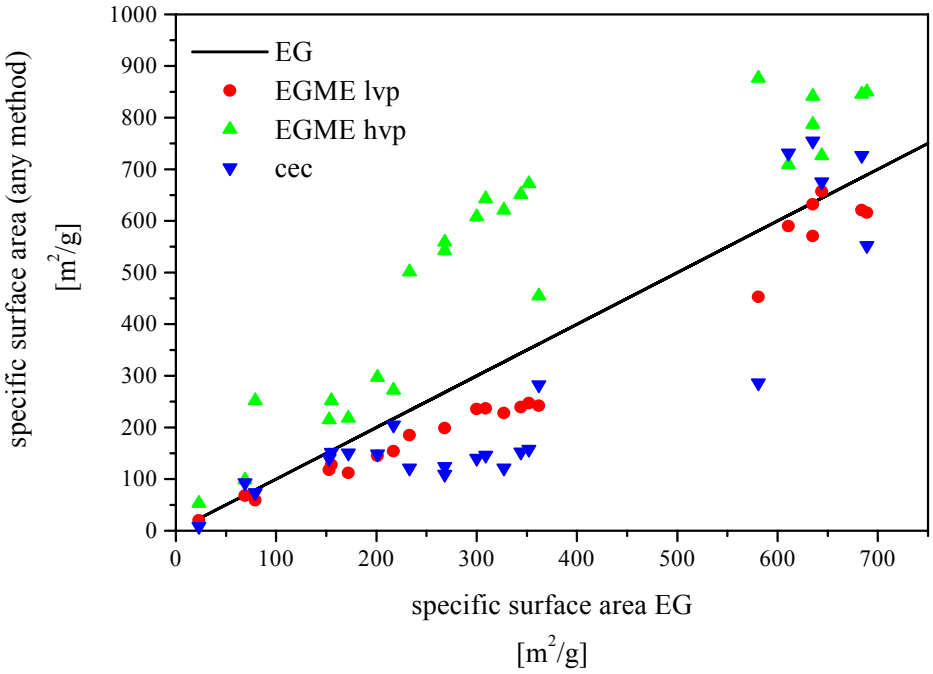

Fig. 6.5 : Specific surface area determined with EG adsorption, EGME retention at lower vapour pressure (lvp) and at higher vapour pressure (hvp) and estimated from cec data.

EGME hvp yielded higher values than EG adsorption, the derived values for some montmorillonites were larger than the maximum specific surface area. Li-M48 retained an amount of EGME corresponding to ten times the maximum specific surface area. EG adsorption, EGME lvp retention and cec data varied considerably. Note, that Li-M48 is not displayed.

[3] The dimension of the cec is meq/g.

Conclusions

Four different methods for the determination of the specific surface area were compared. Surface areas were not calculated from EGDE adsorption data, because this method is not a practicable method. Each method yielded different results. A specific surface area of 760 to 810 m^2/g was assumed for the purified montmorillonites.

- The EGME (hvp) method yielded too high values and the amount of EGME retained depended on the type of the interlayer cations. This method does not seem to be suitable for specific surface area determinations.
- The adsorption of EG also depended on the interlayer cation. However, sodium exchanged montmorillonites yielded reasonable values.
- Only in the EGME (lvp) experiments, the interlayer cation almost did not affect the amount of EGME retained. The derived specific surface areas of the montmorillonites were 590 to 657 m^2/g.
- Estimation of the specific surface area from cec data yields reasonable values for the montmorillonites but no correlation was found between adsorption of EG or retention of EGME.

The experimental setup of the EG, EGME (lvp) and EGDE (hvp) adsorption experiments with a separate container for calcium chloride and the liquids to be adsorbed makes interpretation of the results complicated. If the liquids were applied as calcium chloride saturated solutions a constant vapour pressure of the liquid was ensured. The chosen experimental setup with two separated containers, however, provides a somewhat higher vapour pressure of the liquid which is probably not a fixed value, since the thermodynamic conditions are uncertain. It is likely that a gradient of the vapour pressure exists among the two containers. The diameter and the distance of the containers may also play a role. When no separate container with the liquid is placed in the desiccator, the vapour pressure of the liquid is also not fixed because the solvation state of the calcium chloride depends on the amount of calcium chloride and the amount of the liquid released from the samples.

However, both experimental setups permit to distinguish more and less easily expanding minerals. At lower vapour pressure only the samples HK80 to HK100 are expandable, whereas at high vapour pressure the amount of expandable layers depends on the degree of charge reduction.

The observed reduction of the cec is larger than the lithium content of the exchangeable cations. Therefore, the decrease of the cec cannot be due only to lithium fixation. Probably the layers of the HK70 to HK0 samples collapse and no longer exhibit the swelling properties of the original sample. Therefore, the cation exchange can only take place on the edges of the clay mineral lamellae. This observation corresponds to the estimation (Lagaly, 1993) that about twenty percent of the cec is located on the edges.

6.8 Adsorption on common clays

Adsorption of cetylpyridinium ions

See Chap. 5.3 for the results of cetylpyridinium adsorption.

Adsorption of polyvinyl pyrrolidone (PVP)

0.03 to 0.7 g/g PVP (0.24 to 6.2 mmole/g) were adsorbed onto the clays (Fig. 6.6). The highest amounts were adsorbed by the montmorillonites, the smallest by $Augzin_{sieved}$.

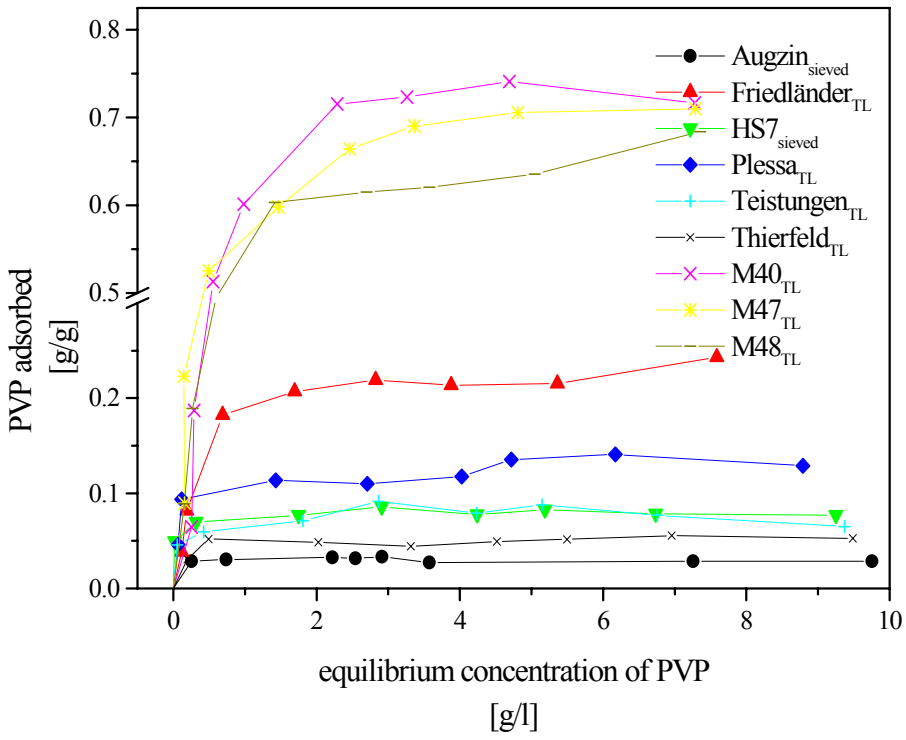

Fig. 6.6 : Amount of polyvinyl pyrrolidone adsorbed by the clays.

Adsorption of methylene blue

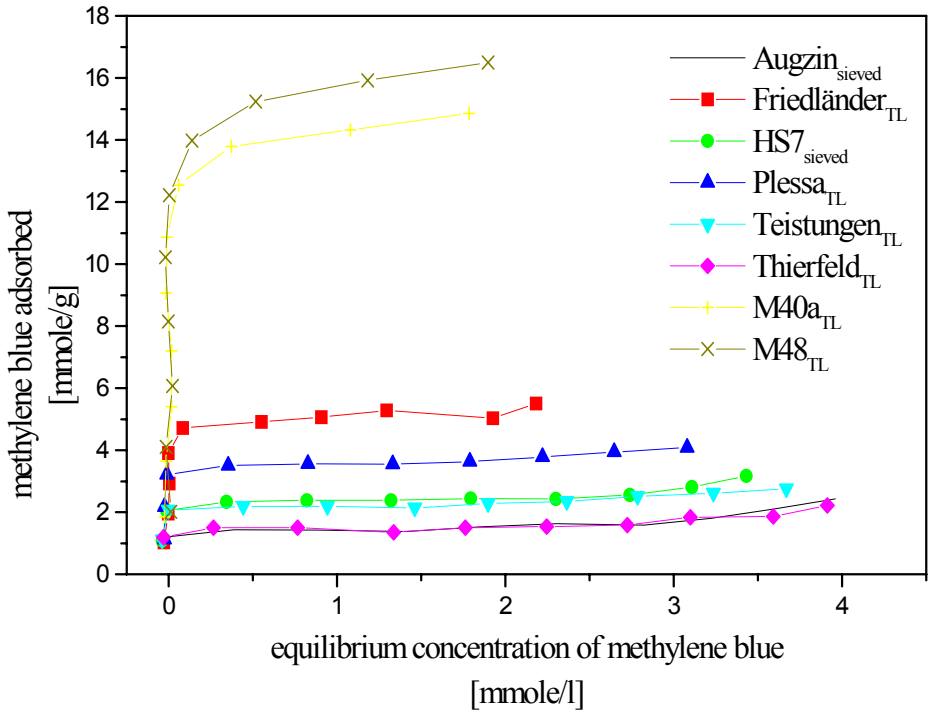

Fig. 6.7 : Amount of methylene blue adsorbed by the clays.

The plateaux of the methylene blue adsorption lie between 0.15 and 1.65 mmole/g (Fig. 6.7), the halo points between 0.1 and 0.6 mmole/g. Thierfeld$_{TL}$ and Augzin$_{sieved}$ adsorbed the smallest amounts of methylene blue, the montmorillonites the largest.

Adsorption of alkylammonium ions

The amount of alkylammonium ions adsorbed by the clays varied between 0.09 and 0.86 mmole/g for decylammonium ions, between 0.12 and 0.82 mmole/g for the dodecylammonium ions and between 0.16 and 0.82 mmole/g for the tetradecylammonium ions. Augzin$_{sieved}$ adsorbed the smallest amounts, the montmorillonites the largest. The results of the adsorption experiments on the mixed layer clay samples are summarised in Tab. 6.2. Results of ethylene glycol, ethylenglycol mono- and diethylether adsorption are given in Tab. 6.1 Chap. 6.7.

Tab. 6.2 : Adsorption capacity of clays: Adsorption of methylene blue (MB) (halo point and saturation adsorption (sat)), adsorption of polyvinyl pyrrolidone (PVP), decylammonium ions (C10), dodecylammonium ions (C12), tetradecylammonium ions (C14) and cetyl pyridinium chloride (CPC).

	MB halo mmole/g	MB sat mmole/g	PVP mmole/g	PVP g/g	C10 mmole/g	C12 mmole/g	C14 mmole/g	CPC mmole/g
				common clays				
$Augzin_{sieved}$	0.1	0.15	0.24	0.03	0.09	0.12	0.16	0.09
$Friedländer_{TL}$	0.4	0.52	1.83	0.20	0.35	0.33	0.35	0.30
$HS7_{sieved}$	0.2	0.24	0.68	0.08	0.19	0.16	0.23	0.16
$Plessa_{TL}$	0.3	0.36	1.16	0.13	0.23	0.22	0.28	0.27
$Teistungen_{TL}$	0.2	0.22	0.67	0.07	0.19	0.20	0.25	0.15
$Thierfeld_{TL}$	0.1	0.15	0.45	0.05	0.14	0.16	0.18	0.11
				montmorillonites				
$M40a_{TL}$	0.6	1.49	6.22	0.69	0.76	0.65	0.72	
$M47_{TL}$			6.03	0.67	0.85	0.78	0.82	
$M48_{TL}$	0.6	1.65	5.66	0.63	0.86	0.82	0.82	

Comparison of the adsorption experiments

A number of adsorption experiments were carried out to study the common clays Augzin, Friedländer, HS7, Plessa, Teistungen and Thierfeld. The cation exchange capacity was determined, and several methods were applied to determine the specific surface area of the samples. One aim was to find out whether the amount of substances adsorbed on the clays depends on the number of charges or the specific surface area. Unfortunately, with this set of samples it is difficult to discriminate if the adsorption is dominated by the charges or the surface area, because these two quantities are highly correlated (Fig. 6.8). This result was surprising because a priori there is no correlation expected between these quantities. However, comparing the main components of the common clays, kaolinite and chlorite have the smallest cec and the smallest specific surface area, smectite the largest whereas illite lies between these minerals. Therefore, the smectite content has the greatest influence on the cec and the specific surface area. This may explain the almost linear correlation for the common clays. Furthermore, the charge density and the ratio of edge charges to basal surface charges play a role.

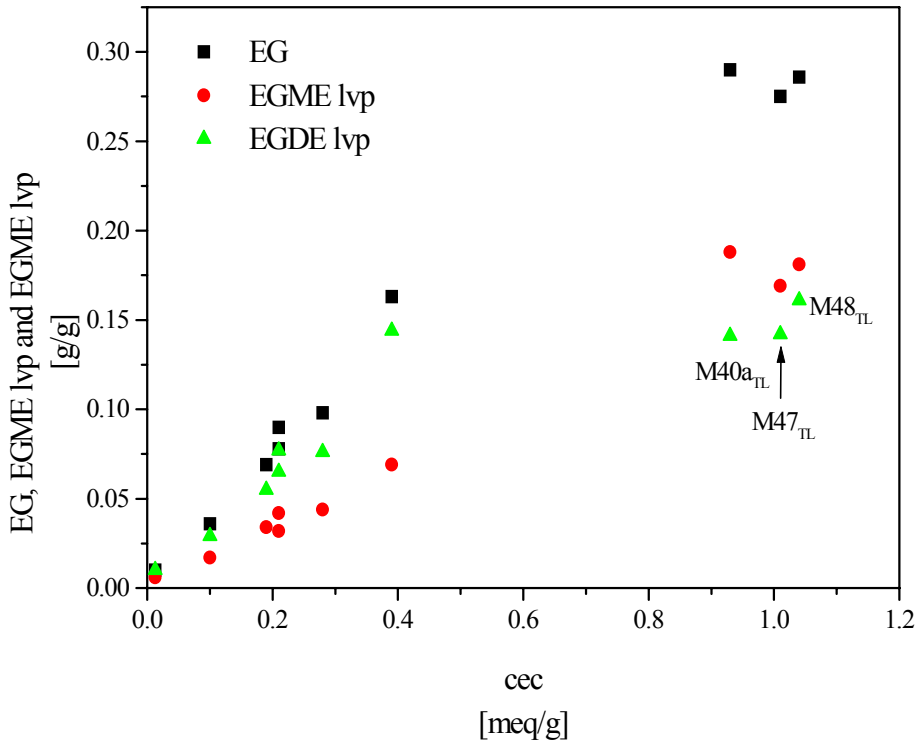

Fig. 6.8 : Adsorption of ethylene glycol (EG), ethylene glycol monoethylether (EGME) at lower vapour pressure (lvp) and ethylene glycol diethylether (EGDE) at lower vapour pressure

Comparing the adsorption of ethylene glycol, ethyleneglycol mono- and diethylether at low vapour pressure with the cation exchange capacity (Fig. 6.8), a general tendency is observed: with increasing cec the adsorbed amount of these substances increases, an almost linear correlation is found for EGME. EG and EGDE have an almost linear correlation for the common clay samples, whereas the values for the montmorillonites lie distinctly below these lines.

The methylene blue adsorption at the halo point and the saturation adsorption were also compared with the cec (Fig. 6.9). Up to 1.65 mmole MB/g were adsorbed by the saturation isotherms. A linear correlation between the cec and the saturation adsorption of methylene blue is observed, indicating that 1.7 methylene blue molecules correspond to one surface charge. A cross sectional area of 130Å^2 for the MB molecule (Kahr and Madsen, 1995) corresponds to a coverage of 783 m^2/mmole. Thus, 1.65 mmole MB/g of M48$_{TL}$ correspond to a surface area of 1292 m^2/g. This value is greater than the crystallographic surface area. The reason is that at higher concentrations the MB molecules are not adsorbed in face to face orientation on the silicate layers. If this value is divided by 1.7, the specific surface area of the basal planes (760 m^2/g) is obtained. Therefore, specific surface areas of the saturation adsorption data were calculated with a conversion factor of 460 m^2/mmole.

The halo point varied within 0.1 mmole/g for $Augzin_{sieved}$ and $Thierfeld_{TL}$ sample to 0.6 mmole/g for the montmorillonites. 0.6 mmole/g methylene blue corresponds to a specific surface area of 470 m^2/g. This is distinctly too low for a montmorillonite, indicating that a determination of the specific surface area cannot be done with the halo point.

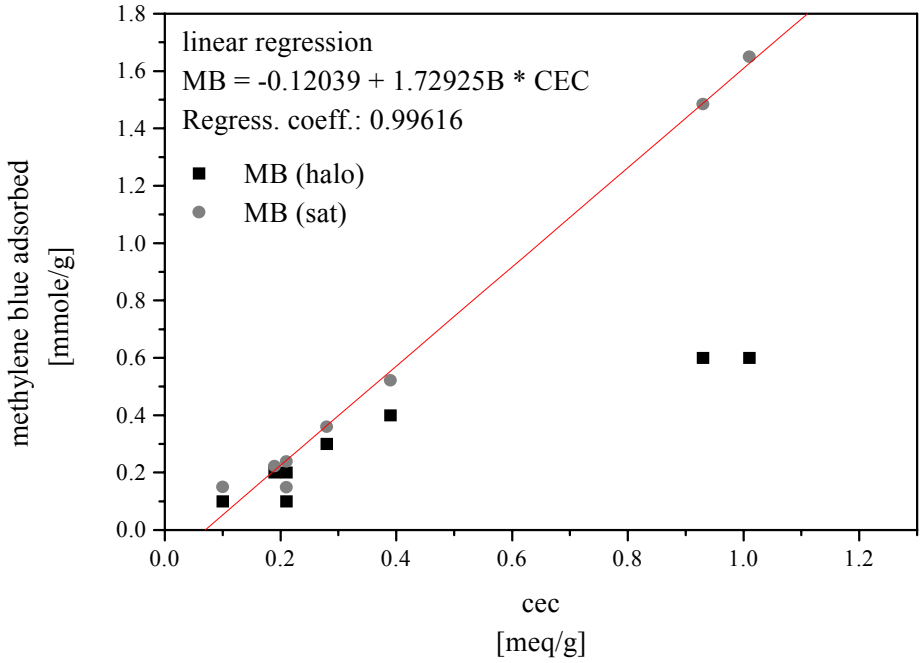

Fig. 6.9 : Adsorption of methylene blue (MB); halo point (halo) and saturation adsorption (sat).

The adsorption of alkylammonium ions and cetylpyridinium chloride is in rather good agreement with the cec (Fig. 6.11) for the common clays, but too low for the montmorillonites. The correlation with the ethylene glycol adsorption is even worse.

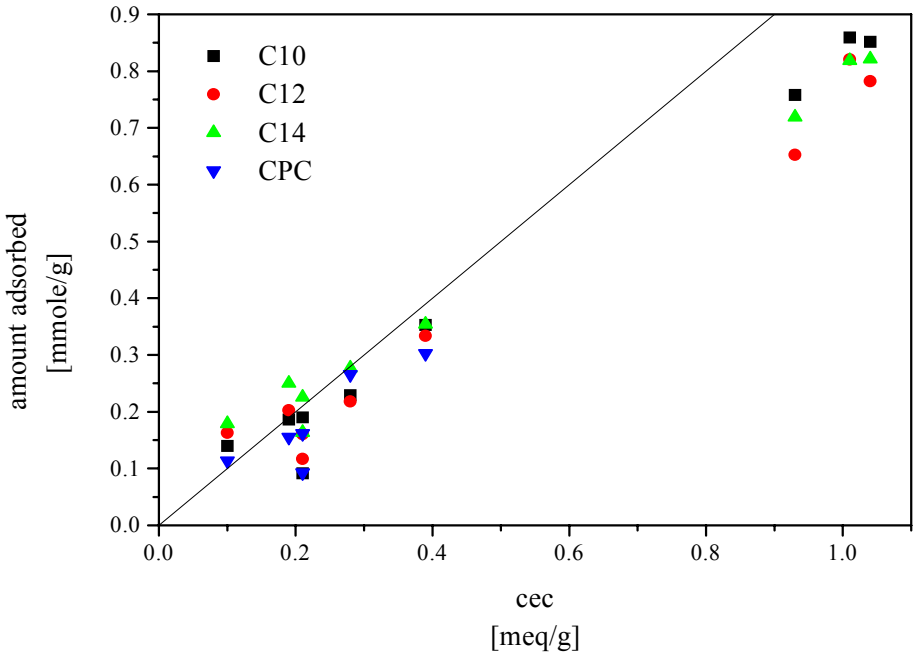

Fig. 6.10 : Adsorption of decylammonium ions (C10), dodecylammonium ions (C12), tetradecylammonium ions (C14) and cetyl pyridinium chloride (CPC).

Tab. 6.3 : Specific surface areas (m^2/g) determined with ethylene glycol (EG) adsorption, ethylene glycol monoethylether (EGME) retention at lower (lvp) and higher (hvp) vapour pressure, adsorption of methylene blue (MB) at the halo point (halo) and saturation adsorption (sat), and estimated from the cec and adsorption of decylammonium ions (C10), dodecylammonium ions (C12), tetradecylammonium ions (C14) and cetyl pyridinium chloride (CPC).

	EG	EGME lvp	EGME hvp	CEC	MB halo	MB sat	C10	C12	C14	CPC
conversion factor	0.45 mg/m^2	0.286 mg/m^2	0.367 mg/m^2	722 m^2/meq	783 m^2/ mmole	460 m^2/ mmole	722 m^2/meq	722 m^2/meq	722 m^2/meq	722 m^2/meq
					common clays					
$Augzin_{TL}$	172	112	218	150						
$Friedländer_{TL}$	362	242	455	282	313	240	255	241	256	218
$HS7_{TL}$	201	145	297	148						
$Plessa_{TL}$	217	154	272	204	235	166	166	158	200	192
$Teistungen_{TL}$	153	118	215	140	157	102	135	146	181	112
$Thierfeld_{TL}$	79	59	252	73	78	69	101	118	129	82
$Augzin_{sieved}$	69	68	98	92	78	69	66	84	118	67
$HS7_{sieved}$	155	128	252	151	157	110	137	116	163	116
	EG	EGME lvp	EGME hvp	CEC	MB halo	MB sat	C10	C12	C14	CPC
					kaolin					
KGa-1	23	20	53	8						
					montmorillonites					

$M40a_{TL}$	644	657	726	675	470	683	548	472	519
$M47_{TL}$	635	632	787	754			615	565	593
$M48_{TL}$	611	590	709	731	470	759	621	593	591
Na-M48	635	571	841						
Li-M48	1935	614	7528						
				reduced charge montmorillonites					
HK 0	233	185	501	121					
HK 10	268	199	542	124					
HK 20	268	199	559	109					
HK 30	300	236	608	140					
HK 40	309	237	643	146					
HK 50	327	228	621	121					
HK 60	344	239	651	152					
HK 70	352	247	672	157					
HK 80	581	453	876	286					
HK 90	689	616	850	552					
HK 100	684	621	845	726					

Conclusions

A general tendency was observed in all adsorption experiments. With increasing cation exchange capacity the amounts of EG, EGME, EGDE, CPC, PVP, MB and alkylammonium ions increase. A decisive conclusion as to whether the adsorption is reigned by the cationic charges or the specific surface area was not reached due to the increase of the specific surface area with the cec. As revealed by the charge-reduced montmorillonites, the choice between EG adsorption and EGME and EGDE adsorption at high and low vapour pressure may be a tool to detect the easily expandable layers. Instead of specific surface area a more accurate term to use is e.g. ”the surface accessible to ethylene glycol under the given conditions”.

7 Discussion and summary

The specific surface area of a clay mineral comprises the external and internal surface area and, finally, the surface area which is exposed to the solution (Chap. 6.1). The aim of this study was to correlate adsorption data of common clays with these specific surface areas.

Gas adsorption is usually considered to occur only on the external surfaces, but Lagaly (1993) mentioned, that gas molecules can partly enter the interlayer space. Kloppenburg (1997) and Bojemüller (2003) found that the specific surface area of montmorillonite differs if the sample is freeze-dried or spray-dried. Therefore, gas adsorption data represent the surface area accessible to gas molecules.

The important but still unsolved question is which surface area is accessible to solutions. In two cases this question can be simply answered: (i) montmorillonite which fully delaminate provide a specific surface area of about 800 m^2/g, (ii) clay minerals which do not swell have a specific surface area similar to the gas adsorption values. However, these ideal systems are seldom found. In particular the degree of delamination of montmorillonite depends sensitively on the composition of the solutions and the purity of the mineral. The problems are still more evident for common clays with mixed-layer structure which contain montmorillonitic interlayer spaces. These interlayer spaces may be accessible to adsorptives or may not. Thus, measurement of the accessible specific surface area of these clays is strongly needed but the problem is still unsolved. A possible application could be the analysis of clays, which are chosen as sealing materials for waste deposits. Among the clays which posses the desired hydraulic permeability and swelling properties, a clay with a larger surface area exposed to the solution is supposed to be capable to adsorb and fix more ions or molecules.

Unfortunately, determination of the specific surface area exposed to the solution by the negative adsorption, could not be applied to the common clays. Many other techniques were employed but the correlation between the different adsorption data was poor or absent. The adsorptives comprised ethylene glycol, ethylene glycol mono- and diethylether, polyvinyl pyrrolidone, methylene blue and alkylammonium ions. Each substance was adsorbed in a different way. Generally, no method permits a correct determination of the specific surface area but some methods permit rather good estimations of the specific surface area.

Adsorption of ethylene glycol, ethylene glycol mono- and diethylether (at lower and higher vapour pressure) was studied in detail. Montmorillonites with different layer charge

and lithium and a sodium exchanged montmorillonites were investigated. In the EG, EGME (hvp), EGDE (lvp, hvp) experiments the amount adsorbed by the lithium exchanged sample was 16 times higher than for the sodium exchanged sample. Therefore, all these methods cannot be suitable to determine specific surface areas. Only the retention of EGME at lower vapour pressure was almost not affected by the nature of the interlayer cation.

Eltantawy and Arnold (1973 and 1974) and Carter et al. (1965) reported the conversion factors to calculate the specific surface area from the amounts of EG adsorbed and EGME retained at lower and higher vapour pressure. If these factors were used, only the EGME retention at higher vapour pressure yielded values of about 800 m^2/g for the montmorillonites. The surface areas calculated with EG adsorption and EGME lvp retention were too low. However, the authors measured the adsorption or retention for one montmorillonite and divided it by the maximum specific surface area, thus 800 to 810 m^2/g. No details were reported, if the sample was purified or not. Therefore the conversion factors could be erroneous.

The adsorption data were also related to the cation exchange capacity (cec). To permit a correct determination of the cec, two methods using copper complexes were evaluated and compared to the ammonium acetate method. Photometric determination was selected as the most simple procedure. Data were erroneous when the procedure was carried out as described in the literature. Addition of buffer was found to be necessary for samples with low pH. Both methods were simplified and the precision could be increased.

The cation exchange capacity and the specific surface area are a priori independent. However, comparing the adsorption experiments with the cec of the common clays, an increasing adsorption capacity was observed with increasing cec. An almost linear correlation was found between the methylene blue saturation adsorption and the cec. The different compounds of common clays contribute in different ways to the specific surface area and the cec. Kaolinite and chlorite have a small cec and small specific surface areas, smectite has the largest and illite lies between these minerals. For this reason, the smectite and illite content contribute the most to the cec and the specific surface area. Estimation of specific surface area from cec data yielded reasonable values for the montmorillonites, but too low values for the common clays or reduced charge montmorillonites. Lagaly (1981) estimated 10 to 20% of the charges to be located on the edges of montmorillonites. The portion of edge charges in arbitrary common clays may be distinctly different.

Besides charges and the specific surface area a third factor can be important to control the adsorption on clay minerals: the quantity and the acidity of acidic sites. Potentiometric titration was employed to study the acidic properties of bentonites and pillared clays.

Shortcomings of the traditional titration experiment are (i): the sample is diluted during the experiment, (ii): one has to chose either concentrated solutions if a large pH range is studied or diluted solutions for a higher resolution (iii): if pH equilibrium is attained slowly, the required time can be very long. To avoid these shortcomings, an alternative titration experiment was designed, the multibatch titration experiment. It permits to study the proton adsorption or release kinetics. Furthermore, concentrated and diluted solutions can be combined. A $\Delta V / \Delta pH$ plot was developed for evaluation and presentation of titration data. It permits the determination of amounts and acid constants of acidic sites. The evaluation is based on simple mathematics. The multibatch titration experiment and the $\Delta V / \Delta pH$ plot permit a new understanding of surface phenomena.

8 Literature cited

Ammann, L., 2000, Aufarbeitung und Charakterisierung von Bentoniten, Diplomarbeit, Universität Kiel

Avena, M., Valenti, L. E., Pfaffen, V., de Pauli, C. P. 2001, Methylene blue dimerization does not interfere in surface-area measurements of kaolinite and soils, Clays and clay minerals **49,** 168-173

Avena, M. J., Cabrol, R., de Pauli, C. P. 1990, Study of some physicochemical propertiers of pillared montmorillonites: acid-base potentiometric titrations and electrophoretic measurements, Clays and clay minerals **38,** 356-362

Bandosz, T. J., Jagiello, J., Putyera, K., Schwarz, J. A. 1994, Characterization of acidity of pillared clays by proton affinity distribution and drift spectroscopy, J. Chem. Soc. Faraday Trans **90,** 3573-3578

Behrens, H., 1996, Perkolationsversuche zur Untersuchung des Einflusses organischer Schadstofflösungen und Sickerwäasser auf tonige Deponieabdichtungen, Verlag Dr. Köster

Bergaya, F., Vayer, M. 1997, CEC of clays: Measurement by adsorption of a copper ethylendiamine complex, Applied clay science **12,** 275-280

Blum, T., 2001, Charakterisierung und Quantifizierung von Bentoniten, Diplomarbeit, Universität Kiel

Bojemüller, E., 2003, Porenstruktur und Adsorptionsverhalten von Tonmineralen, Dissertation, Universtität Kiel

Bolt, G.H., Warkentin, B.P. 1958, The negative adsorption of anions by clay suspensions, Kolloid-Zeitschrift **156,** 41-46

Bowden, J. W., Posner, A. M., Quirk, J. P. 1977, Ionic adsorption on variable charge mineral surfaces. Theoretical-charge development and titration curves, Aust. J. Soil Res. **15,** 121-136

Bower, C. A., Geschwend, F. B. 1952, Ethylene glycol retention by soils as a measure of surface area and interlayer swelling, Soil Sci. Soc. Am. Proc. **16,** 342-345

Bower, C. A., Gortzen, J. O. 1959, Surface area of soils and clays by an equilibrium ethylene glycol method, Soil Sci. **87,** 289-292

Brindley, G. W., 1965, Ethylene glycol and glycerol complexes of smectites and vermiculites, Clay minerals **6,** 237-59

Brindley, G. W., Gözen Ertem 1971, Preparation and solvation properties of some variable charge montmorillonites, Clays and clay minerals **19,** 399-404

Bujdák, J., Janek, M., Madejová, J., Komadel, P. 1998, Influence of the layer charge density of smectites on the interaction with methylene blue, Journal Chemical Society, Faraday Transactions **94,** 3487-3492

Bujdák, J., Komadel, P. 1997, Interaction of methylene blue with reduced charge montmorillonite, Journal Physical Chemistry **101,** 9065-9068

Burba, J. L., McAtee, J. L. Jr. 1977, The orientation and interaction of ethylenediamine copper (II) with montmorillonite, Clays and clay minerals **25,** 113-118

Calvert, C. S., 1984, Simplified, complete CsCl-hydrazin-dimethylsulfoxide intercalation of kaolinite, Clays and clay minerals **32,** 125-130

Carter, D. L., Mortland, M. M., Kemper, W. D. 1986, Methods of soil analysis, Part I. Physical and mineralogical methods - agronomy monograph n 9 (2nd edition), **,** 413-423

Cenens, J., Schoonheydt, R.A. 1988, Visible spectroscopy of methylene blue in hectorite, laponite b, and barasym in aqueous suspension, Clays and Clay Minerals **36,** 214-224

Chhabra, R., Pleysier, J., Cremers, A. 1975, The measurement of the cation exchange capacity and exchangeable cations in soils: A new method, Proc. Int. Clay Conf. 1975 **,** 439 - 449

Chorover, J., Spsito, G. 1995, Surface charge characteristics of kaolinitic tropical soils, Geochimica et Cosmochimica Acta **59,** 875-884

Contescu, C., Jagiello, J., Schwarz, J. A. 1993, Heterogeneity of proton binding sites at the oxide/solution interface, Langmuir **9,** 1754-1765

Davis, C. E., Ahmad, N., Jones, R. L. 1971, Effect of exchangeable cations on the surface area of clays, Clay minerals **9,** 258-261

Dohrmann, R., 1997, Kationenaustauschkapazität von Tonen
Bewertung bisheriger Analysenverfahren und Vorstellung einer neuen und exakten Silber-Thioharnstoff-Methode, Dissertation, Aachener Geowissenschaftliche Beiträge **26**

Dyal, R. S., Hendricks, S. B. 1950, Total surface of clays in polar liquids as a characteristic index, Soil science **69,** 421-432

Eberl, D. D., Nuesch, R., Sucha, V., Tsipursky, S. 1998, Measurement of fundamental illite particle thickness by x-ray diffraction using pvp-10 intercalation, clays and clay minerals **46,** 89-97

Eltantawy, I. M., Arnold, P. W. 1973, Reappraisal of ethylene glycol mono-ethyl ether (EGME) method for surface area estimations of clays, Journal of soil science **24,** 232-238

Eltantawy, I. M., Arnold, P. W: 1974, Ethylene glycol sorption by homoionic montmorillonites, J. Soil Sci. **25,** 99-110

Ewald, W., 1995, Die Zugänglichkeit von Schichtzwischenräumen bei der Gasadsorption, Dissertation, Universität Kiel

Greenland, D.J., Quirk, J.P. 1964, Determination of the total specific surface area of soils by adsorption of cetyl pyridinium bromide, J. Soil Sci. **15,** 178-191

Hang, P.T., Brindley, G.W. 1970, Methylene blue adsorption by clay minerals. Determination of surface areas and cation exchange capacities (clay-organic studies XVIII), Clays and clay minerals **18,** 203-212

Heilman, M. D., Carter, D. L., Gonzalez, C. L. 1965, The ethylene glycol monothyl ether (EGME) technique for determining soil-surface area, Soil science **100,** 409-413

Helmy, A. K., Ferreiro, E. A., de Bussetti, S. G. 1994, Cation exchange capacity and condition of zero charge of hydroxy-Al montmorillonite, Clay and clay minerals **42,** 444-450

Helmy, A.K., Ferreiro, E.A., de Bussetti, S.G., Peinemann, N. 1998, Surface areas of kaolin, a-Fe2O3 and hydroxy-Al montmorillonite, Colloid and Polymer Science **276,** 539-543

Hofmann, U., Giese, K. 1939, Über den Kationenaustausch an Tonmineralien, Kolloidzeitschrift **,** 21-36

Hofmann, U., Klemen, R. 1950, Verlust der Austauschfähigkeit von Lithiumionen an Bentonit durch Erhitzung, Zeitschrift für Anorganische Chemie **262,** 95-99

Hrobárikova, J., Madejová, J., Komadel, P. 2001, Effect of heating temperature on Li-fixation, layer charge and properties of fine fractions of bentonites, Journal of materials chemistry **11,** 1452-1457

Jagiello, J., 1994, Stable numerical solution of the adsorption integral equation using splines, Langmuir **10,** 2778-2785

Janek, M., Komadel, P. 1999, Acidity of proton saturated and autotransformed smectites characterized with proton affinity distribution, Geologica Carpathica **50,** 373-378

Janek, M., Komadel, P., Lagaly, G. 1997, Effect of autotransformation on the layer charge of smectites determined by the alkylammonium method, Clay Minerals **32,** 623-632

Janek, M., Lagaly, G. 2001, Proton saturation and rheological properties of smectite dispersions, Applied Clay Science **19,** 121-130

Janek, M., Lagaly, G. 2003, Interaction of a cationic surfactant with bentonite: a colloid chemistry study, Colloid Polym Sci **281,** 293-301

Jaynes, W. F., Bigham, J. M. 1987, Charge recuction, octahedral charge, and lithium retention in heated, Li-saturated smectites, Clays and clay minerals **35,** 440-448

Kahr, G., 1991, Water vapor adsorption on clays to deduce the surface area, Proc. 7th Euroclay Conf. Dresden 1991 **,** 573-575

Kahr, G., Madsen, F.T. 1995, Determination of the cation exchange capacity and the surface area of bentonite, illite and kaolinite by methylene blue adsorption, Applied Clay Science **9,** 327-336

Kallay, N., Hlady, V., Jednacak-Bisca, Miljonic, S. 1993, Techniques for the study of adsorption from solution. In: Rossitzer, B.W.; Baetzold, R.C. (eds) Investigations of surfaces and interfaces. Part A. Physical methods of chemistry series, 2nd edn., John Wiley & Sons **,** 73-140

Kloppenburg, S., 1997, Kolloidchemische Steuerung der Porosität aggregierter Tonminerale, Dissertation, Universität Kiel

Komadel, P., Janek, M., Madejova, J., Weekes, A., Breen, C. 1997, Acidity and catalytic activity of mildly acid-treated Mg-rich montmorillonite and hectorite, J. Chem. Soc. Faraday Trans. **93,** 4207-4210

Kraehenbuehl, Stoeckli, H. F., Brunner, F., Kahr, G. Mueller-Vonmoos, M. 1987, Study of the water-bentonite system by vapour adsorption, immersion calorimetry and x-ray techniques: I. Micropore volumes and internal surface areas, following Dubinin's theory, Clay Minarals **22,** 1-9

Lagaly, B., Mermut, A.R. (ed) 1994, Layer charge determination by alkylammonium ions., CMS workshop lectures Vol. 6. The clay mineral soc **,** 1-46

Lagaly, G., 1981, Characterization of clays by organic compounds, Clay Minerals **16,** 1-21

Lagaly, G., Schulz, O., Zimehl, R. 1997, Dispersionen und Emulsionen, Steinkopff Verlag. Darmstadt

Laglay, G., 1993, Tonminerale und Tone. Edit: Jasmund, K., Lagaly, G. Steinkopff Verlag, Darmstadt.

Levy, R., Francis, C. W. 1975, A quantitative mehtod for the determination of montmorillonite in soils, Clays and clay minerals **23,** 85 - 89

Lim, C. H., Jackson, M. L. 1986, Expandable phyllosilicate reactions with lithium on heating, Clays and clay minerals **34,** 346-352

Lyklema, H., 1995, Fundamentals of interface and colloid science. II. Solid-liquid interfaces., Acad. Press, London

Mandalia, T., Crespin, M., Messad, D., Bergaya, F. 1998, Large interlayer repeat distances observed for montmorillonite treated by Al-Fe and Fe pillaring solution, Chem. Commun. **19,** 2111-2112

Mantin, I., Glaeser, R. 1960, Fixation des ions cobaltihexamine par les montmorillonites acides, Bull Gr. Fr. Argiles **12,** 83-88

Martin, R. T., 1955, Ethylene glycol retention by clays, Soil Sci. Soc. Am. Proc. **19,** 160-164

McNeal, B. L., 1964, Effect of exchangeable cations on glycol retention by clay minerals., Soil Sci. **97,** 96-102

Mehlich, A., 1948, Determination of cation- and anion-exchange properties of soils, Soil Sci. **66,** 429-445

Meier, L.P., Kahr, G. 1999, Determination of the cation exchange capacity (CEC) of clay minerals using the complexes of copper(II) ion with triethylenetetramine and tetraetylenepentamine, Clays and Clay Minerals **47,** 386-388

Moore, D. M., Reynolds, R. C. Jr. 1989, X-ray diffraction and the identification and analysis of clay minerals, Oxford university press

Morel, R. 1958, Observation sur la capacité d'échange et les phénomène d'échange dans les argiles, Bull. Fr. Gr. Argiles **10,** 1958

Müller-Vonmoos, M., Kahr, G., Madsen, F. 1994, Intracrytalline swelling of mixed-layer illite-smectite in K-bentonites, Clay minerals **29,** 205-213

Nennemann, A., 1997, Anionenausschluß in Montmorillonitdispersionen, Diplomarbeit, Universität Kiel

Nennemann, A., Ammann, L., Mecking, O., Permien, T., Lagaly, G. 2000, Specific surface area by co-ion exclusion measurements: influence of experimental conditions, Scripta--Geology **28,** 37-42

Newman, A.C.D., 1983, The specific surface of soil determined by water sorption, J. Soil Sci. **34,** 23-32

Orsini, L., Remy, J. C. 1976, Utilisation du chlorure de cobaltihexamine pour la détermination simultanée de la capacité d'échange et des bases échangeables des sols, Science du sol **4,** 269-275

Parker, J. C., Zelazny, L. W., Sampath, S., Harris, W. G. 1979, A critical evaluation of the extension of zero point of charge (zpc) theory to soil systems, Soil Sci. Soc. Am. J. **43,** 668-674

Pleysier, J., Cremers, A. 1975, Stability of silver-thiourea complexes in montmorillonite clay, Farad. Trans **71,** 256-264

Polubesova, T.A., Ponizovskiy, A.A., Stawinski, Y. 1989, Application of the theory of the double electrical layer to the evolution of anion exclusion moisture in soils, Soviet Soil Science **22,** 59-66

Ristori, G.G., Sparvoli, E., Landi, L. Martelloni, C. 1989, Measurement of Specific Surface Areas of Soils by p-Nitrophenol Adsorption, Applied Clay Science **4,** 521-532

Roempp 1995, Falbe, J., Regitz, M. (eds):Roempp Chemie Lexikon,

Rosenqvist, J., Persson, P., Sjöberg, S. 2002, Protonation and Charging of Nanosized Gibbsite Particles in Aqueous Suspension, Langmuir **18,** 4598-4604

Schofield, R.K., 1947, Calculation of surface areas from measurement of negative adsorption, Nature **160,** 408-410

Schofield, R.K., 1949, Calculation of Surface Areas of Clays from Measurement of Negative Adsorption, Trans British Ceram Soc **48,** 207-213

Schoonheydt, R.A., Heughebaert, L. 1992, Clay adsorbed dyes: methylene blue on laponite, Clay Minerals **27,** 91-100

Schramm, L.L., Kwak, J.C.T. 1982, Influence of exchangeable cation composition on the size and shape of montmorillonite particles in dilute suspension, Clays and Clay Minerals **30,** 40-48

Schramm, L.L., Kwak, J.C.T. 1982, Interactions in clay suspensions: The distribution of ions in suspension and the influence of tactoid formation, Colloid & Surfaces **3,** 43-60

Schroth, B. K., Sposito, G. 1997, Surface charge properties of kaolinite, Clays and clay minerals **45,** 85-91

Sequaris, J. M., Hild, A., Narres, D., Schwuger, M.J. 2001, Polyvinyladsorption an Na-montmorillonite, J. Colloid Interface Sci **233,** 367

Sor, K., Kemper, W. D. 1959, Estimation of hydrateable surface area of soils and clay from the amount of adsorption and retention of ethylene glycol, Soil Sci. Soc. Am. Proc. **23,** 105-110

Srasra, E., Bergaya, F., Van Damme, H., Aribuib, N. K. 1989, Surface properties of an activated bentonite - decolorisation of rape-seed oils, Applied clay science **4,** 411-421

Srodon, J., 1980, Precise identification of illite/smectite interstratifications by x-ray powder diffraction, Clays and clay minerals **28,** 401-411

Tributh, H., Lagaly, G. 1986, Aufbereitung und Identifizierung von Boden- und Lagerstättentonen, GIT Fachz. Lab. **30,** 524-529

Tributh, H., Lagaly, G. 1991, Identifizierung und Charakterisierung von Tonmineralen, Berichte der Deutschen Ton und Tonmineralgruppe **,** 86-130

Tributh, H., Lagaly, G. 1991, Identifizierung und Charakterisierung von Tonmineralen, Berichte der Deutschen Ton- und Tonmineralgruppe **,** 63-85

Van den Hul, H.J., Lyklema, J. 1967, Determination of specific surface areas of dispersed materials by negative adsorption, Journal of Colloid and Interface Science **23,** 500-508

Wanner, H., Albinssong, Y., Karnland, O., Wieland, E., Wersin, P., Charlet, L. 1994, The acid/base chemistry of montmorillonite, Radiochimica acta **66,** 157-162

Weiss, A., Lagaly, G., Beneke, K. 1970, Steigerung der Nachweisempfindlichkeit von quellungsfähigen Dreischichttonmineralen in Gemengen, Zeitschrift für Pflanzenernäherung und Bodenkunde **129,** 193-202

9.1 Co-ordinates of the complexes

Copper bisetyhlenediamine $[Cu(en)_2]^{2+}$ complex

Tab. 9.1 : Co-ordinates of $[Cu(en)_2]^{2+}$ complex.

atom	x	y	z
Cu	0	0	0
N	1,39022	-0,00654	1,53130
H	1,79944	0,93446	1,60510
H	2,16451	-0,65869	1,36134
C	0,67738	-0,36548	2,82321
H	0,56088	-1,45433	2,85241
H	1,27360	-0,06849	3,69276
C	-0,68033	0,33718	2,82877
H	-0,56377	1,42545	2,87616
H	-1,27731	0,02601	3,69281
N	-1,39264	0,00000	1,53054
H	-2,16071	0,66092	1,36638
H	-1,81039	-0,93818	1,59102
N	-1,39112	-0,00654	-1,53100
H	-1,79320	-0,95085	-1,60226
H	-2,17048	0,63977	-1,36227
C	-0,68003	0,35484	-2,82343
H	-1,27538	0,05521	-3,69265
H	-0,56735	1,44404	-2,85293
C	0,67980	-0,34342	-2,82850
H	0,56662	-1,43208	-2,87288
H	1,27472	-0,03239	-3,69395
N	1,39202	0,00000	-1,53176
H	2,16175	-0,65844	-1,36567
H	1,80756	0,93892	-1,59557

Copper triethylenetetramine $[Cu(trien)]^{2+}$ complex

Tab. 9.2 : Co-ordinates of $[Cu(trien)]^{2+}$ complex.

atom	x	y	z
Cu	0	0	0
N	-1,24624	-0,10827	1,62070
H	-1,39371	0,83439	2,00539
H	-2,17507	-0,49608	1,42210
C	-0,50637	-0,98210	2,61976
H	-0,99380	-0,95597	3,60072
H	-0,55147	-2,01418	2,25584
C	0,94174	-0,48184	2,73358
H	0,97306	0,47334	3,26972
H	1,55005	-1,19699	3,29956
N	1,52150	-0,24937	1,35487
H	2,16252	0,55132	1,39286
C	2,22203	-1,42625	0,70983
H	3,13117	-1,69094	1,26351
H	1,54544	-2,28740	0,76074
C	2,56726	-1,07843	-0,76346
H	3,56140	-0,62358	-0,83344
H	2,58670	-1,99488	-1,35993
N	1,54797	-0,10827	-1,35529
H	1,98445	0,81832	-1,40455
C	0,98272	-0,42996	-2,72761
H	1,66060	-1,08555	-3,28443
H	0,90772	0,51073	-3,28556
C	-0,40255	-1,07702	-2,59196
H	-0,33411	-2,09326	-2,18829
H	-0,89192	-1,13864	-3,57057
N	-1,22867	-0,24937	-1,62111
H	-1,46975	0,66083	-2,03517
H	-2,11422	-0,72228	-1,40889

9.2 Excel macro for the polynomial interpolation

```
Sub polynomial_interpolation()
Dim n%, p%, x#, r#, s#
n = 6                                   'number of line to search the data
p = 6                                   'number of line to print the results

r = Cells(2, 4)                         'read pH-max
s = Cells(3, 4)                         'read pH-min

For x = r To s Step -0.1                'pH-range and increment

  Do While Cells(n, 2) <> ""            'search only cells which are not empty
    If Cells(n, 2) <= x Then
      Cells(p, 4) = x                   'print the pH

        Dim i%, j%, l#, V#
        V = 0
        For i = -2 To 1 Step 1
          l = 1
          For j = -2 To 1 Step 1
            If j <> i Then
              If (Cells(n + i, 2) <> Cells(n + j, 2)) Then  'to avoid division by zero
              l = l * (x - Cells(n + j, 2)) / (Cells(n + i, 2) - Cells(n + j, 2))
              End If
            End If
          Next j
          V = V + l * Cells(n + i, 1)
        Next i

      Cells(p, 3) = V                   'print the calculated volume
      p = p + 1
      Exit Do
    End If
    n = n + 1
  Loop
Next

End Sub
```

Comments on the macro

- The macro is designed only to search from high pH to low pH. For ab titrations the data have to be changed in order before running the macro.

- Before running the macro the user must choose pH_{min} and pH_{max} (Fig. 9.1) of the range to be interpolated. Note that two data points before and after the desired pH are required for the interpolation polynomial.
- It is strongly recommended to plot the titration data and the interpolated data in the same graph to check if both curves match. Artefacts arise from the interpolation if two data pairs within the interpolated data have a very small or no difference in pH. In this case the user should delete manually one of the data pairs and run the macro again.

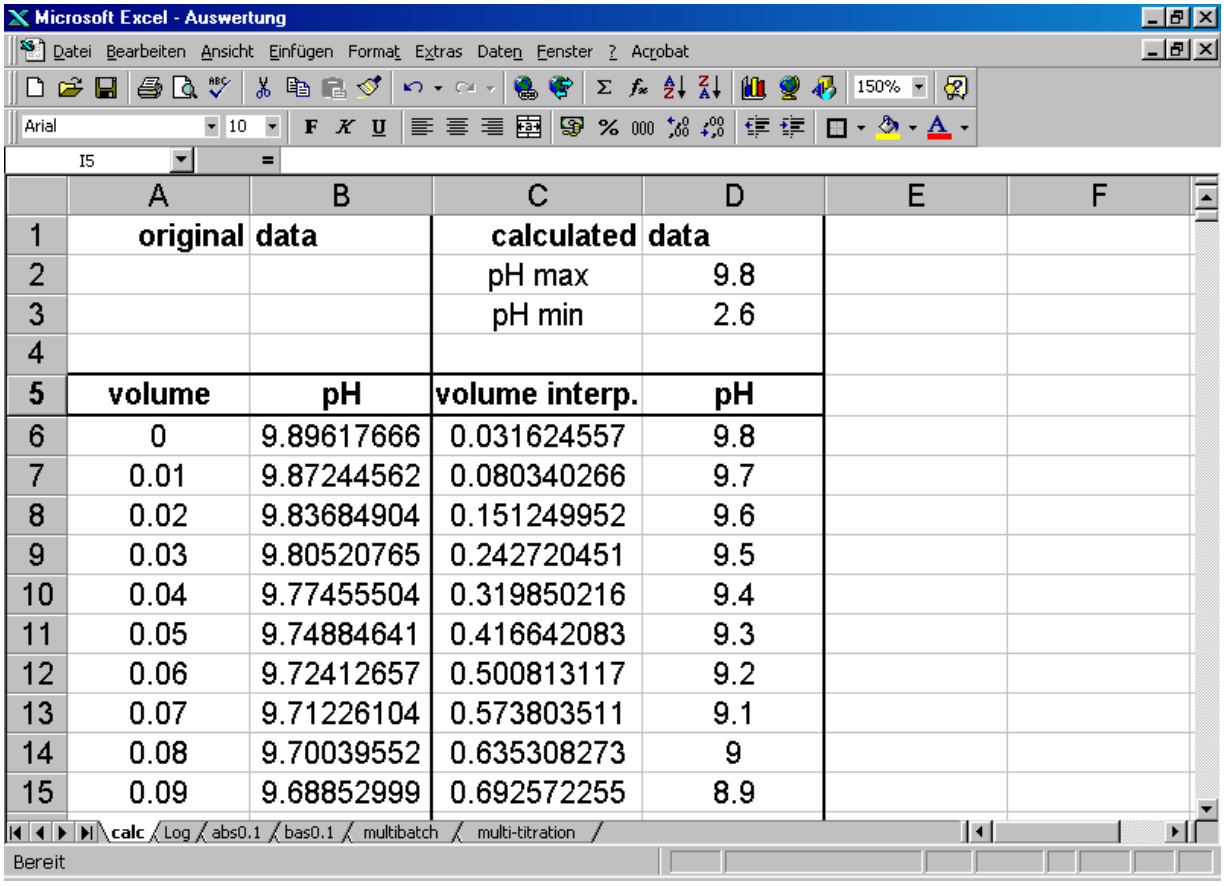

	A	B	C	D	E	F
1	**original**	**data**	**calculated**	**data**		
2			pH max	9.8		
3			pH min	2.6		
4						
5	**volume**	**pH**	**volume interp.**	**pH**		
6	0	9.89617666	0.031624557	9.8		
7	0.01	9.87244562	0.080340266	9.7		
8	0.02	9.83684904	0.151249952	9.6		
9	0.03	9.80520765	0.242720451	9.5		
10	0.04	9.77455504	0.319850216	9.4		
11	0.05	9.74884641	0.416642083	9.3		
12	0.06	9.72412657	0.500813117	9.2		
13	0.07	9.71226104	0.573803511	9.1		
14	0.08	9.70039552	0.635308273	9		
15	0.09	9.68852999	0.692572255	8.9		

Fig. 9.1 : Screenshot of the polynomial interpolation worksheet.

9.3 Adsorption of ethylene glycol

The amount of ethylene glycol adsorbed per gram of dry clay was plotted vs. the duration of the experiment (days). A linear regression was performed for the fast adsorption phase and for the slow phase. Co-ordinates of the point of intersection are given. The specific surface area was calculated by dividing the amount of ethylene glycol adsorbed per gram of dry clay by 0.45 mg/m^2.

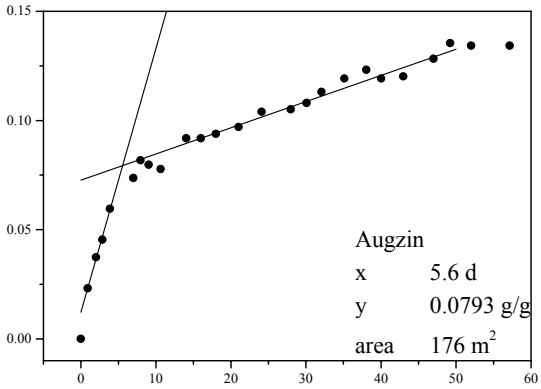

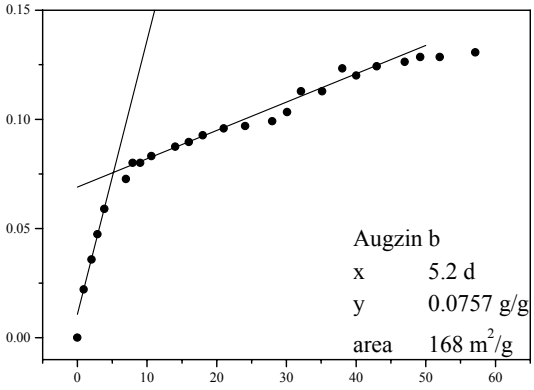

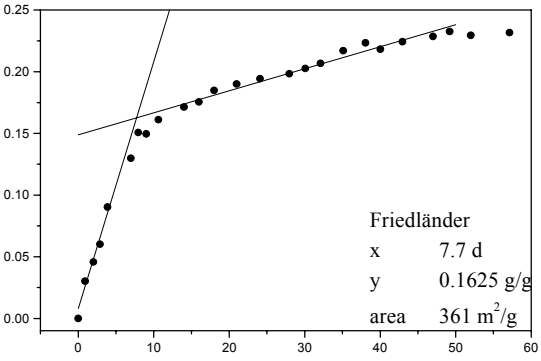

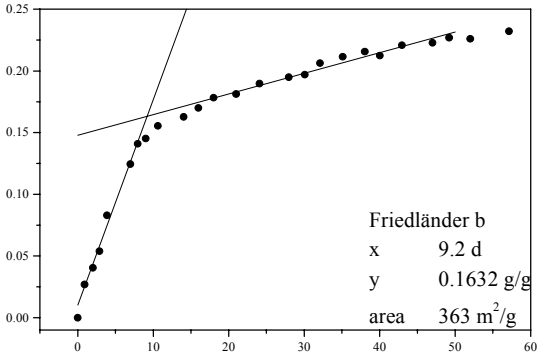

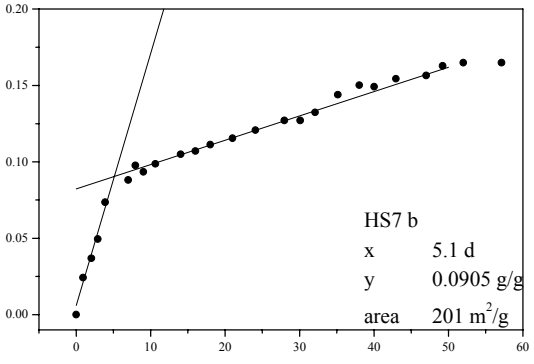

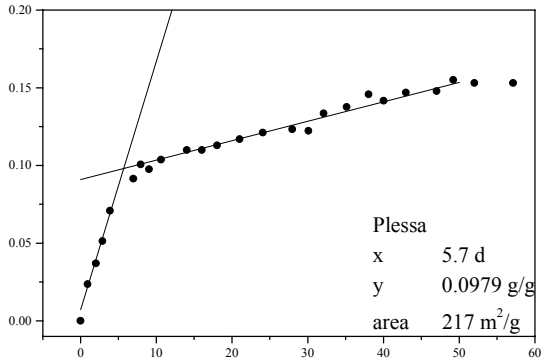
Plessa
x 5.7 d
y 0.0979 g/g
area 217 m²/g

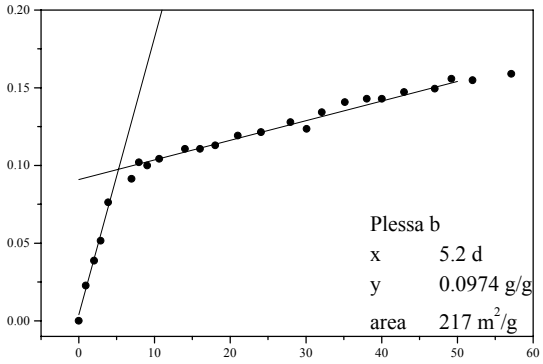
Plessa b
x 5.2 d
y 0.0974 g/g
area 217 m²/g

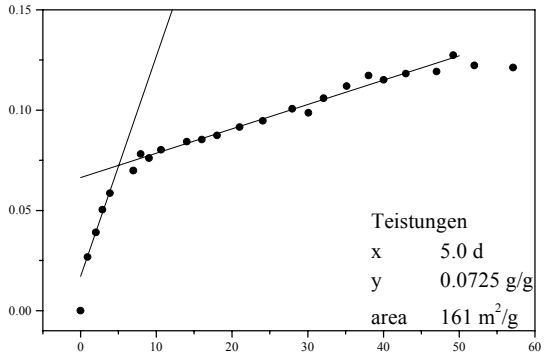
Teistungen
x 5.0 d
y 0.0725 g/g
area 161 m²/g

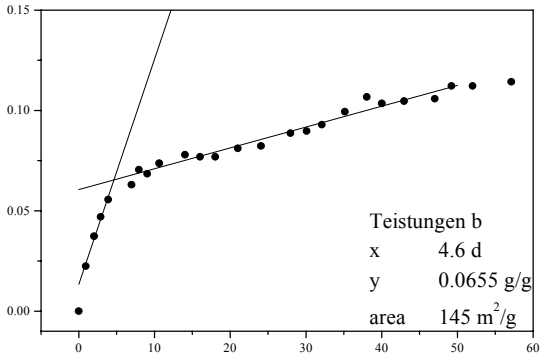
Teistungen b
x 4.6 d
y 0.0655 g/g
area 145 m²/g

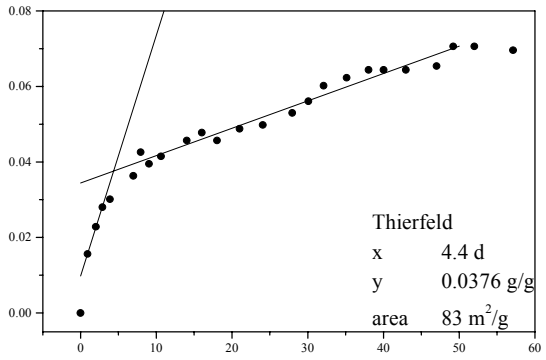
Thierfeld
x 4.4 d
y 0.0376 g/g
area 83 m²/g

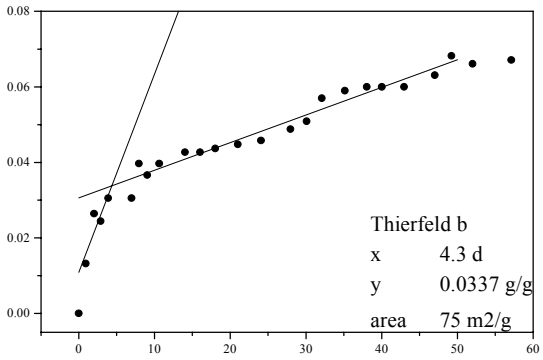
Thierfeld b
x 4.3 d
y 0.0337 g/g
area 75 m2/g

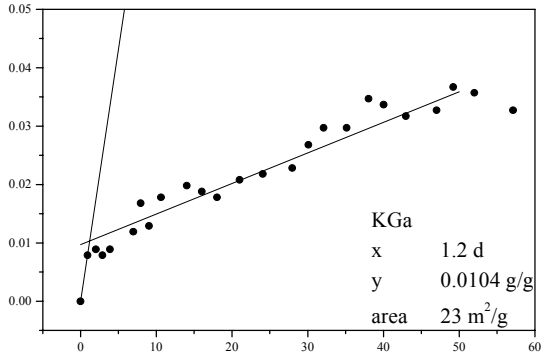
KGa
x 1.2 d
y 0.0104 g/g
area 23 m²/g

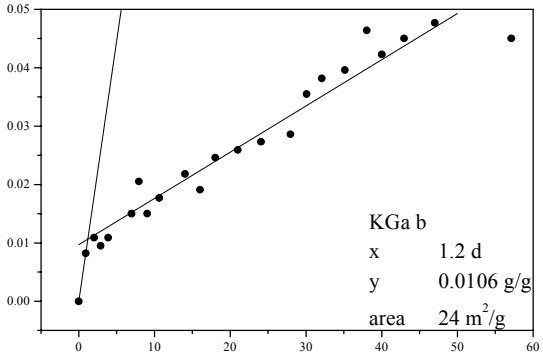
KGa b
x 1.2 d
y 0.0106 g/g
area 24 m²/g

9.4 Glossary of abbreviations

AA	ammonium acetate
AAS	atomic adsorption spectroscopy
ab	ab indicates that a titration was performed from **a**cidic to **b**asic by adding base (Chap. 4)
ba	titration performed from **b**asic to **a**cidic by adding acid (Chap. 4)
cec	cation exchange capacity
cip	common intersection point
$[Cu(en)_2]^{2+}$	Copper bisethylenediamine complex
$[Cu(trien)]^{2+}$	Copper triethylenetetramine complex
DMSO	dimethyl sulfoxide
EG	ethylene glycol
EGDE	ethylene glycol diethylether
EGME	ethylene glycol monoethylether
en	ethylenediamine
HK0, 10, 20...	Reduced charge montmorillonites prepared with the **H**ofmann-**K**lemen effect; 0, 10, 20% sodium exchanged before calcination (Chap. 2.1).
hvp	high vapour pressure
iep	isoelectric point
lvp	low vapour pressure
MB	methylene blue
PC0, 50, 100	pillared clay containing 0, 50 or 100% iron pillars
PCD	particle charge detector
PVP	polyvinyl pyrrolidone
pzc	point of zero charge
pznc	point of zero net charge
pznpc	point of zero net proton charge
pzse	point of zero salt effect
rcf	relative centrifugal field
SCHN	elemental analyzer capable to determine **s**ulfur, **c**arbon, **h**ydrogen and **n**itrogen content
TL	TL as an index of a sample name indicates that the sample has been

	purified by the method of Tributh and Lagaly (Chap. 2.2)
trien	triethylenetetramine
$\Delta V / \Delta pH$ plot	differentiated acid or base more adsorption isotherm